

NASA TECHNICAL
TRANSLATION



NASA TT F-701

e. 1

NASA TT F-701

LOAN COPY: RETURN TO
AFWL (DOUL)
KIRTLAND AFB, TX

0069051



TECH LIBRARY KAFB, NM

THE RINGS OF SATURN

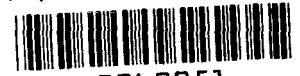
by M. S. Bobrov

Academy of Sciences USSR, Astronomical Council

"Nauka" Press, Moscow, 1970

NATIONAL AERONAUTICS AND SPACE ADMINISTRATION • WASHINGTON, D. C. • JUNE 1972

TECH LIBRARY KAFB, NM



0069051

THE RINGS OF SATURN

By M. S. Bobrov

Translation of "Kol' tsa Saturna."
Academy of Sciences USSR, Astronomical Council,
"Nauka" Press, Moscow, 1970

NATIONAL AERONAUTICS AND SPACE ADMINISTRATION

For sale by the National Technical Information Service, Springfield, Virginia 22151

\$3.00

Present-day knowledge of Saturn's rings is reflected. The results of observations of Saturn's rings are analyzed in detail, and a number of conclusions as to the nature of the rings are formulated. Particular attention is given to the quantitative theory of change in the brightness of the rings with phase angle, which is then used to estimate the principal physical magnitudes that characterize the rings as a whole, as well as a typical particle of the rings. Questions concerned with the dynamics of the rings are discussed. The book is intended for scientists, graduate students, and students interested in research on objects in the solar system.

Table of Contents

Introduction	1
I. Details of the Structure that Differ from Those of the Earth	3
#1. The zonal structure, The A, B, and C rings	3
#2. More precise detail	4
#3. Ring dimensions	6
II. Changes in Ring Openings. View from the Edge	7
#4. Cycle of changes in ring openings	7
#5. Observations of the dark side of the rings	8
#6. "Disappearance" of the rings	9
III. Astrophysical and Radioastronomy Data	10
#7. Introductory remarks	10
#8. Linear rotational velocities of the rings	10
#9. Visible and near ultra-violet spectral reflectivity ...	11
#10. Infrared spectrometry	19
#11. Polarization	21
#12. Change in surface luminance with phase angle	21
#13. Other photometric data	27
#14. Optical thickness	29
#15. Radiometric and radioastronomical data	34
IV. Model of the B Ring. Properties of a Typical Particle	39
#16. Absolute surface brightness of the B ring	39
#17. Model of the ring. Albedo of a particle	41
#18. The mechanism responsible for the observed ring phase curve	49
#19. Conclusions concerning the structure of the B ring and properties of a typical particle	51
V. Analysis of Observations Made During Extremely Small Ring Openings	53
#20. Introductory remarks	53
#21. Illumination of the dark side of the rings	54
#22. Analysis of observations for estimating the physical thickness of the rings	60
#23. "Atmosphere" of the rings	70
VI. Ring Dynamics	72
#24. Ring rotation law	72
#25. Differential rotation and Its Consequence	73
#26. The physical condition of the ring material	74
#27. Stability	75
#28. Mechanisms that possibly prevent complete flattening of the rings	81

VII. Theory of the Effect of Mutual Shading and Its Comparison with Observations	85
#29. Introductory remarks	85
#30. The Seeliger approximation	85
#31. The "cone-cylinder" approximation, without variance in the sizes of particles taken into consideration	87
#32. The "cone-cylinder" approximation with variance in particle size taken into consideration	99
#33. Other solutions	114
#34. Discussion of the results. Values of the Principal physical parameters of the rings	114
APPENDIX. List of Designations in the Formulas Used in the Theory of the Effect of Mutual Shading	118
REFERENCES	120

"When we in fact see how this majestic arc is suspended over the equator of the planet with no visible means of support or connection, our mind can no longer remain at ease. We cannot become reconciled to this phenomenon as if it were some simple fact, we cannot describe it simply as the result of observations, and we cannot accept it without seeking for an explanation for it."

45*

James Clerk Maxwell

On the Stability of the Motion of Saturn's Rings

Introduction

Saturn's rings are, in essence, a satellite object. At the same time, the great many bodies that are contained within it, and the comparative shortness of the distance between those bodies, makes them into a single, compact system in which the individual satellite loses its individuality.

Saturn's rings have a dual interest for the researcher. First of all, it is the only cosmic formation of its type that we know of. It has its own special geometry, dynamics and other features. Furthermore, it is one of the elements in the solar system, and in its own way is as characteristic as the ring of asteroids, as the Galilean satellites of Jupiter, or of the moon. In

* Numbers in the margin indicate pagination in the foreign text.

other words, the problem of Saturn's rings is not one of a narrow problem of a single object, but rather part of an incomparably broader problem of physics and cosmogony of the solar system.

It can be pointed out, for example, that the particles of Saturn's rings are subjected to continuous bombardment by micrometeoroid bodies and by corpuscular solar radiation. A quantitative estimate of the pitting of the surface of a typical ring particle is, at the same time, an indirect estimate of the intensity of the flow of micrometeoroid bodies and of solar corpuscles at the distance of Saturn.

Another example of the physical connection between Saturn's rings and the environment is the probable interaction of their material with the magnetic field of the planet (the latter should be strong, as can be anticipated because of the similarity of Saturn to Jupiter). The presence of rotating rings in Saturn's magnetosphere should deform the magnetic lines of forces significantly (Zheleznyakov, 1964; Zlotnik, 1967).

/6

To simply speak of cosmogony makes the very fact of the existence of Saturn's rings in the solar system important, and something that cannot be ignored. The properties of a typical ring particle are of particular cosmogonic interest. In fact, according to contemporary hypotheses, the rings are the zone of the presatellite cluster of Saturn, within which the tidal forces prevented the material of the cluster from forming into a single satellite. If this is so, then the zone of Saturn's rings is virtually the only place in the solar system where one can find and investigate the remains of preplanetary material.

Saturn's rings as a whole also are of considerable interest to the cosmogonist because the dynamics of the rings are, in many respects, similar to the dynamics of a protoplanetary cloud, and can be described by similar equations.

This monograph attempts to give a sequential account of all of the observational and theoretical material bearing on Saturn's rings (with the exception of those works that are of little significance, or which are obsolete) and to point out the conclusions that can be drawn as a result concerning the nature of the rings. Our task was made very much more complicated because of the complexity of the problem. Investigation of Saturn's rings

requires the application of many branches of science; astrophysics, celestial mechanics, astrometry, cosmogony, meteor astronomy, the physics of the interplanetary medium, the physics of the surface layer of the moon, optics of ice crystals and of microscopic particles of various shapes, the dynamics of systems with not completely elastic collisions, and others. So it is obvious that one author is in no position to deal with all sides of the problem with the same completeness. In order to avoid the possibility of making serious errors, we here have cited only those facts, data, results, and conclusions that we checked personally, or that were completely evident to us. In those rare instances when we were forced to depart from this rule we have pointed this out in the text and have indicated the sources from which the materials were taken, and we have given our views concerning them.

We should add that it was not the task of the monograph to provide precise numerical data. These data can be found quite readily in handbooks. We preferred to use rounded estimates, or to indicate the orders of magnitude.

I. Details of the Structure that Differ from Those of the Earth

/7

#1. The Zonal Structure. The A, B, and C Rings.

The ring structure susceptible to resolution in telescopes on earth (even including those in observatories high in the mountains with excellent image quality) is absolutely concentric, with no light or dark details of any description, giving the appearance of rotation around the planet. The rings, when they open wide enough, appear in the form of a system of concentric zones with different brightnesses (Figure 1a). The boundary of a particular zone is seen as a sharp, radial change in brightness or as a narrow, dark slit ("division") between the rings, as if devoid of matter.

The principal parts of the zonal structure are the A ring (the outer), the B ring (the middle), and the C ring (the inner). The latter sometimes is called the "crape" ring because of its very low brightness [about $1-3 \cdot 10^{-2} b_c$, where b_c is the brightness of the center of Saturn's disk, this is the approximate estimate made by Bell (1919)]. The B ring is the brightest part of the system (in opposition approximately equal to the center of Saturn's disk in brightness. The A ring visually is 0.6^m weaker (Schoenberg, 1921) and is partially transparent. Hepburn (1914), studying images of Saturn on plates

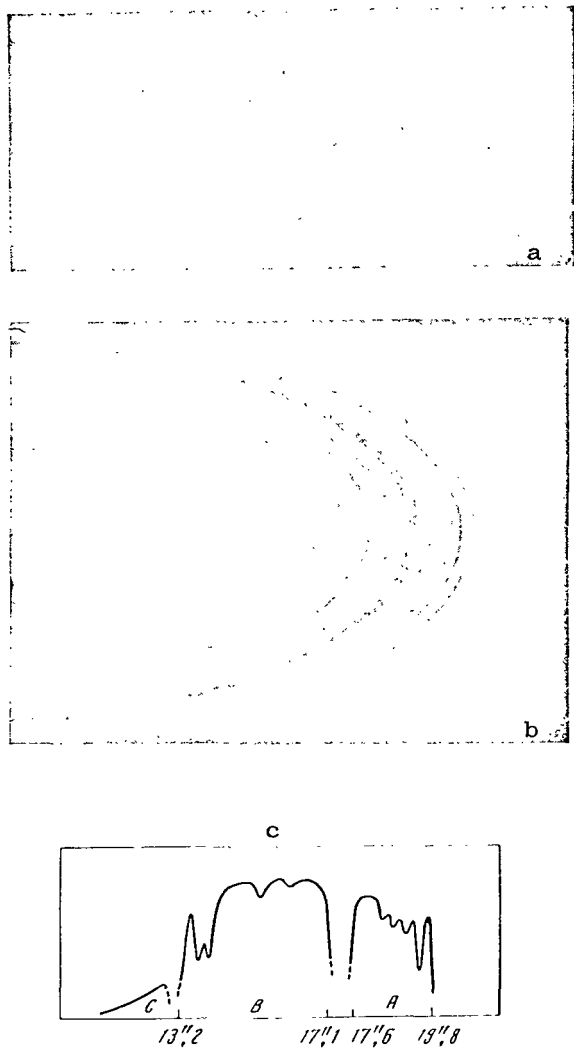


Figure 1. a - Saturn with rings opened wide (photograph by Camichel, 1958). Ring A is somewhat underexposed and ring C can be seen in a projection on the disk of Saturn. Resolution is $\sim 0.4''$; b - The rings of Saturn from visual observations from Pic du Midi (sketch by Lyot, 1953). Contrast is somewhat overdrawn; c - Distribution of brightness in the eye of the rings of Saturn along the major axis of the rings (from visual observations made by Dollfus, 1963). The angular dimensions of the rings are shown for the mean distance of Saturn from the sun (9.539 AU).

taken by Barnard (1914), was able to see Saturn's disk, translucent through the A ring at their edges. The crape ring is very transparent. The ball of the planet is readily distinguishable through it when observed visually (it goes without saying that these observations require the corresponding objective lens opening and a good quality image, because the crape ring itself is an almost inaccessible object).

The main division in the system is located between the A and B rings. It has been named the "Cassini division" from the name of its discoverer in 1675, Jean Dominique Cassini, the first director of the Paris Observatory (see Berry, 1964). The width of the Cassini division is about 5,000 kilometers, according to Barnard (1914).

#2. More Precise Detail.

Lyot (1953), observing Saturn visually in a 60 centimeter telescope from the Pic du Midi Observatory, with resolution approximately that of theoretical ($0.23''$), was able to distinguish some 10 divisions with different degrees of darkening of the rings (Figure 1b). Dollfus made similar observations (1936 b) in large telescopes in France and in the United States, enabling him to construct an approximate curve of brightness distribution

along the major axis of the rings (Figure 1c). The curve shows that in essence the system brightness changes with distance from Saturn, and that it is solely the presence of minima created by the divisions that lead to the conventional separation of the system into the "individual" A, B, and C rings.

Comparing Dollfus' curve with Lyot's sketch, one is readily persuaded that they are in good concordance. Attention is drawn to the wide zone of reduced brightness near the middle of the A ring created by the three close minima. Earlier observers, working under conditions of lesser resolution, took this to be a single division (the so-called "Encke division").

Kuiper (1957 a) is of the opinion that only the Cassini division is a real lane, containing very little material, and that all of the other divisions recorded in the literature on the subject are zones of somewhat reduced brightness (by 10 to 15 percent), or are fictitious. Kuiper's conclusion is based on a single visual observation he made of the rings in the Mount Palomar Observatory's 5 meter reflector with a magnification of 1170. Atmospheric turbulence on the night of the observation was unusually low and the resolution was 0.05" to 0.10". Three zones of darkening were seen in the B ring. The zone that divides the B and C rings was not observed (despite the fact that its existence had been noted by Lyot, as well as by many other observers; some weak divisions can change intensity markedly, so the possibility is not ruled out, however). Kuiper estimated the width of Cassini's division as one-fifth the width of the A ring. A region of darkening that was, at the same time, the region of an abrupt change in the brightness of the A ring was seen at the site of the "Encke division." Observation of a star occulted by the rings is an effective method to use to obtain information on the width, position, and optical thickness of the divisions. We shall discuss this method in #14. The mean time interval between two successive occultations of up to 9th magnitude stars by Saturn is 1.9 years. (Seeliger, 1881). The elements of the occultations of stars by planets are computed regularly by the British Astronomical Association, and are published on a systematic basis in that organization's annual.

Kirkwood (1884) was the first to explain the existence of the divisions by resonant perturbations in the orbits of the particles of Saturn's satellites. Actually, the period of revolution of a particle inside any of the divisions

is very close to 1/2, 1/3, ... the sidereal period of one, or of several internal satellites of Saturn, or of the most massive of them, Titan. This question has been discussed as well by Lowell (1910), Goldsbrough (1921, 1922), and Greaves (1922 a, 1922 b).

#3. Ring Dimensions.

Saturn's rings have been measured by many authors (with micrometers, with heliometers, and by measuring the images of the planets on negatives). Halation is the principal cause of fixed errors. In view of this, it is desirable in the near future to check accepted dimensions by using observations made of the occultations of stars by the rings.

Table 1 lists the ring dimensions, according to Rabe (1928).

TABLE 1

Detail	Visible radius (distance 9.5388 AU) seconds of arc	Actual radius, kilometers	Width	
			Seconds of Arc	Kilometers
A ring, outer edge	20.14	139,300	2.46	17,100
A ring, inner edge	17.68	122,200	0.73	5,000
B ring, outer edge	16.95	117,200	4.04	27,900
C ring, outer edge	12.91	89,300	2.49	17,300
C ring, inner edge	10.42	72,000		
Equatorial radius of Saturn	8.72	60,300		

Barabashov and Semeykin (1933), using photographic photometry and light filters, and excluding instrumental error by the "artificial planet" method (see #9), found that in blue light the space between the visible, inside boundary of the C ring and Saturn's equator is not completely dark. Negatives obtained in red and yellow light show no such effect. The authors interpreted their results as indicative of the fact that this space is filled with rarefied material stretching to the ball of Saturn itself. Consequently, it can be said that the inner edge of the C ring coincides with the external, visible, boundary of the planet's ball.

#4. Cycle of Changes in Ring Openings.

The plane of the rings coincides very precisely with the plane of Saturn's equator. The latter is tilted to the plane of Saturn's orbit by 26.7° , and to the plane of the earth's orbit by 28.1° . As the planet moves in its orbit, the plane of its equator, and the plane of the rings, move parallel to each other. The result is that the angles of elevation of the sun and of the earth above the plane of the rings, A and A' , change constantly, depending on the position of Saturn in its orbit. There are, in the course of one sidereal period of revolution of Saturn (29.46 years), two times of maximum opening of the rings, and two times when the rings are turned to the sun precisely on edge (or, in other words, the sun intersects the plane of the rings). This is what the observer on earth sees, basically, but it must be remembered that the earth does not coincide with the sun, but instead has its own orbital motion. Generally speaking, therefore, $A' \neq A$. Angle A' will change with the sidereal period of Saturn, and there will be small changes in its synodic period as well. These latter are more significant near the times when $A = 0$. As will be seen from Figure 2, a fixed time (that is, 360 days) is required for the intersection of the plane of the rings by the earth orbit. A more detailed examination of the question shows that during this period of time the earth can intersect the plane of the rings once, or three times (the number of intersections must be odd because the earth, in the final analysis, will be moving from one side of the plane of the rings to the other). In extremely rare cases two of these three intersections can take place almost simultaneously (case equivalent to two intersections). In certain other cases the earth can intersect the plane of the rings once, and in place of the other two intersections there is simply a more or less close approach to the plane of the rings. A typical example of the triple intersection of the plane of the rings by the earth is the one that took place in 1966 (Figure 3).

Let us add that the intervals between the successive intersections of the plane of Saturn by the sun are not equal. This can be explained by the difference in the orbital velocity of Saturn near the perihelion and near the aphelion. The rounded, respective intervals are 13.75 and 15.75 years.

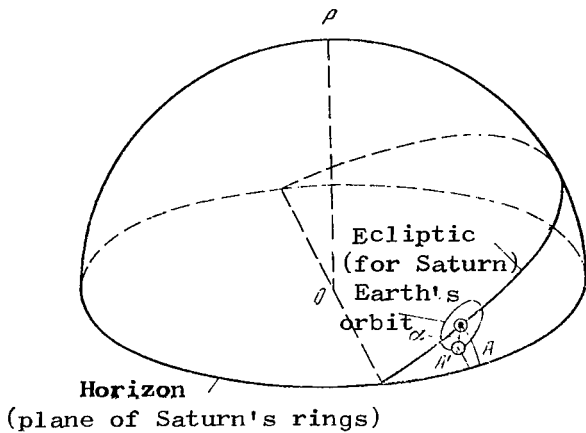


Figure 2. Northern hemisphere of the celestial sphere in the case of an observer standing on the side of Saturn's rings illuminated by the sun (near the time of intersection of the plane of the rings by the sun).

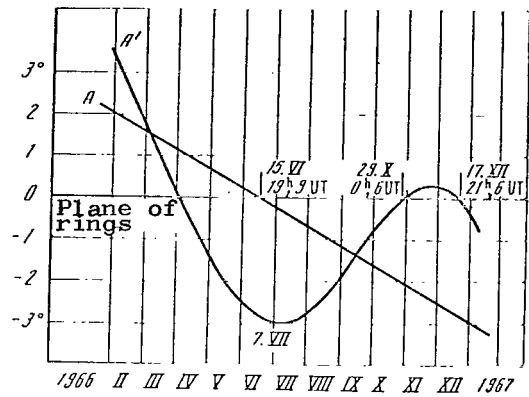


Figure 3. Change in the angles of elevation of the sun and the earth, A and A', above the plane of the rings in 1966. The earth intersected the plane of the rings three times.

#5. Observations of the Dark Side of the Rings.

Figure 2 can be used to find $|A - A'| \leq 3.5^\circ$. What follows in particular is that near time $A = 0$ (when $|A - A'|$ has its greatest value) the signs of angles A and A' can be opposite, that is, the earth can be over the dark side of the rings (Figure 3). Despite the fact that at this time the surface of the rings turned to the observer is not illuminated by the direct rays of the sun, the narrow ellipse of the rings is seen quite well, given a good quality image and not too small a telescope aperture. Russel (1908) pointed out that the illumination of the rings by the ball of Saturn is intense enough for their dark side to be seen visually by an observer in a telescope on earth. A recent reconsideration of the question (see #21) leads to the conclusion that there must be another source of dark side illumination, specifically solar light diffused through the rings in optically thin zones. The brightness of the dark side is less than that of the center of Saturn's disk by a factor of between 2 and 2.5.

Barnard (1908 a) described the view of the dark side in detail. Photography of the dark side has not yet been published. All that is available are drawings, and the best of them were made by Barnard. Figure 4 is an example. A typical feature of the dark side is the two pairs of bright "condensations" (Bardnard's expression). The outer condensations coincide

/13

with the Cassini divisions, the inner with the crape ring. They are attributable to solar light filtering through the corresponding zones of the rings (#21).

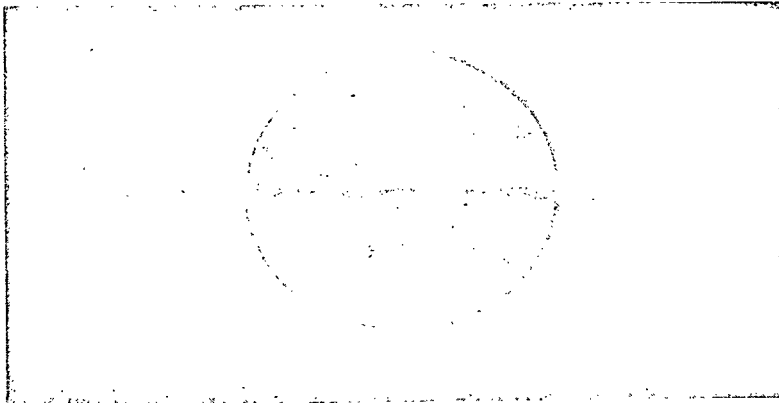


Figure 4. Drawing of the dark side of Saturn's rings (Barnard, 1908 a).

#6. "Disappearance" of the Rings.

/14

Many sources contain the assertion that the gaps of the rings disappear completely when one of the angles of elevation (A or A') is zero. But it is obvious that when $A = 0$, generally speaking, $A' \neq 0$, so the earth-bound observer will see the dark side of the rings illuminated by the ball of Saturn. Accordingly, the gaps will be seen (#5), so long as angle A' is not too small. The case when $A = 0$, that is, the time of intersection of the plane of the rings by the earth, actually has not been observed under conditions necessary for this to occur up to as late as 1966. Further details, and the results that follow, are contained in Chapter V.

#7. Introductory Remarks.

The angular width of Saturn's rings (see Table 1) is small, making it very difficult to investigate them. Ring B, because of its brightness, and because it is located in the center of the system, is relatively more accessible for astrophysical work. Study of the A ring requires greater skill because it is not as bright and because it is adjacent to the dark background of the surrounding sky. The crape ring is weaker than the B ring by approximately one and a half orders of magnitude, and is located between the B ring and Saturn's disk. The nearness of these bright objects makes for very serious difficulties. Astrophysicists ordinarily cannot be certain that they are studying the light reflected by the C ring, or the light that is scattered by the B ring which is directly contiguous to it, and by the disk of the planet.

This is why most of the astrophysical investigations made to date of the rings of Saturn involve the B ring. Data on the A ring are very meager, and the crape ring is, for all practical purposes, terra incognita.

#8. Linear Rotational Velocities of the Rings.

One of the earliest applications of spectral analysis to the physics of the planet was the study of the law of rotation of Saturn's rings by measuring the Doppler shift of the lines in the spectrum of the gaps of the rings. Observations were made independently by Belopol'skiy (1895) in Pulkovo, by Deslandres (1895) in Paris, and by Keeler (1895) in the Licks Observatory. The principles involved in making the measurements are clear in Figure 5. Table 2 lists the numerical results (Sharonov, 1958).

As will be seen from the data in Table 2, the measured velocities are in good concordance with Kepler's. Consequently, any ring particle can be considered a separate, independent, satellite of Saturn, moving around the planet in a circular orbit at Keplerian velocity. In fact, however, this is just the first approximation of the real motion of the particles. Perturbations by satellites, mutual perturbations, and collisions force the particles to oscillate near their mean positions. But the rings are so thin when compared with their radial distances that the velocities at which the particles oscillate are many orders of magnitude below their Keplerian velocities. The

problems alluded to here will be discussed in Chapter VI.

TABLE 2

Detail	Linear velocity, km/s			
	Belopol'skiy	Deslandres	Keeler	Theoretical (Kepler)
A ring, outer boundary	15.5	15.4	16.4	16.6
Middle of the ring	-	-	18.0	18.3
B ring, inner boundary	21.0	21.0	20.0	20.5

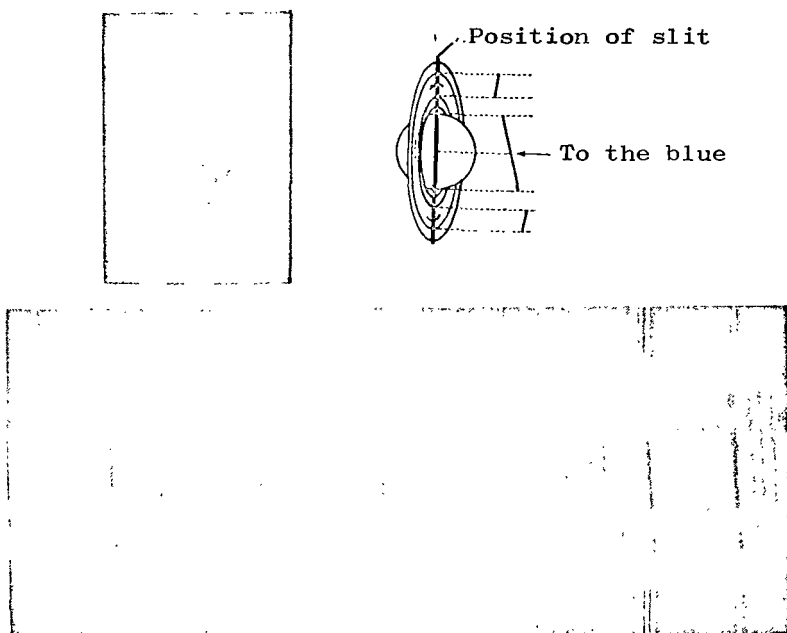


Figure 5. Position of the spectrograph slit and the Doppler shift of the lines in the spectra of the eyes of Saturn's rings and of the planet's disk caused by rotation (from Belopol'skiy, Deslandres, and Keeler).

#9. Visible and Near Ultra-violet Spectral Reflectivity.

/17

The pioneering research on this question was done by Belopol'skiy and Tikhov in Pulkovo. Belopol'skiy earlier (1896) had noted that the spectrum of Saturn's rings (the reference is to the more intense B ring zone) extends

toward the violet side much further than does the spectrum of the equatorial belt of the planet's disk. Thus, in the April 13, 1895, photograph the disk spectrum is extremely faint when $\lambda = 4100 \text{ \AA}$, whereas the ring spectrum extends to $\lambda = 4000 \text{ \AA}$, virtually without attenuation. Consequently, the light from Saturn's rings should differ from the light from its disk. Tikhov (1911) made a detailed check of the effect, using a great deal of material obtained from observations (spectra of Saturn and of the rings, taken by Belopol'skiy in 1906 and 1909, negative of Saturn with moderately open rings made by Tikhov in 1909 and by Belopol'skiy in 1911, using the 30 inch Pulkovo refractor with light filters to separate, respectively, the red-orange, the yellow-green, the green, and the blue-violet parts of the spectrum). Tikhov found that the disk could be seen up to 6950 \AA at the red end of the spectrum, but that the ring spectrum could only be seen to 6800 \AA . The disk spectrum was brighter than that of the rings over virtually all of the visible part, but the difference in brightness gradually decreased with reduction in λ . Near 4500 \AA the brightness of the spectra was the same, after which the ring spectrum brightened as compared with the disk spectrum. The ring spectrum could be traced to 3970 \AA , that of the disk spectrum only to 4020 \AA .

The results of the examination made of the photographs taken using light filters were in good concordance with these conclusions. It was established that Saturn's equatorial belt gradually attenuated with transition from the red to the violet, with the brighter part of the disk in the red, and the darker in the violet. The change in the brightness of the rings is the direct opposite; it was less than the mean brightness of the disk in the red, then increased and became much brighter than the mean brightness of the disk in the violet.

Tikhov's work, taken in the whole, establishes the fact that the blue is the most intense zone of the B ring in Saturn's equatorial belt. Lack of a tie with the sun, or with stars of the sun class, makes it impossible to explain whether or not the scattering of solar light by the B ring is neutral, or selective. Tikhov was inclined to the latter view, and based it on the following considerations. He found that darkening of Saturn's disk at the edges, substantial in the red, gradually became unremarkable with decrease in λ , and disappeared near the G band. According to Tikhov, this could be explained by the increase in the reflectivity of the atmosphere of Saturn with reduction in the wavelength. Furthermore, it was found that the brightness

/18

of the B ring near the points of its meeting with the planet's disk was the equal of that at the edges of Saturn's disk, and this was the case for all rays. This then led Tikhov to conclude that it was possible that the material of the ring was very similar in its reflectivity to that of Saturn's atmosphere, that is, that the mean diameter of the ring particles was less than the length of the light wave (recognizing however that special research would be required to arrive at a final answer to this question). This conclusion has never been confirmed.

Later on the famous American optician Robert Wood (1916) used light filters to obtain photographs of Saturn in the Mount Wilson Observatory (60 inch reflector), as did astrophysicist Wright in the Lick Observatory (1927). The new approach, as compared with that used by Tikhov and Belopol'skiy, was the use of infrared and ultraviolet filters. There still were no photometric scales. The equatorial belt on the disk of Saturn was particularly dark in the ultraviolet. Wood raised the question, "Is this effect due (albeit in part) to the hypothetical cloud of material filling the space between the crape ring and the spheroid of the planet?" In point of fact, the geometry of the equatorial belt is such that such interpretation cannot be precluded. However, Wright found that on his photographs the crape ring made a dark belt on the disk only in the red, whereas there was no shadow of the crape ring on the disk in the ultraviolet. Consequently, if the darkening of the equatorial belt in the ultraviolet was in fact connected to with the above-mentioned cloud of material, it would be necessary, at the very least, to postulate that its light scattering properties differed significantly from the light scattering properties of the crape ring.

Wood's photographs too show a gradual reduction in the difference in the brightness of the A and B rings with reduction in the wavelength, with A much weaker than B in the infrared and yellow, but only slightly weaker than B in the violet and ultraviolet. Wright's photographs, on the other hand, show approximately the same ratio of ring brightness for all filters. Present day data on the spectral reflectivity of the A and B rings show that Wright's results were close to the true results. The results obtained by Wood are the result of simple overexposure of the B ring image in the violet and ultraviolet photographs.

It would be necessary to use light filters for the photography, to print photometric scales, and, if possible, to eliminate instrumental effects, in order to judge the relationship between the reflectivity of the A and B rings and that of Saturn's disk in various parts of the spectrum. Barabashov and Semeykin (1933) did just this in their work, already mentioned in #3. Saturn was photographed through red, yellow, and blue filters in the 20 centimeter refractor in the Khar'kov Astronomical Observatory, using a magnification system. /19

An "artificial Saturn," that of the image of the planet with open rings corresponding to the real image, but with no gradations of brightness, was cut from thick white paper, and was photographed parallel to the instrument in order to exclude instrumental errors (diffraction, chromatic aberration, scattering in the photographic layer, errors in the microphotometer, and others). The artificial planet was photographed through the same filters, and with the same exposures, as was the real Saturn. Lighting of the artificial planet was selected so that the background and the density of the image on the negatives would be as close as possible to the real Saturn.

The density drop at the boundaries of the image on the microphotograms of the artificial planet was more or less smooth, rather than step-like. This was then used to correct the microphotograms of the real Saturn for errors attributable to the plates used, to the microphotometer, and to the instrument, and to obtain a brightness distribution along the central meridian and along the intensity equator.

The second of these graphics (Figure 6) provides, in particular, the radial progress of brightness in the eyes of the rings along their major axes. The completeness with which instrumental errors were eliminated can be judged by the position and depth of the minimum, corresponding to the Cassini division, and by the ratio of the A and B ring brightnesses. The position of the minimum coincides extremely well with the accepted distance of the Cassini division. The brightness at the minimum differs somewhat from zero, and increases with decrease in the wavelength, reaching 0.08 the brightness of the center of the disk in the blue. The A ring brightness was definitely underestimated [in the yellow by 2.06^m below the brightness of the B ring, whereas the visual surface photo-

metry provided by Schoenberg (1921), the photographic photometry provided by Camichel (1958) using a yellow filter, and the photographic photometry of Franklin and Cook (1965), provide magnitudes of $0.^m59$, $0.^m47$, and $1.^m00$ respectively]. Thus, the effect of fuzziness of the image is not done away with entirely (apparently because the artificial planet method does not correct for drive and atmospheric flicker errors) and this should be remembered during interpretation.

The authors found that the brightness of the most intense A ring zone changed from 0.129 to 0.150 and 0.154 (in terms of the brightness of the center of the disk) with transition from red to yellow and blue. The corresponding magnitudes were 0.585, 0.775, and 0.862 for the most intense B ring zone. From whence the ratio of A and B ring brightnesses in the red, yellow, and blue, were 0.221, 0.194, and 0.179. In other words, the brightness of the A ring changed less than did that of the B ring as the wavelength decreased when

/20

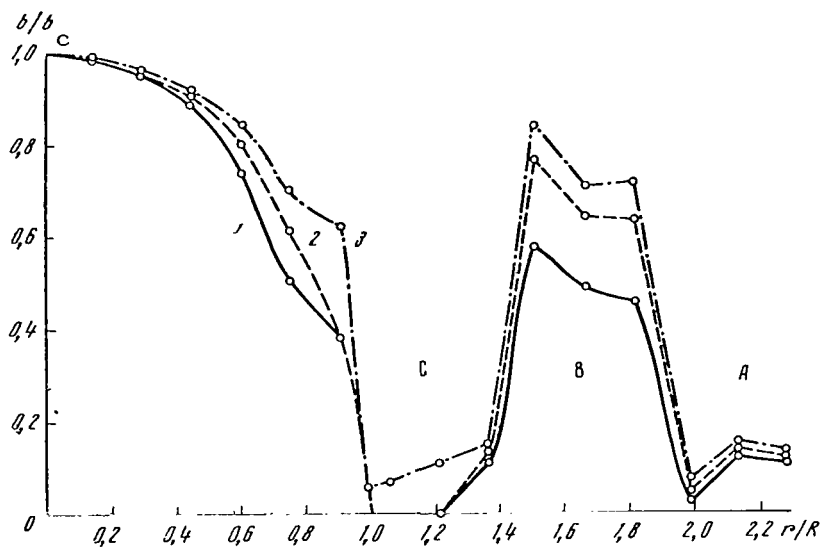


Figure 6. Distribution of brightness along the intensity equator for Saturn and for fuzziness of the image by the artificial planet method (Barabashov and Semeykin, 1933).

r/R is the distance from the center of the disk in parts of the equatorial radius of the planet. b/b_c is the brightness as a percentage of the brightness of the center of the disk. Curves 1, 2, and 3 were constructed for photographs in which red, yellow, and blue filters, respectively, had been used.

equated to the center of the disk. Note that Franklin and Cook (1965) obtained 0.398 and 0.403, with a probable error of 0.003, for the ratio of A and B ring brightnesses, that is, for all practical purposes there was no difference in the observed course of the reflectivity of both bright rings with wavelength. This question, it would appear, is in need of further investigation.

The B ring brightness in terms of the center of Saturn's disk increased greatly with decrease in the wavelength, in complete concordance with the results obtained by Belopol'skiy and Tikhov.

Finally, it was found (and this already has been pointed out in #3) that in blue light the space between the inner edge of the C ring and the ball of Saturn has a brightness differing significantly from zero, indicative of the presence in this space of evacuated, selectively diffusing matter. This region is completely dark in yellow and red lights, indicating a strong dependence of brightness on λ , and, as a result, on the smallness of the sizes of the diffusing particles. It even is possible that the matter discovered is gaseous in nature.

Shayn (1935) used the one-meter reflector in the Simeiz Observatory for spectrophotometry of the B ring with a tie-in to the sun, and to class G stars. Spectra of Saturn (disk and rings), the Moon, the Sun, and of two class G dwarf stars, 9 Ceti and 51 Pegasi, were obtained. The author comments that because of the low altitude of Saturn above the horizon (the declination of the body was about -16°) the image was not sufficiently still. Details of the order of 2" to 3" were partially washed out by nearby, brighter, details. He was unsuccessful in obtaining A and C ring spectra suitable for measurement purposes. The spectrophotometric measurements were made in two stages: (1) comparison of the disk and B ring spectra (using spectrograms with a dispersion of 36 \AA/mm near H_{γ}); (2) comparison of the spectra of Saturn, of the Sun, and of 9 Ceti (using spectrograms with low dispersion).

High dispersion spectrograms of Saturn were taken for phase angles $\alpha = 0^\circ 5' .5$, $0^\circ 37' .7$, and $2^\circ 38' .5$. Comparison with the disk showed the marked effect of the phase of the B ring, comprising almost 0.30^m in this α interval (see #12 for a detailed explanation of the effect of the phase of the rings). It was discovered that in the interval of wavelengths investigated, (4260-6500 \AA) the magnitude of the effect of the phase did not depend on λ , and that this was

/21

so with the accuracy of within 0.01^m . This is an important conclusion for interpreting the mechanism of the effect. The measurement data were then reduced to a single α value and averaged.

The tie-in to the sun and to the stars presented greater difficulties. Without going into detail, let us simply point out that the average from the comparisons made of the spectrum of Saturn's disk with the spectra of the Sun, Moon, and 9 Ceti, was taken as the final behavior of the differences $m_{\odot} - m_{\text{H}}$ with λ . The values obtained for 9 Cetus were considered to be the ones most free of systematic errors, and were taken with a weight of 2 in the averaging. The control comparison of the 9 Ceti and 51 Pegasi spectra showed good concordance in the distribution of their brightnesses over the spectrum.

Knowing $m_{\text{B}} - m_{\text{H}}$ and m_{\odot} , it is easy to find the unknown difference $m_{\odot} - m_{\text{B}}$. Figure 7 shows this graphically. As will be seen, $m_{\odot} - m_{\text{B}}$ does not depend on λ in the interval 4000 - 4600 Å, and for large λ there is a slight rise, ending near 5700 Å. Consequently, the B ring is somewhat more yellow than the sun. The disk of Saturn, in turn, is much more yellow than the B ring. In fact, as will be seen from Figure 7, in the interval of change in λ investigated (4000 - 6500 Å) the magnitude $m_{\odot} - m_{\text{H}}$ changes 1.5^m , whereas the change in the magnitude of $m_{\odot} - m_{\text{B}}$ is 0.5^m . The widely held view as to the blue color of the B ring is based on its comparison with the disk of Saturn, which is much more yellow than the sun. From all of this, Shayn came to the conclusion that the B ring particles should be longer or even much longer, than the length of the light wave.

There is no more recent work in spectrophotometry of Saturn's rings. Cook and Franklin (1965) found the blue and visual brightness of the A and B rings in stellar magnitudes per square second of arc in the so-called UBV* system. The result was the same value for the color index, $B - V = +0.86^m$, for both rings. For the sun $B - V = +0.64^m$ (Stebbins and Kron, 1956), for Saturn $+0.98^m$, according to Franklin and Cook (1965), and $+1.04^m$, according to Harris (1963). Giving preference to the data furnished by Cook and Franklin in the case of Saturn, we come to the color differences in the objects we are interested in as compared with the sun (see Table 3; the moon has been added as a

/22

*UBV (ultraviolet - blue - visual) is a photometric system in which the stellar magnitude is found for each body in three parts of the spectrum, the ultraviolet, the blue, and the visual.

typical body in the solar system devoid of atmosphere).

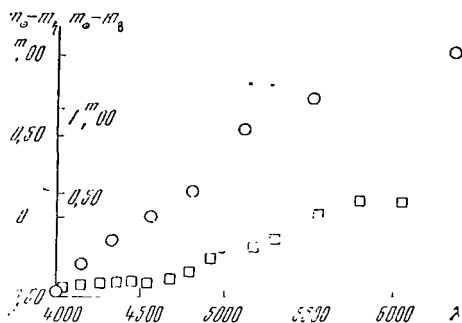


Figure 7. Spectral reflectivity of Saturn's disk (circles) and of the B ring (squares) from Shayn's observations (1935).

Quantitatively, these results are not in very good concordance with Shayn's spectrophotometry (his color differences for Saturn and for the B ring in blue light are $0^m.77$ and $0^m.40$, respectively), but his chief conclusion remains valid from a qualitative standpoint; the B ring, in any event, is not blue because of its illumination by the sun.

The slight increase in the spectral reflectivity of the B ring with increase in λ noted in these papers is not, in any event, connected with the illumination of the ring by Saturn's disk. Calculations (see #21) show that the intensity of the illumination by Saturn is at least two orders of magnitude lower than the intensity of the direct solar light. An independent confirmation of this fact is Shayn's observation that no traces of even the most powerful absorption belts observed in the spectrum of Saturn's disk were discovered in the spectrum of the ring.

TABLE 3

Object	B	V	Reference
Saturn's disk	$+0^m.34$	$0^m.00$	Cook and Franklin (1965)
A and B rings	$+0.22$	0.00	Same
Moon	$+0.29$	0.00	Harris (1963)

Nor can the evacuated "atmosphere" (dust or gas; see #13) blanketing the ring be responsible for the effect discussed. Maggini (1937) established that it can only result in significant increase in the color index for the rings in the case of extremely small elevations of the sun over their plane ($A \gtrsim 1.5^\circ$). It therefore is more plausible to associate the color of the B ring directly with the color of the surface of the ring particles. Although infrared observations (#10) show that the particles are covered with hoarfrost, the reflectivity of individual particles (#19) is not so high that it can be considered that the hoarfrost completely covers the individual particle. Also possible is

23

the fact that the color of the particle is affected by constant bombardment by micrometeorites and solar corpuscles.

#10. Infrared Spectrometry

Kuiper (1951) found that at $\lambda \sim 1.5$ microns, the reflectivity of the rings dropped significantly, and that the intensity of the spectrum was low for $\lambda > 1.5$ microns. Additional laboratory research by this same author showed that this spectrum is typical of a thin layer of hoarfrost deposited on dry ice ($t = -78^\circ\text{C}$). In terms of magnitude of absorption, this is the equivalent of a water filter $2/3$ mm in thickness. These facts were interpreted by the observer as the result of the presence of hoarfrost, or of snow, on the surface of the particles. Some years later Kuiper (1957 b) made a second series of observations with better equipment, and these observations confirmed the previous results.

Not too long ago the infrared spectrum of Saturn's rings was once again investigated by Moroz (1961) and by the team of Shnyrev, Grechushnikov, and Moroz (1964). The former investigated the integral radiation from Saturn, including the disk, and the widely opened rings, in the 0.9 to 2.5 micron range. The traces showed intensity maxima at 1.63 to 1.80 and 2.0 to 2.5 microns. Comparison with the infrared trace of Jupiter, obtained using the same instrument, led to the conclusion that these maxima are attributable to Saturn's rings, and not to its disk. The reflected spectra of snow and hoarfrost were studied as part of the program. Hoarfrost crystals are smaller than snow crystals, and are of the order of 0.1 mm, or smaller, in size. The infrared spectrum of the rings is closer to the hoarfrost spectrum.

Shnyrev, Grechushnikov, and Moroz used the infrared interferometric technique and obtained separate interference patterns for the disk and for the rings. The authors applied the Fourier transform to these patterns and constructed spectrograms of these objects (Figure 8a). The 1.4 micron band in the ring spectrum turned out to be wider than in disk spectrum. The intensity at 1.5 microns in the ring spectrum was lower than in the disk spectrum. Similar characteristics could be present if the ring particles consisted of ice, or were covered by ice.

On the other hand, Mertz and Coleman (1966), who used a spectrometer

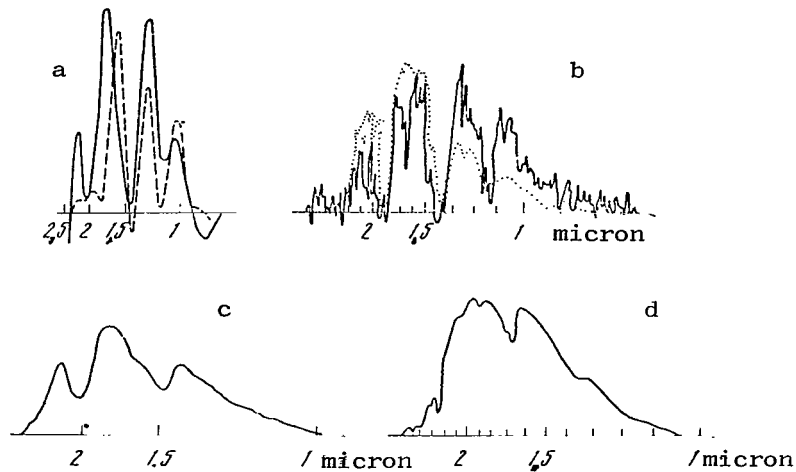


Figure 8. a - Infrared spectra of rings (solid lines) and of Saturn's disk (dashed lines), according to Shnyrev, et al. (1964); b - infrared spectrum of Saturn's rings according to Mertz and Coleman (1966); c and d - laboratory spectra of ice (hoarfrost) and paraformaldehyde (powder), according to Mertz and Coleman (1966).

with a Fourier transform (Mertz, 1965) coupled to a 61 inch telescope, are very hard pressed to find agreement between the ring spectrum and the ice particle hypothesis. These authors found heavy absorption in the ring spectrum at $\lambda = 1.66$ microns (Figure 8b), and this was ascribed to paraformaldehyde (the spectrum of reflection of the latter has a similar characteristic; see Figure 8d). The authors are not entirely confident that their results are correct because the observations were made when the ring openings were very small (16-17 October 1965, $A = 3.6^\circ$, $A' = 5.6^\circ$), so the fact that some part of the "spectrum of the rings" actually is attributable to the halo of the disk cannot be excluded. It is proposed that the observations be repeated during the next epoch of large ring openings.

As a matter of fact, the results obtained by Mertz and Coleman are extremely doubtful. First of all, the spectrum of the rings obtained by Shnyrev, et al (during large opening) showed no traces of absorption at 1.66 microns. Second, if one makes a graphical summation of the traces of the infrared spectra of rings and disk, one easily obtains the 1.66 micron minimum observed by Mertz and Coleman (as will be seen quite well in Figure 8a). We tend to the view that the effect of the scattered light from the disk was actually substantial during these observations, and that there is no basis

25

for the rejection of the ice particle (or of particles covered with a layer of ice) hypothesis.

It might appear strange that the layer of ice crystals has not yet evaporated. Kuiper (1951) anticipated this objection. Using the data in the International Critical Tables, he extrapolated the rate of evaporation of ice at the extremely low temperatures that could be present on the surface of the particles (near 60 to 80°K). It was found that when $T = 70^{\circ}\text{K}$ the evaporation rate is exceptionally low (the pressure of water vapor is of the order of 10^{-28} mm Hg). At the time of the observations (see #15, below) the information is that the temperature of the surface of the particles was about 65°K.

#11. Polarization.

Lyot (1929) found that the A and B rings were not identical in terms of polarization properties. Ring B is close to earth materials, but the A ring has many special characteristics.

The recent observations made by Dollfus (1963a) revealed that the light reflected by the B ring is partially ($1 - 6 \cdot 10^{-3}$) polarized in a plane passing through the sun and the earth. This type of polarization is in concordance with the conclusion that the particles are covered with ice crystals, or with the more general idea that the surface layer of a typical particle consists of some type of good reflecting powder. There also is partial polarization in a plane normal to that indicated above. This type of polarization indicated that the particles are elongated, or striated in the direction of their orbital motion. The characteristics of the polarization of the A ring are more complex.

#12. Change in Surface Luminance with Phase Angle.

Although the maximum phase angle at Saturn (the angle Sun-Saturn-Earth) is not in excess of 6.5° , the surface luminance of the rings changes very greatly with phase. The finding of the phase function of the luminance of the rings was the purpose of several series of photometric observations. In astronomy, observers usually express surface luminance in stellar magnitudes per unit area (per square second of arc, for example) and plot it on a graph as a function of the phase angle α . This graph is known as the phase curve. Knowledge of phase curves for Saturn's rings is as important as a knowledge of

/26

the light curves for eclipsing double stars. In both cases we obtain information that, after it has been deciphered, provides data on the features of structure beyond the limits of resolution of earth-bound telescopes.

The first systematic measurements of the surface luminance of Saturn's rings as a function of α were made photographically by Hertzsprung (1919), and visually by Schoenberg (1921) (with the aid of his "microphotometer"; see Schoenberg, 1917). Both observers used the center of the disk as the photometric standard. Hertzsprung obtained the surface luminance of the A and B rings individually, and Schoenberg obtained the mean luminance of the A and B rings (some subjective magnitude not strictly defined by the observer). Schoenberg was not satisfied with his results and later on made a second series of observations (Schoenberg 1933), using the same photometer. The second series differed from the first in many respects: (1) four filters (red, yellow, green, and blue) were used; (2) many more points near $\alpha = 0$; (3) the object measured was the surface luminance of the most intense zone of the B ring.

The observer found that the phase curves obtained using the different filters showed no systematic differences. This opened up the possibility of presenting Schoenberg's data in the form of a single phase curve less susceptible to random errors than the curves obtained when the filters were used. Complete tables of observations of surface luminance values were not published. Schoenberg's article contains but seven averages of the values for each filter, and indicates the number of observed values for each average. These averages make it possible to compute the mean weighted luminance for all four filters as a function of α (weight taken in accordance with the number of observed values for each filter). This mean visual phase curve for the B ring is one of the best to date. Its empirical equation is in the form

$$\beta_B(\alpha) - \beta_B(0) = 0.270 \lg \alpha - 0.213 \quad (12.1)$$

where

β_B is the stellar magnitude of the luminance* of the B ring (stellar

* The "stellar magnitude of luminance" β , frequently required in astrophotometry, is associated with the conventional surface luminance, b , by the relationship $\beta = -2.5 \log b + C$, where the value of the constant C depends on the units chosen. Specifically, if b is expressed in apostilbs ("white luxes"), and if β is expressed in stellar magnitudes per square second of arc, then $C = 13.92$

magnitude/ square second of arc);

α is the phase angle at Saturn (minutes of arc).

Here we have taken it that $\beta_B(0) = \beta_{\text{center}}$, where β_{center} is the stellar magnitude of the luminance of the center of the disk of Saturn. Eq. (12.1) provides a good approximation of Schoenberg's phase curve in the interval ($0^\circ 20' \lesssim \alpha \lesssim 6^\circ 30'$). We should point out that Eq. (12.1) reveals an interesting feature of the B ring phase curve; it is linear in the coordinates ($\log \alpha, \beta_B$).

More recent photometric measurements of surface luminance of the B ring as a function of α have been made by Lebedinets (1957) and Franklin and Cook (1965).

Lebedinets used the photographic photometry methodology in the form developed by Barabashov in the Khar'kov Observatory. He found 20 B ring surface luminance values as functions of α between $0^\circ 16'.6$ and $6^\circ 0'$. The results are quite dependable, although random scattering of the points is quite broad.

Franklin and Cook measured the total luminous flux for Saturn, and for the widely opened rings, and did so photoelectrically. Four filters, yellow, blue, ultraviolet, and red, were used. In order to evaluate the contribution of fluxes from the disk and from the A and B rings, the observers simultaneously obtained a series of large-scale, photometrically calibrated negatives of Saturn on effective wavelengths extremely close to those for the photoelectric observations. These latter were obtained by using another telescope. The photographs taken with the red and ultraviolet filters were unsatisfactory, hence the observers selected only the yellow and blue (some 20 of the best negatives in each color).

Without going into further detail, let us simply point out that the measurement of the optical density of the rings and of the disk appearing on the negatives selected made it possible to determine (as a function of α) the percentage of luminous flux attributable to the disk and to the rings individually. Luminances then were expressed in B and V units on the UBV scale.*

* See the footnote on page 17.

An obvious shortcoming in the observations made by Franklin and Cook is the indirect method they used to obtain the surface luminance of the rings. The calculation of final luminance values required many intermediate reductions that could have introduced systematic errors, and the use of photographic photometry increased significantly the probable errors in the measurements. In our view, the best way to indicate the magnitude of the probable errors would be to construct A and B ring luminance phase curves directly from the photographic data. The authors did not do this, unfortunately, and all of this detracts from the confidence one has in their results, despite the fact that the deviation of the computed points from the meancurve is small. The advantage of the work done by Franklin and Cook however, lies in the great number of observed luminance values that are more or less uniformly distributed over the entire phase curve.

The B ring phase curves obtained by Lebedinets, like those of Franklin and Cook, are in good concordance with Schoenberg's curve (1933), so it can be asserted that the basic features of the B ring phase curve now are quite well known. At the same time, it is extremely desirable to have at least one series of purely photoelectric measurements of the surface luminance of the A and B rings individually, because such a series would be able to detect finer effects that now are masked by random and systematic errors. /28

Let us hasten to add that there is no satisfactory A ring phase curve in existence, and the situation with respect to the crape ring is even worse, because there is nothing available that remotely resembles precise measurements of its surface luminance.

Turning once again to the observed B ring phase curve, we encounter the need to reduce all the curves to a single zero [or to a single amplitude of phase changes in the interval $(0, \alpha_{\max})$]. The significant difficulty here is that no one has observed the ring when $\alpha = 0$, so the only way the surface brightness, $b_B(0)$, of the B ring when $\alpha = 0$, can be obtained is by extrapolation. Schoenberg (1933) took it that $b_B(0) = b_{\text{center}}$, where b_{center} is the brightness of the center of the disk, but in earlier work he took $b_B(0)$ as $1.10b_{\text{center}}$.

The data provided by Franklin and Cook, including a certain number of points extremely close to $\alpha = 0$, show that evidently $\beta_B(0) \approx \beta_{\text{center}} 0^m.06$,

where β is the stellar magnitude of the brightness (see the footnote page 22.)

Taking all of this into consideration, we can reduce all B ring phase curve observations to a single zero by comparing them with Eq. (12.1), and basing the comparison on the assumption that $\beta_B(0) = \beta_{\text{center}}$. Today there is a more basic assumption, namely, that $\beta_B(0) = \beta_{\text{center}} - 0^m.06$, in which case, rather than Eq. (12.1), we come to the expression

$$\beta_B(\alpha) - \beta_B(0) = 0^m.270 \log \alpha - 0^m.153 \quad (12.2)$$

where α , as before, is expressed in minutes of arc. Now let us change the ordinates of the Lebedinets and Franklin and Cook phase curves in such a way that for a single, definite value of α , say 3° , they have $\beta_B(\alpha)$ values identical with those of Eq. (12.2). We arrive at the curve shown in Figure 9a. As will be seen quite readily, the phase curves derived by all the authors are in good concordance each with the other.

The phase curve shape is very characteristic. The curve can be broken down, somewhat conventionally, into three sections: (1) the initial section ($0^\circ \lesssim \alpha \lesssim 0^\circ 25'$) with a steep, almost linear rise in the stellar magnitude with α ; (2) the transition section ($0^\circ 25' \lesssim \alpha \lesssim 3^\circ$); and (3) the saturation section, which, once again is almost a straight line, but has a phase coefficient that is much smaller than is the case for the initial section.

Let us point out further the extreme acuteness of the maximum for the brightness $\alpha = 0$. This property stands out particularly sharply if polar coordinates are used to plot the phase function curve (Figure 9b). It suggests that within 30 the narrow interval of phase angles in which the ground observer can investigate the reflectivity of the rings the contribution of multiple scattering to the resultant brightness is small. Actually, in the majority of systems of multiple scattering encountered in nature, the tendency is toward severe smoothing of the first order phase function maximum. The sharper the maximum, the firmer the basis for supposing that first order scattering is "operating" for the most part in the particular direction. In order to establish whether or not this argument is applicable to Saturn's rings, we must know the mechanism responsible for the observed change in brightness of the rings with phase. As will be pointed out in #18, this mechanism is the mutual shading of the particles, one by the other. In this case multiple scattering is not sharply directional

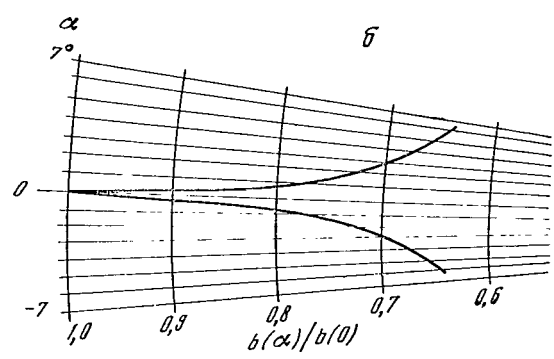
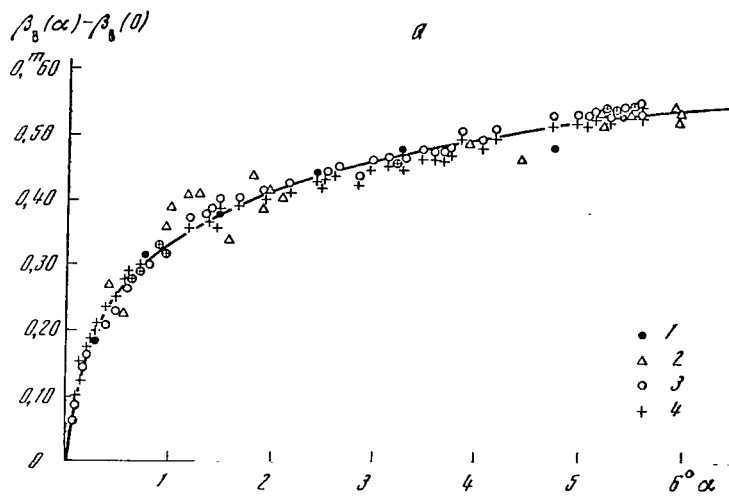


Figure 9. Observed B ring phase curves (a) reduced to a single zero [1 - Schoenberg (1933; mean weighted values for four filters); 2 - Lebedinets (1957); 3 and 4 - Franklin and Cook (1965; blue and visual stellar magnitudes, respectively)]; luminance of B ring (σ) as a function of the phase angle α (in polar coordinates). The extreme acuteness of the maximum when $\alpha = 0$ forces one to conclude that in this direction the contribution of scattering of the highest orders to the total brightness is small.

in nature. Its role reduces to one of attenuating the deepness of the shadows, or, and this is the same thing, of reducing the sharpness of the peak when $\alpha = 0$. Quantitative evaluations lead to the conclusion that in the region of the peak shown in Figure 9b the contribution of multiple scattering is not in excess of 10 percent, something that henceforth will simplify greatly our interpretation of observed facts.

#13. Other Photometric Data

Schoenberg (1921) detected a systematic difference in the luminance of the eyes of the rings. The eastern eye was steadily more luminous than the western for one whole period of observations (1913-1918). The mean difference in luminances was $0^m.039$. This effect was confirmed by Fesekov (1926, 1927, 1928), who found the eastern eye to be more luminous than the western by from $0^m.06$ to $0^m.20$. Difference in luminances decreased with increase in ring opening.

Fesekov used a reversing prism to show that this effect is not physiological in nature. The direct cause of the effect is unknown, but it should be remembered that the eastern eye differs from the western in terms of time of insolation. The particles of the eastern eye only come out of the shadow of the ball of Saturn, whereas the region of the western eye is occupied by particles subjected to the effect of direct solar radiation for approximately half the period of revolution.

The dependence of the surface brightness of the rings on the angles of elevation of the sun and of the earth, A and A', above the plane of the rings was the subject of wide-ranging investigation by Camichel (1958), who used the photographic method, and by Maggini (1937), who used the photoelectric method.

Camichel's research was conducted under excellent astronomical climatic conditions from the Pic du Midi Observatory. The series of photographs (taken with a yellow filter) cover the period 1943-1957, or approximately half of the orbital period of Saturn. The change in A and A' was from between 2 to 3° to between 26 to 27° . Resolution, estimated by photographing double stars, was $0''.4$. Microphotographs taken along the major axis of the rings detected a considerable amount of residual luminance in the Cassini division. This indicates that the influence of halation is not negligibly small. Figure 10 shows the

31

luminance of the A and B rings, as corrected by us for the phase dependence by using Eq. (12.1), and plotted as a function of A. Despite the considerable scattering of the points, the reduction in the B ring luminance with reduction in the angle of elevation A, is readily seen. The other ring shows no marked effect.

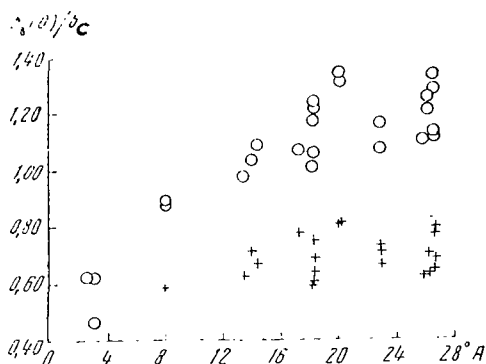


Figure 10. Luminance of the A (crosses) and B (circles) rings as a function of the angle of elevation of the sun above their plane (Camichel, 1958).

In this regard, let us note the visual results obtained by Barnard (1909), in accordance with which the A ring can be more luminous than the B ring when openings are small.

The luminance values obtained by Camichel near $A = 2$ to 3° are significantly underestimated because of halation, so are not completely dependable. Maggini studied the region of very small values of A photoelectrically. The results (also corrected by us for phase effect) are shown in Figure 11 as a function of A. A decreased from $2^\circ 06'$ to $1^\circ 01'$ over the period of observation and A' increased from $0^\circ 38'$ to $3^\circ 01'$. Maggini noted a sharp decrease in ring luminance with reduction in A. Dependence of luminance on the angle of elevation of the earth, A', was not observed. This fact, as well as the increase in the visible opening over the period of observation, shows that the darkening of the rings with reduction in A is a real effect, and is not the result of irradiation. The correctness of this conclusion can be confirmed independently by the simultaneous increase in the color equivalent for the rings (curve J in Figure 11). At the same time, no definite dependence of J on A' was observed. Coloration of the rings at extremely small values of angle of elevation of the sun probably is indicative of the stratification of the ring particles in terms of size along the z-coordinate; the percentage of small particles increases with distance

from the mean plane of the rings. In other words, it is possible that the rings are surrounded by their own type of "atmosphere." The fact that it can contain a gas component is not precluded. We shall return to this question in #23.

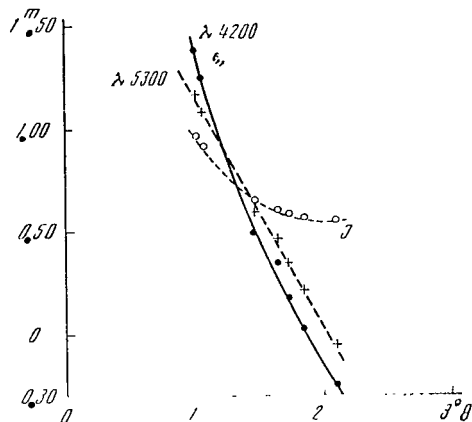


Figure 11. Color equivalent $J = m_{4200} - m_{5300} + 0^m.75$ and ring brightness when $\lambda_{\text{eff}} = 4200$ and 5300 \AA as a function of the angle of elevation of the sun (processed Maggini data, 1937).

Camichel not only found a dependence of surface luminance on angle of elevation A , but also some interesting azimuthal effects: (1) the surface luminance of the B ring decreases from the eyes to the minor axis; (2) there is a systematic difference between the nearest and farthest (with respect to the earth) branches of the A ring; the nearest branch is more luminous in the case of the eastern eye, and weaker in the case of the western.

#14. Optical Thickness*

33

There are two methods that can be used to assess this important parameter, one that characterizes the degree of transparency of the rings: (a) observations of the visibility of Saturn's disk through the rings; (b) observations of the occultations of stars by the rings.

The starting point for method (a) is the obvious relationship

* Let us recall that the optical thickness of a plane-parallel layer for a normally incident beam can be defined by the relationship $\tau_0 = -\ln(I/I_0)$, where I_0 and I are light intensities before and after the beam has passed through the layer. In other words, $(I/I_0) = \exp - \tau_0$.

$$b' = b \exp - \left(\frac{\sin A + \sin A'}{\sin A \sin A'} \tau_o \right) \quad (14.1)$$

where

b' is the visible surface brightness of that part of Saturn's disk covered by the ring under consideration and illuminated by the sun through this ring;

b is the surface brightness of that part of Saturn's disk when it is not covered by the ring and is illuminated by the sun directly;

A and A' are the angles of elevation of sun and earth above the plane of the rings;

τ_o is the optical thickness of the ring in a direction normal to its plane.

Camichel's data (1958) permit the use of this formula to evaluate $\tau_o A$, the optical thickness of the A ring. This observer found a mean of $b_A = 0.57b_e$, where b_A and b_e are the surface brightness of the A ring and of Saturn's equatorial zone, respectively. The A ring is partially transparent, and Saturn's polar zone can be seen through it. This creates additional brightness corresponding to $0.08b_e$. Polar zone brightness is equal to $0.87b_e$, when not occulted. From whence, and in accordance with Eq. (14.1)

$$\begin{aligned} \tau_{oA} &= 2.30 (\lg b - \lg b') \frac{\sin A \sin A'}{\sin A + \sin A'} = \\ &= 2.30 (\lg 0.87 - \lg 0.08) \frac{0.429 \cdot 0.426}{0.429 + 0.426} \approx 0.5, \end{aligned} \quad (14.2)$$

where

0.429 and 0.426 are the mean values of the sines of angles A and A' at the time of the observations used here.

Evaluation of Eq. (14.2) will yield a correct order of magnitude, but can contain some degree of error attributable to halation, and for which Camichel's data were not corrected (see #13). Let us take it that the minimum contrast in brightness that could be observed in Camichel's observations was about 0.05. Accordingly, he was able to see the polar zone of Saturn through the A ring when $b' = 0.05b_A = 0.028b_e$. Substituting this in Eq. (14.1), we obtain $\tau_{oA} = 0.7$.

In all probability, the interval

$$0,5 \leq \tau_0 \leq 0,7 \quad (14.3)$$

will provide a quite correct representation of the value of the optical thickness of the A ring, but it is desirable to make further assessments, precisely corrected for halation.

Method (b), as has been pointed out, is based on observations of occultations of stars by the rings. To date the only types of such observations are visual ones. They have been made mostly by amateurs using low and medium powered instruments ($D \leq 50$ cm). Here we will consider the case of good images (for details see Bobrov, 1962).

Let us suppose that the radial distribution of the intensity in the image of a star is identical to that in a diffraction picture of a point source, but that the first minimum occurs at $r_t = r_1 + t$, where r_1 is the first diffraction minimum, and t is the angle of turbulence. Let b_r be the surface brightness of the zone of the ring occulting the star, and let ϵb_r be the minimum brightness of the image of the star needed in order for the eye to distinguish it through the ring. Let us note that the radius of the image of the star visible through the ring is $r_* < r_t$. It is obvious that

$$\bar{b}_*(G) = \bar{b}_{t_0}(G_0) \frac{G_0^2}{G^2} \exp -(\tau_0/\sin A'); \quad (14.4)$$

where G_0 is the equipupillary magnification;

G is the magnification resolving the image of the star;

$\bar{b}_{t_0}(G_0)$ and $\bar{b}_*(G)$ are the mean brightness of the star when not occulted (G_0 magnification), and during occultation (G magnification), respectively.

On the other hand

$$\bar{b}_*(G) = \epsilon b_r(G_0) \frac{G_0^2}{G^2}. \quad (14.5)$$

Remembering that

$$r_* = p_e/2G, \quad (14.6)$$

where p_e is the angle resolved by the naked eye, substituting Eq. (14.5) in Eq. (14.4), and changing from brightnesses to their stellar magnitudes per square second, we obtain

$$\tau_0 = \frac{\sin A'}{1,036} [\beta_K - m_{t_0} - 2,5 \lg \epsilon + 5 \lg G + 2,5 \lg / (r_*/r_t) - 10^m 32]. \quad (14.7)$$

Here the function $f(r_*/r_t)$ signifies the percentage of luminous flux from the part of the stellar image bounded by radius r_* . In Eq. (14.7) we took it that $p_e = 120''$, based on the experiments made by Maksutov (1946) and Pavlov (1961); that m_{t0} was the stellar magnitude of the star (at the zenith). The minimum contrast ϵ depends on the brightness of the background. Sytinskaya (1949) made the corresponding laboratory investigations.

The value of t during the observation can be estimated by using the Danjon-Coudé image quality scale, bearing in mind that the case of good images is satisfied by the condition that $(t/r_1) \lesssim 1/2$.

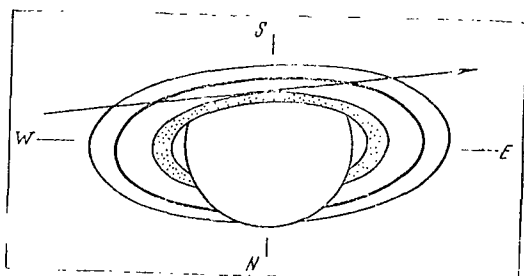


Figure 12. Path of a star during its occultation by Saturn's disk and rings on 28 April 1957

Needless to say, the assumptions on which Eq. (14.7) are based are but a rough approximation of occultation conditions. This is why two of its shortcomings will be found in all of the available observed data in which the equation was used. First of all, the computed value of τ_0 turns out to be somewhat exaggerated as compared with the value obtained through method (a). The difference disappears if we change the last term in the equation, putting it equal to $-10^m.81$. This means that only 54 percent of the luminous flux from the star is concentrated in the central circle of the turbulent image of the star, rather than 84 percent (as is the case in the classical diffraction pattern, and as we assumed in deriving Eq. (14.7)). Moreover, this is not the only possibility. Strictly speaking, Eq. (14.1), on which our estimate of τ_0 through method (a) is based, is correct only for a point source of light, whereas Saturn's disk is an extended source. Disregard for this feature can lead to exaggerating the true value of τ_0 and it is possible that herein lies the reason for the discrepancies discussed.

Second, the numerical values of τ_0 give a greater random scatter. It is likely that the above computed concentration of luminous flux is 54 percent

only in the middle, and there could be cases when there could be a significant deviation from this magnitude.*

At the same time, observation of a star occulted by the rings undoubtedly is a solid and fruitful method to use to investigate the optical thickness of the rings, their radial structure, and the like. The advantages of this method have not yet attracted the attention of the professional observers.

One of the most interesting of the occultations occurred on 28 April 1957. The path of the star (BD - 20°4568; 8^m.0) can be seen in Figure 12. The phenomenon was observed visually by Westfall (see Heath, 1958) in a 20 inch refractor (magnification 320). The observer did not have a photometer and estimated the change in the magnitude of the star during the occultation by eye. We have attempted, in Figure 13, to show these changes graphically in accordance with the qualitative description given by Westfall. His observations are important in that they demonstrated for the first time the partial transparency not only of the A ring, but of the B ring as well (at least of its outer zone and of a small part near the center). Figure 13 also shows that the optical thickness of the A ring changes markedly with r, decreasing in the central zone, and, it seems possible, having narrow lanes near the outermost boundary of the entire ring system.

/36

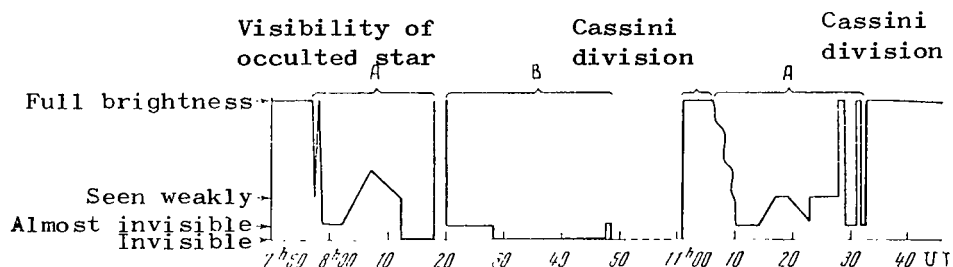


Figure 13. Schematic representation of the change in the brightness of a star during its occultation by Saturn's rings on 28 April 1958, observed visually by Westfall.

Let us attempt to estimate τ_{OB} by comparing Westfall's results for the A ring with the results for the B ring. Westfall observed zones in both rings that were not transparent for the star. These zones were wider in the B ring. Zones that were partially transparent for the star were observed in both rings.

* Note that the values of the magnitudes p_e and ϵ can change significantly, depending on observation conditions.

They were narrower in the B ring. We can conclude, therefore, that in general τ_{OB} is higher than τ_{OA} , but not much. If τ_{OA} is 0.5 to 0.7 [see Eq. (14.3)], we can take the average for the B ring as

$$\tau_{OB} \sim 1. \quad (14.8)$$

Some B ring zones are even more transparent.

The methods described here cannot be applied to the C ring because of the specific difficulties that arise in connection with its lack of brightness. The values adopted for τ_{OC} all are based on the old observation made by Barnard (1890). These were estimates of the attenuation of the brightness of Iapetus as a function of time in the shadow of the C ring. Cook and Franklin (1958) made a detailed analysis of this observation and concluded that τ_{OC} increases monotonically with distance from the center of Saturn from 0.0 for $9''/3$ to 0.18 for $13''.2$.

#15. Radiometric and Radioastronomical Data

/37

Kuiper (1951) estimated the equilibrium temperature of a typical particle of Saturn's rings to be between 60° and 70°K . It was supposed that the particles were covered by hoarfrost and that they were screened periodically from the sun by each other, and by the ball of Saturn. At this low temperature the Planckian maximum of intrinsic heat radiation of the particle will be 41-48 microns, that is in the wave band that is longer than the region of the transmission window for the earth's atmosphere. Consequently, heat radiation from the rings at infrared wavelengths can be observed only by extra-atmospheric observations, and such observations have not yet been made.

Conversely, radioastronomical observations of Saturn make it possible, in principle, to detect heat radiation from the rings without going beyond the limits of the earth's atmosphere. Moreover, radioastronomical observations can be used to obtain estimates of the optical thickness of the rings at radio wavelengths, and these, in turn, can be used to make a ready determination of the typical size of a particle (we will recall that when $2\pi\rho/\lambda < 1$, where ρ is the radius of the particle, the transmission for the system increases sharply).

Unfortunately, present data on radio radiation from Saturn is such that one cannot do these tasks without ambiguity. Still, discussion of the available data is of interest.

Radio radiation from Saturn has been measured by Kuzuza et al. (1965), at $\lambda = 8$ mm, by Welch et al. (1966), at 1.53 cm, by Cook et al. (1960), at 3.45 cm, by Hughes (1966), at 6.0 cm, by Rose et al. (1963), at 9.4 cm, by Drake (1962), at 10.0 cm, by Davies et al. (1964), at 11.3 cm, and by Davies and Williams (1966), at 21.2 cm. The values for the brightness radio-temperature of Saturn, T_b , obtained by these authors are shown in Figure 14 as a function of the wavelength (the open circles; the vertical lines show probable errors in the determinations as cited in the articles). As will be seen, T_b rises with $C\lambda$, although the considerable scatter in the points does not enable us to fix the law of rise with confidence. The reason for the rise is the greenhouse effect (the larger λ , the deeper the layers of the atmosphere from which the radiation is being recorded), or the presence of a nonthermal component (radiation from the radiation belts, similar to that observed for Jupiter). If the second possibility is what occurs, radio radiation from Saturn definitely should be polarized, and this is what has been found by Rose et al. (1963), at 9.4 cm. These authors reported strong ($20 \pm 8\%$) polarization with orientation of the electric vector parallel to the axis of rotation of the planet (in the case of the corresponding radiation from Jupiter the electric vector is perpendicular to the axis of rotation; Zheleznyakov (1964) showed that the difference in orientation can be explained by the effect of the rings on the shape of the radiation belts). However, observations made by other radio astronomers have not confirmed Rose's results. For example, Davies et al. (1964), observed no polarization at 11.3 cm, and arrived at the conclusion that its upper limit is less than 6 percent. So, the question /38 is not completely settled, and further observations are needed in order to resolve it.

But whatever the nature of the rise in T_b with $C\lambda$, it can be expected that when λ is small enough the radio brightness temperature of Saturn should be close to the infrared brightness temperature. Today we can place the old results obtained by Pettit and Nicholson (1924), and by Menzel, Coblentz, and Lampland (1926), which yielded $T_b \sim 125^\circ$ to 130°K , as well as more recent observations by Murray and Wildey (1963), and by Low (1964, 1966), at infrared wavelengths. Murray and Wildey used a germanium photoresistance on a 19-inch reflector and worked in the transmission window between 8 and 13 microns. No traces of infrared emission from Saturn were found, so it follows that in this band of

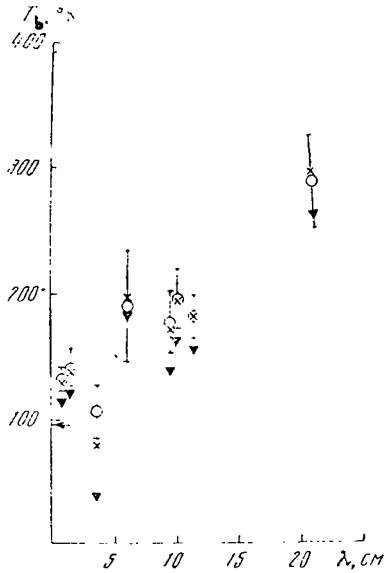


Figure 14. Brightness temperature of Saturn at radio wavelengths. The circles are for temperature normalized for the full disk of Saturn (the "cold, completely transparent" rings hypothesis). The crosses and triangles are for temperature calculated through Eq. (15.2) when $T_K = 30^\circ$ and 65°K (the "warm, partially transparent" rings hypothesis). The horizontal arrow is the infrared brightness temperature at $\lambda = 10$ and 20 microns (Low, 1964, 1966) normalized for the part of Saturn's disk not screened by the rings.

Let us turn now to the question of the thermal emission from the rings. Low (1966) notes that his value for the brightness temperature of Saturn is corrected for absorption in the rings, which, in his words, proved to be very much colder than Saturn's disk. He does not provide numerical values for ring temperatures, however. So far as the radio wavelengths are concerned, all of the radioastronomers proceed from the assumption that the emission source is the total area of Saturn's disk when they make the transition from the measured flow of the emission to T_b . This, however, ignores the visible area of the rings, not only in the eyes, but in front of the disk as well. This is the equivalent

wavelengths $T_b < 105^\circ\text{K}$. Low measured the emission from Saturn with an infrared photometer in the Cassegrain's focus of an 82-inch reflector in the McDonald Observatory at $\lambda = 10$ and 20 microns. This time emission was found. The corresponding T_b values were $93 \pm 3^\circ\text{K}$, confirming the correctness of the conclusions reached by Murray and Wildey, and showing that the old estimates of the infrared brightness temperature of Saturn apparently were exaggerated.

The mean of Low's results is shown by the horizontal arrow at the axis of ordinates in Figure 14. As will be seen from the figure, all T_b estimates obtained at radio frequencies are higher than this value, but it still is hard to say whether the temperature found by Low is the asymptote to which the radio temperature tends with reduction in λ . The data still are too sparse for this.

39

of the "cold, completely transparent" rings. In the general case, that of the "warm, partially transparent" rings, however, the mean radio brightness temperature of the Saturn plus rings system can be found through the expression (with an accuracy up to first order scatter)

$$\bar{T} = \frac{1}{x+y} \{x[1 - \exp - (\tau_0/\sin A')] T_r + [y + (1-y) \exp - (\tau_0/\sin A')] T_d\}, \quad (15.1)$$

where

- T_r and T_d are the radio temperatures of Saturn's rings and disk;
- x is the visible area of the rings (in the eyes and in front of the disk);
- y is the area of that part of Saturn's disk not screened by the rings;
- τ_0 is the optical thickness of the rings for a given wavelength;
- A' is the angle of elevation of the earth above the plane of the rings.

The magnitudes x and y are expressed in percentages of the total area of Saturn's disk. They have been tabulated by Schoenberg (1929) as a function of A' .

It is not difficult to see that $\bar{T} = T_b/(x+y)$, where T_b is the brightness temperature cited by the radio astronomers. Hence, the radio temperature of the disk is

$$T_d = \frac{T_b - x[1 - \exp - (\tau_0/\sin A')] T_r}{y + (1-y) \exp - (\tau_0/\sin A')}. \quad (15.2)$$

We used Eq. (15.2) to find T_d values for two assumptions, $T_r = 65^\circ\text{K}$ and $T_r = 30^\circ\text{K}$ (with τ_0 taken as equal to 0.8), in order to see how existing radio measurements agree with the "warm, partially transparent" rings hypothesis. The corresponding points are shown by the triangles and crosses in Figure 14.

As will be seen from the figure, in all but one case the computed values of T_d are higher than the infrared temperature of Saturn as found by Low; that is, they agree with the "warm, partially transparent" rings hypothesis when $T_r = 30^\circ\text{K}$, as well as when $T_r = 65^\circ\text{K}$. The point where they are not in agreement ($\lambda = 3.45$ cm) is that found by Cook et al. (1960), the first time an observation had /40 been successful in detecting radio emission from Saturn. Perhaps this is the explanation of why Cook's point in Figure 14 clearly "breaks" downward, as compared with adjacent points. It would appear that the measurement provided an exaggerated value for T_b . In fact, one should expect $T_b \sim 140^\circ\text{K}$ at $\lambda = 3.45$ cm. Substituting this figure in Eq. (15.2), we find 75°K and 116°K for T_d when

$T_r = 65^\circ\text{K}$ and 30°K , respectively. It can be taken therefore, that when $T_r = 30^\circ\text{K}$, the "warm" rings hypothesis satisfies all the available observational data, remembering that the rings are no more transparent at the radio wavelengths than they are at the optical wavelengths. $T_r = 65^\circ\text{K}$ is too high a value, although this conclusion is based on just one point in Figure 14, Cook's point.

At the same time it should be emphasized that the 30°K value obtained here for the temperature of the rings is unjustifiably low, so the fact that Saturn's rings are more transparent at radio wavelengths than they are at optical wavelengths cannot be precluded. In fact, all that need be done to satisfy all existing data is to reduce τ_o to 0.4 when $T_r = 65^\circ\text{K}$. Further observations are needed in order to arrive at a final answer to this problem. The most effective observations would be of two types. The first would involve obtaining long series of measurements of T_b as a function of A' . The second would involve observations with high angular resolution, the purpose being to establish the shape and size of the radio emitting region, and the distribution of radio brightness in it. If it should develop that Saturn, like Jupiter, has radiation belts, the question of the temperature of the rings will call for a new discussion, different from that undertaken in the foregoing.

IV. Model of the B Ring. Properties of a Typical Particle.

#16. Absolute Surface Brightness of the B Ring

The preceding chapters have dealt with observational data. Let us now set about analyzing all of this primary information. As before, the primary object of our attention will be the B ring. Let us, as our first step, compute the absolute surface brightness, $b_B(0)$, of the most intense zone of the B ring when $\alpha = 0$. Knowledge of $b_B(0)$ will make it possible to estimate the spherical albedo* of a particle and to draw some conclusions as to the particle's natural phase function. The term "absolute brightness" will be used in the sense of "brightness in b_o units," where b_o is the brightness of an absolutely white, orthotropic area, positioned normal to the incident solar radiation at the mean distance of Saturn.** We shall express b_o in a visual system.

As was noted in #12, not too much credence can be placed in the extrapolation of the brightness of the ring to $\alpha = 0$. The most reasonable thing to do is to represent the value as

$$\beta_B(0) = \beta_c - 0.06, \quad (16.1)$$

where β is the brightness, expressed in stellar magnitudes (see footnote on p. 22); c is the center of Saturn's disk. Converting the magnitudes in Eq. (16.1) into conventional brightnesses, we obtain

$$b_B(0) = 1.06b_c. \quad (16.2)$$

Thus, the task is reduced to finding b_c in b_o units. It should be noted /42 that we consider the b_c used in Eq. (16.2) as the photometric standard to be a magnitude that is completely stable with respect to Saturn's axis of rotation, and with change in angles A and A' . This stability is not absolute, of course, but the many observations already made indicate that when the rings are wide open, b_c is stable enough, as a rule, to serve as a good photometric standard.

* Spherical albedo is a dimensionless magnitude equal to the ratio of the luminous flux scattered in all directions by the body to the luminous flux incident on it (given the condition that the body is illuminated by a beam of parallel rays). The analogous magnitude for a plane area is called the plane albedo. If the rays are incident on the area in a direction normal to it, one can then speak of the plane-normal albedo.

** Brightness, expressed in b_o units, is also called the "luminance factor," or "visible albedo," in astrophotometry.

Moreover, in our calculations b_c is only an intermediate magnitude. We will, in the end, express $b_B(0)$ in b_o units, and b_o is in fact stable.

Absolute measurements of b_c were made by Sharonov (1935, 1939), visually and photographically, and by Lebedinets (1957) photographically, by comparing this magnitude with the brightness of a white screen illuminated by very weak solar radiation. Brightness was reduced to a visual system in the photographic work done by Sharonov (1939). Lebedinets used four filters (red, yellow, green, and blue) and obtained the respective four b_c values. From these one can deduce a single b_c value in a visual system, proceeding from the standard curve for visual acuity, and the effective wavelengths for the filters. This procedure results in the data listed in Table 4.

TABLE 4

Observer	Method	b_c/b_o
Sharonov (1935)	Visual	0.30
Sharonov (1939)	Photographic	0.68
Lebedinets (1957)	Photographic	0.48

Absolute measurement techniques are complicated, and involve many intermediate operations with all of the systematic and random errors inherent in such operations, the magnitude of which it is difficult to estimate. This is precisely why the divergence in the b_c/b_o values listed in Table 4 is so great.

But one can readily calculate b_c/b_o independently, and estimate the probable error in the calculations, by starting with the visual stellar magnitude of Saturn (without the rings) m_p , the area of Saturn's disk ω (in seconds of arc), and the darkening toward the limb of Saturn's disk, and which can be expressed by the ratio \bar{b}/b_c , where \bar{b} is the mean brightness of Saturn's disk.

We obtain

$$\lg (b_c/b_o) = 5,57 - 0,40m_p - \lg \omega - \lg E_{\odot} - 2 \lg R_p - \lg (\bar{b}/b_c), \quad (16.3)$$

where E_{\odot} is the brightness of an orthotropic, absolutely white surface placed 43 at a distance from the earth normal to the incident solar radiation (outside the earth's atmosphere); R_p is the mean distance of Saturn from the sun.

The value of \bar{b}/b_c , found from observations of the darkening toward the limb of Saturn (Schoenberg, 1921; Barabashov and Chekirda, 1952; Lebedinets, 1957; Camichel, 1958), has a mean of $0.66 \pm 5\%$; $m_p = + 0^m.89 \pm 7\%$; $E_\odot = 1.35 \cdot 10^5$ lx $\pm 5\%$ (both values taken from Russel, 1916); $\omega = 270''$ (Rabe, 1928); $R_p = 9.54$ AU. The addend 5.57 is based on Fabry's formula for a stellar magnitude of 1 lux. The probable error is 5 percent.

Substituting all of these magnitudes in Eq. (16.3) will give $(b_c/b_o) = 0.62 \pm 22\%$, and, as a result

$$\frac{b_B(0)}{b_o} = 0.65 \pm 22\% = 0.51 - 0.79. \quad (16.4)$$

The middle of the interval is very close to the result obtained in Sharonov's second effort.

#17. Model of the Ring. Albedo of a Particle.

The spherical albedo* of a typical ring particle can be obtained by using the value $b_B(0)/b_o$ from Eq. (16.4) if we know the magnitude of the phase integral, q (expressing the angular distribution of the light scattered by the particle) and if we have selected some model of the ring. Two alternative models can exist. One of the models has properties such that at any point on the ring normal to its surface one will find no more than a single particle

$$z_o \approx 2 \rho \quad (17.1)$$

where z_o is the ring thickness; ρ is the particle radius. It is not shown as a true equality because the particles can complete small oscillations around the middle positions. We shall call this model a "one-particle thickness system."

The alternate model can be written by the expression

$$z_o \gg \rho \quad (17.2)$$

This is a "many-particle thickness system." The inequality of Eq. (17.2) signifies that the inclinations of the particle orbits to the plane of the ring are not very small. That is,

$$i \gg \frac{\rho}{r} \quad (17.3)$$

where i is the mean inclination; r is the mean radius of the particle orbit.

* See footnote, p. 39.

Recognizing that $\tau_o \sim 1$, we see that the Eq. (17.2) model can be characterized /44 by frequent collisions between the particles. Jeffreys (1947b) drew attention to the fact that the collisions are in part inelastic. The energy dissipation that takes place as a result of nonideal elasticity of collisions results in a secular reduction in inclinations and eccentricities in particle orbits. Calculations led Jeffreys to the conclusion that over a period of time that was short as compared with the age of the solar system, Saturn's rings should have been transformed into a one-particle thickness system. But, as will be seen in Chapter V, the data from observations quickly indicate in favor of the many-particle thickness system. Chapter VI will take up the possible reason for the non-concordance between Jeffrey's result and the real ring structure. We will not, at this point, opt in favor of either model.

(a) One-particle thickness system. The upper limit of the spherical albedo, a_{\max} , is equal to one for visual rays. This is the case for microscopic dielectric particles. They will be particles of ice (#10) in the case of Saturn's rings. But the very concept of rings consisting only of microscopic particles encounters very serious difficulties. One of the major difficulties is cosmogonic in nature. Microscopic particles would experience the strong influence of planetocentric radiative braking, which is analogous to the atmospheric braking of artificial earth satellites and which would force the particles to fall into the central body (the planet). This problem was reviewed by Radziyevskiy (1952), who derived the formula

$$t = 0.95 \cdot 10^7 \rho R^2 \delta \ln(r_o/r_t), \quad (17.4)$$

where ρ is the particle radius (cm); δ is the particle density (g/cc); R is the distance of the central body from the sun (AU); t is the time interval (years) during which the radius of the circular orbit of a particle will decrease from r_o to r_t . Applying Eq. (17.4) to Saturn's rings, Radziyevskiy introduced a correction factor that took into consideration the shielding of the particle from direct solar radiation by the ball of Saturn, and by other particles. The true value of t turns out to be greater than that computed through Eq. (17.4) by a factor of approximately three.

Schoenberg (1933) was of the opinion that ρ could be 3.6 microns. Franklin and Cook (1965) arrived at 310 microns in their "Model II." Substituting these

values for ρ in Eq. (17.4), and taking $\delta = 0.9 \text{ g/cm}^3$ (ice), $R = 9.54 \text{ AU}$, $r_o = 14 \cdot 10^4 \text{ km}$ (the present outer limit of the A ring), and $r_t = 7 \cdot 10^4 \text{ km}$ (the present inner limit of the C ring), we obtain $6 \cdot 10^5$ years and $5 \cdot 10^7$ years, respectively. In other words, even if $\rho = 310$ microns, all of the ring material should have undergone complete renewal over the period of time that the solar system has been in existence ($\sim 5 \cdot 10^9$ years) some 100 times! Another possibility (also of slight probability) is that the rings are several orders of magnitude /45 younger than any typical body in the solar system.

Thus, we have eliminated from further consideration microscopic particles, and will now proceed to look into particles of macroscopic size ($\rho \gtrsim 3 \text{ cm}$). It can be expected that the action of micrometeorites and solar corpuscular radiation would have left the surface layer of this sort of particle very rough, and that it would resemble the moon's surface layer (somewhat similar to "castles in the air," "lichens," and the like). Consequently, the value close to that of the phase integral for the moon ($q_p = 0.585$), can be taken for the phase integral, q , for the particle. It also is natural to suppose that the surface layer is thick enough for $\tau_o = \infty$. Moreover, we know that the brightness of the ring in opposition is $[b_B(0)/b_o] \approx 0.65$. Let us recall that we do have a case in the one-particle thickness system when $\tau_o = \tau_{oB} \approx 1$. The indicatrix for the individual particle with the surface layer described above is badly asymmetrical, with the scatter maximum directed backward (toward the light source). The spherical albedo of the particle in this system need not be high in order to ensure that $b_B(0) = 0.65b_o$. Then we can ignore multiple scattering from particle to particle, just as we can the dark lanes between particles (errors have opposite signs and cancel each other, approximately), and we can identify $b_B(0)$ with the mean brightness of the disk of the particle in the full phase

$$\bar{b}(0)/b_o = b_B(0)/b_o. \quad (17.5)$$

This approximation results in a readily obtainable majorizing estimate of the spherical albedo of a particle in the system. Actually, the magnitude on the left hand side of Eq. (17.5) is, by definition, the geometric albedo of the particle

$$\bar{b}(0)/b_o = a_{gp} \quad (17.6)$$

But the geometric albedo of any body is linked with its spherical albedo by the relationship

$$a_{sp} = qa_g, \quad (17.7)$$

where q is the phase integral. Consequently, in our case we can write

$$a_{sp\ p} = (q_p a_{g\ p} / q_{\text{moon}} a_{g\ \text{moon}}) (a_{sp\ \text{moon}}), \quad (17.8)$$

where the subscripts p and moon are magnitudes that equate to the particle and to the moon.

Now note that $a_{g\ p} > a_{g\ \text{moon}}$. As a matter of fact, in the Eq. (17.5) approximation $a_{g\ p} = 0.65$, whereas the tabulated value is $a_{g\ \text{moon}} = 0.106$ (Allen, 1960). Since the indicatrix for the particle can be considered to be close to the indicatrix for the moon, this inequality means that the particle's reflectivity is /46 higher than the moon's. But general considerations, as well as laboratory investigations (Hapke and van Horn, 1963), suggest that when the body has a lunar type surface, the elongation of the indicatrix (toward the light source) decreases with increase in the body's reflectivity. In such case $q_p / q_{\text{moon}} > 1$, and we can write the following in place of Eq. (17.8)

$$a_{sp\ p} > (a_{g\ p} / a_{g\ \text{moon}}) (a_{sp\ \text{moon}}). \quad (17.9)$$

The values of all the magnitudes on the right hand side are known, so all that needs to be pointed out is that the $a_{g\ \text{moon}} = 0.106$ cited above should be corrected for the effect of the moon's opposition. This will give $a_{g\ \text{moon}} = 0.145$. Then, when $a_{g\ p} = 0.65 \pm 22\%$, and $a_{sp\ \text{moon}} = 0.067$

$$a_{sp\ p} > 0.30 \pm 22\%. \quad (17.10)$$

In #18 it will be shown that this albedo is too high to be able to ascribe the "logarithmic" shape of the phase curve for the B ring to the effect of shading in the surface layer of an individual ring particle. Consequently, the Eq. (17.10) result indicates that the B ring is not a one-particle thickness system.

It now becomes of interest to turn to microscopic particles with a spherical albedo close to unity. They appear to be unsatisfactory from the photometric point of view, apart from cosmogonic considerations. To show this, let us calculate the brightness of the layer as applicable to dielectric particles scattered

in accordance with Mie's formulas. We see that even when $a_{sp} = 1$, the brightness of this layer is much less than that observed for Saturn's rings, $0.65b_0$.

In this case we are not justified in ignoring the multiple scattering from particle to particle because the albedo is high. The resultant system brightness therefore should be written in the form

$$b = b_1 + \Delta b, \quad (17.11)$$

where the first and second summands designate the contribution to the resultant brightness of first and higher orders of scattering. Since the calculation is being made for a one-particle thickness system and for the moment of precise opposition, the magnitude b_1 is the geometric albedo of the particle. If q is known, the calculation is readily made through Eq. (17.7).

The monochromatic phase function of dielectric microscopic spheres with indices of refraction $m = 1.33$ and 1.50 yields q values that vary from 1.72 to approximately 130 (Walter, 1957, 1959; Giese et al., 1961), depending on the parameter $\kappa = 2\pi\rho/\lambda$, where λ is the wave length of the incident radiation, and ρ is the radius of the sphere. Walter's tables list the parameter κ with values from 10 to 400 , and Giese's tables list it from 10 to 159 . Assuming $\lambda = 0.555$ micron, we obtain ρ limits 0.9 - 35.4 microns and 0.9 - 14.1 microns, respectively. When we use the data in these tables we should take into consideration the fact that the incident radiation is not monochromatic in our case, and that ρ can have dispersion (considerable, in all probability). What should be taken for q , therefore, is a mean value around 7.15 . Assuming $a_{sp} = 1$, we obtain

$$b_1 = a_g = 1/7.15 = 0.14. \quad (17.12)$$

We can estimate the term Δb through formulas from the theory of multiple scattering. Unfortunately, this theory holds only with many-particle thickness systems. Let us take an exaggerated value for τ_0 , say 3, in order to avoid underestimating Δb . Then the isotropic phase function will yield $\Delta b/b_1 = 0.41$ for absolutely reflecting particles and wide open rings ($A = A' = 25^\circ$) [in our case the light is scattered forward, primarily, and this reduces $\Delta b/b_1$ as compared with the isotropic problem; the value of 0.41 used in Eq. (17.11) therefore should give some exaggeration in the estimate of system brightness, but, as will be seen below, this merely served to strengthen the argument]. So, the total brightness of the layer is

$$b = 0.41 \cdot 1.41 = 0.20. \quad (17.13)$$

Comparing this result with $\bar{b}_B(0) = 0.65$ (as well as with the other in b_0 units) we see that the system just reviewed will be less bright than the B ring by at least a factor of three. Thus, the one-particle thickness system consisting of microscopic dielectric spheres does not satisfy the photometric data.

One can raise the objection that microscopic particles expected in Saturn's rings should be crystals, rather than true spheres. Unfortunately, there are no phase function calculations for crystals. However, if crystal orientation is chaotic, the results should be close to those for spheres. If the orientation is systematic, meteorological data can be used (optical phenomena in ice crystals in the earth's atmosphere; see Minneart, 1958, for example). These data fail to indicate back scattering strong enough to ensure a high degree of brightness for the B ring. Moreover, crystals are incapable of creating the observed "logarithmic" shape of the phase curve for the B ring with its rapid drop in brightness near $\alpha = 0$. The latter comment is valid as well for microscopic, opaque white spheres reflecting in accordance with Lambert's law (although the amount of light scattered backward in this case is sufficient).

(b) Many-particle thickness system. This is the classical case considered /48 in the theory of multiple scattering of light (a flat layer of scattering medium with optical thickness τ_0 in the direction normal to the layer, the particles of which have albedo a). Formulas and tables can be found in Chandrasekhar (1953), Sobolev (1956), Chandrasekhar, Elbert, and Franklin (1952). Table 5 lists our calculations for the B ring (again when $A = A' = 25^\circ$). We selected 0.62 as the

mean value of $b_B(0)$, rather than 0.65. This produces no significant change in the results.

TABLE 5

τ_0	$b_B(0)$	x_1 for second and higher order scattering	a	$x(\pi)$	$\frac{\Delta b}{b}$	Under study
1	0.62	0	1	3.3	0.24	Effect of $b_B(0)$
1	0.48	0	1	2.7	0.31	
1	0.76	0	1	4.9	0.20	
1	0.62	0	1	4.0	0.17	Effect of τ_0
3	0.62	0	1	3.7	0.31	
1	0.62	+3	1	4.4	0.08	Effect of x_1
1	0.62	-3	1	4.1	0.14	
1	0.62	0	0.8	5.5	0.12	Effect of a
1	0.62	0	0.7	6.6	0.08	
1	0.62	0	0.6	7.9	0.06	

In Table 5, τ_0 is the optical thickness of the layer, $b_B(0)$ is the brightness of the layer in opposition, a is the spherical albedo of a particle in the layer, $x(\pi)$ is the value of the phase function of particle $x(\gamma)$ for time when the angle of scattering $\gamma = \pi$, that is, also in opposition and $\Delta b/b$ is the ratio of the brightness attributable to multiple scattering to total brightness. The following parameter was used to calculate scattering of orders higher than the first

$$x_1 = \frac{3}{2} \int_0^\pi x(\gamma) \cos \gamma \sin \gamma d\gamma, \quad (17.14)$$

and is a measure of the elongation of the indicatrix. x_1 is equal to zero in the case of isotropic scattering, is positive for an indicatrix with forward elongation, and negative for an indicatrix with backward elongation. $|x_1| = 3$ corresponds to an indicatrix with extremely great elongation. As will be seen from the data listed in the table, the dependence of $x(\pi)$ and $\Delta b/b$ on x_1 is weak, so in future calculations it can be taken that multiple scattering is isotropic. /49

The phase function $x(\gamma)$ was normalized such that its mean value over the entire sphere was $\bar{x}(\gamma) = 1$. In order to avoid any confusion, let us point out that in astrophotometry the normalization of the phase function is different, that is, it is taken that $x(\pi) = 1$ for any shape of the indicatrix. In this

case the magnitude in the fifth column in Table 5 is $x(\pi)/\bar{x}(\gamma) = 1/\bar{x}(\gamma) = 4/q$, where q is the phase integral [and for the calculation of which it also is taken that $x(\pi) = 1$].

There is yet another comment to be made, one based on principle, in addition to the purely formal comment already made. The magnitude of a listed in Table 5 is not the albedo of an individual particle in the system, strictly speaking, but the albedo of an element of the volume of the system containing a sufficiently large number of particles, according to the derivation of the formulas of the theory of multiple scattering. We introduce an error by identifying a with the albedo of the particle. But it is obvious that this error will be smaller the smaller the magnitude of the $\Delta b/b$ ratio. At the end of #12 we emphasized the fact that the observed extreme sharpness of the B ring phase function maximum when $\alpha = 0$ (Figure 9b) suggests the primacy in this direction of the effects of first order scattering; that is, on the smallness of $\Delta b/b$ as compared with unity. The results of the direct calculations in terms of the theory of multiple scattering, as listed in Table 5, confirm this fact, so long as the $\Delta b/b$ value is not greater than 0.31, even when $a = 1$. It is more realistic to put $a \sim 0.6$ to 0.7 , and then $\Delta b/b = 0.06$ to 0.08 . There is no objection to identifying a with the albedo of an individual particle under similar circumstances. After these necessary comments, let us proceed to the substantive analysis of the data in Table 5.

We will consider the τ_o and $b_B(0)$ values listed in the table as parameters known from observation (the accuracy of which is within definite bounds). In such case the data in the table enable us to establish what the $x(\pi)$ and $\Delta b/b$ values for some a ought to be so that, when $\tau_o \sim 1$, a $b_B(0)$ value satisfying the observations will be obtained. In turn, this will make it possible for us to conclude that:

1. Microscopic, dielectric, diffracting (consequently transparent) spheres for which $a \sim 1$, $x(\pi) \sim 0.56$ (Walter, 1957, 1959; Giese et al, 1961) do not satisfy the many-particle thickness models, because they cannot provide the observed $b_B(0)$ value.
2. Absolutely white spheres, scattering in accordance with Lambert's law [$x(\pi) = 2.7$], almost satisfy the minimum observed value $b_B(0) = 0.51$ of Eq. (16.4).

At the same time, $a = 1$ indicates that the spheres are microscopic and have a fresh ice surface. Recalling that cosmogonic considerations lead to a very short /50 life span for microscopic particles in Saturn's rings, we should suppose that the sole source of particles such as these is the fractionation of macroscopic particles when they collide with each other. Consequently, the percentage of microscopic white particles in the total mass of the ring ought to be small.

3. The preceding conclusion can be expressed in a different way. The main mass of the B ring is made up of macroscopic particles. It can be anticipated that because of the constant activity of micrometeorites and of solar corpuscular radiation on the surface of the particles, their phase function will be extremely close to the moon's phase function, for which, with the effect of opposition taken into consideration, $x(\pi) = 9.43$. For the same reasons, it can be anticipated that the spherical albedo of a typical macroscopic particle of the B ring will be significantly less than unity. The data in Table 5 confirm this. Actually, a ring with $\tau_0 = 1$, and consisting of particles with $a = 0.6$ and $x(\pi) = 7.9$, will have a surface brightness $b_B(0) = 0.62$ when $A = A' = 25^\circ$.

Finally, it can be stated that a many-particle thickness system having the brightness of the B ring, and consisting primarily of macroscopic particles with a phase function similar to that of the moon (reflecting surface in terms of mass) will have an albedo for the particles of

$$\alpha \sim 0.5 - 0.6 \quad (17.15)$$

or approximately double that of the one-particle thickness system.

#18. The Mechanism Responsible for the Observed Ring Phase Curve

Three explanations have been advanced for the shape of the phase curve observed for Saturn's rings. They are, in historical sequence:

1. mutual shading of the particles (Seeliger, 1887, 1893; see as well a detailed review of these papers, written by Schoenberg, 1929);
 2. diffraction of light by an individual ring particle (Schoenberg, 1933);
 3. the shadow effect on the surface layer of an individual particle (Gehrels, 1956, 1957; Gehrels et al, 1964; Hapke, 1963; Hapke and van Horn, 1963).
- We shall call it the Gehrels-Hapke effect, for purposes of brevity.

The observed phase curve can be attributed to one of these effects, or to combinations of them.

Let us attempt to estimate the relative contribution of each effect to the 51 resultant phase curve. The contribution of diffraction is small. As a matter of fact, in #17 we saw that a ring with a reflecting surface attributable mainly to diffracting particles would be weaker than the B ring in brightness by more than one stellar magnitude. Recalling that $\beta_A - \beta_B \approx 0^m.6$ (#1), we can add that a ring such as this will be much weaker even than the A ring.

The contribution of the Gehrels-Hapke effect too is small. As a matter of fact, this effect can give a phase curve resembling in shape the phase curve for Saturn's rings only for the condition that the albedo of the particle is very low. This can be seen quite well in the example of the Galilean satellites of Jupiter, Io, Europa, Ganymede, and Callisto. Harris (1962), proceeding from a reasonable assumption that $q = q_y = 0.585$ for all these bodies, found spherical albedo values of 0.54, 0.49, 0.29, and 0.15, respectively, for them.

The phase curves for the satellites are quite reliably known from the electrophotometric observations made by Stebbins and Jacobsen (1928). Only in the case of Callisto does the phase curve resemble the phase curve for the B ring with respect to the "logarithmic" behavior near opposition. In the case of the other Galilean satellites, the phase curves are practically straight lines, or are only slightly curved, with a curvature that remains almost unchanged with α . But the main photometric feature of Callisto is its very low albedo (0.15, as compared with 0.29 to 0.54 for the other three satellites). Another satellite with a phase curve resembling the phase curve for Saturn's rings is the moon (Gehrels et al, 1964). Its albedo too is very low (0.07).

Theoretical research (Hapke, 1963) and laboratory experiments (Hapke and van Horn, 1963) also confirm that the "logarithmic" behavior of the phase curve near opposition can be observed only in the case of bodies with low albedo. In particular, artificial laboratory surface structures in this case should have a normal albedo not exceeding 0.15 (a spherical body with a surface such as this would have a $\lesssim 0.09$).

At the same time, we saw in #17 that even a one-particle thickness system with the brightness of the B ring should have a ~ 0.3 , and in the case of the

many-particle thickness system (matching more closely the real structure of the B ring) the value of this parameter should be increased to 0.5 to 0.6, approximately. These figures do not concord with the strong Gehrels-Hapke "logarithmic" effect near opposition.

On the other hand, mutual shading is the principal effect responsible for the observed shape and amplitude of the ring's phase curve. The arguments raised in favor of this point of view are as follows:

1. It is not mandatory that ring particles be microscopic. In this regard, 52 cosmogonic considerations vanish. If the radius of a particle, ρ , has an order of magnitude of a few centimeters, or more, the life of the ring satisfies cosmogonic requirements.

2. The spherical albedo of the particle can have any value between 0 and 1. Specifically, it can be 0.5 to 0.6, that is, have a value satisfying the observed brightness of the B ring.

3. Theoretical phase curves for the effect of mutual shading can yield extremely good concordance with available observations of the B ring. Concordance can be achieved when the values of the theoretical parameters are reasonable (see, in addition, Chapter VII).

#19. Conclusions Concerning the Structure of the B Ring and Properties of a Typical Particle

So, it is more probable that the principal effect responsible for the shape and amplitude of the phase curve for the B ring is mutual shading. This postulation leads immediately to certain quite specific conclusions as to ring structure.

First, the ring should be a many-particle thickness system. This is the consequence of the requirement that the physical thickness of the ring, z_0 , ought to satisfy the condition

$$z_0 \sim l \sin A, \quad (19.1)$$

where l is the length of the dark cone of the particle, and A is the angle of elevation of the sun above the plane of the ring. In Chapter VII it will be shown that if Eq. (19.1) is not satisfied, the phase curve will be almost a straight line in the interval $0 < \alpha < 3^\circ$. It is obvious that the one-particle thickness system can satisfy the condition of Eq. (19.1) only when values of A

are very small. At the same time, the observed phase curve for the B ring is extremely nonlinear in this interval to $A \sim 28^\circ$.

Second, the mean distance between adjacent particles ought to be short enough to provide for a comparatively high probability of mutual shading. In other words, the percentage of the volume of the ring occupied by particles, or the so-called volumetric density, D , should not be too small. Calculations using the formulas from the theory of mutual shading (Chapter VII) reduce to the condition

$$D \gtrsim 10^{-3}. \quad (19.2)$$

Once the B ring model is selected, it becomes possible to describe the properties of a typical ring particle. Strictly speaking, they were described in #17, when we reviewed the many-particle thickness system with $\tau_0 = 1$, and 53 brightness at opposition equal to B ring brightness. With this in mind, we can represent a typical B ring particle as a macroscopic, opaque, diffusely reflecting body with a surface layer similar to the lunar surface, and with spherical albedo $a \sim 0.5$ to 0.6 .

Macroscopic particles with these properties ("blocks") should comprise the overwhelming percentage of the mass and reflecting surface of the ring, but this does not preclude the presence of smaller particles ("dust") in the volume of the ring. The life of such system ("blocks + dust") can be quite long, cosmogonically speaking. Actually, although the "dust" will be swept out of the ring volume continuously because of radiative braking, the collisions between "blocks" will result in the fragmentation of their surface layer and to the appearance of new "dust particles." Collisions in a many-particle thickness system in which $\tau_0 \sim 1$ should be frequent (#28). The presence of "dust" in Saturn's rings was detected reliably by Maggini (1937) photometrically. The presence of the "dust" is readily apparent only when the openings are extremely small (see Figure 11).

V. Analysis of Observations Made During Extremely Small Ring Openings

#20. Introductory Remarks

It is obvious that observations of the rings when openings are extremely small (including times when A , or A' , equals zero) can provide important additional information on the shape and nature of the rings.

First of all, these observations make it possible to estimate the physical thickness of the rings, z_0 . [Let us emphasize the fact that angle φ , corresponding to z_0 , as seen from the earth, is uncommonly small, and cannot be resolved by the largest telescopes, even when images are excellent. For example, if $z_0 = 1$ km, $\varphi = 1.4 \cdot 10^{-4}$ second of arc. See #22, Eq. (22.2)].

There are two ways in which the problem can be solved.

1. Observe the rings when A' is exactly equal to zero. At this time the rings should be seen edge-on (providing the plane of the rings has no significant deformations of the figure-8, or other types), and the luminous flux from the rings should depend solely on the value of their physical thickness.

2. Observe the dark side of the rings (the eyes). The observer should, in principle, detect a bright, narrow, band created by the edge of the system, at the limb of the semi-ellipse of the rings closest to the earth. Since the edge is illuminated by direct solar light, its true brightness, b_e , should be of the order of brightness of the B ring at large openings, whereas the brightness of the dark side, b_d , should be from 2 to 2 1/2 orders of magnitude less (the subscripts "e" and "d" designate the edge and dark side of the rings, respectively). As a practical matter, the magnitude of the b_e/b_d ratio will be greatly reduced because of the apparent expansion of the image of the edge, but despite this fact, given the corresponding visibility conditions, the presence of a bright edge will show up in the form of some asymmetry in the photometric section of the eyes.

Further details dealing with these two methods of arriving at an observed estimate of z_0 will be discussed in #22.

Other tasks of observations at extremely small A and A' are explaining the sources of illumination of the dark side, estimating b'_d/b_1 (where the subscript "1" designates the lighted side of the rings), studying the distribution of particles by size along the z-coordinate, searching for a gas, or dust, atmosphere, possibly, blanketing the rings, estimating the optical thickness of the divisions, and others. The majority of these problems can be solved because the periods when A and A' have opposite signs provide the observer with the distinct possibility of studying the rings in diffusely transmitted light, rather than in diffusely reflected light (as is customary).

#21. Illumination of the Dark Side of the Rings

(a) Illumination of the dark side of the ball of Saturn. Russel (1908) was the first to obtain the correct order of magnitude of this effect. His calculation can be expressed by the formula

$$(b'_d/b_1) = 1/2 [(I_\gamma R^2 \sin^2 P)/(I_\odot r^2 \sin^2 p)] f_\gamma(\alpha_\gamma) f_p(\alpha_p) \quad (21.1)$$

where b'_d is a brightness component for the dark side attributable to the illumination of the rings by the ball of Saturn;

b_1 is the brightness of the lighted side (the most intense zone of the B ring when $\alpha \sim \alpha_{\max}$);

I_γ and I_\odot are the intensities of the light from Saturn and from the sun, as observed from the earth;

R and r are the mean heliocentric distances of Saturn and the earth;

P and p are the apparent magnitudes of the polar radius of Saturn for the observer at a given point on Saturn's rings and on the earth;

f_γ and f_p are the phase functions of the ball of Saturn and of a typical particle of Saturn's rings;

α_γ is the phase angle at Saturn (in the conventional sense; that is, when the sun is taken as the light source);

α_p is the phase angle for the particle at a given point at the rings (in a special sense; the source of light is the ball of Saturn). Figure 15 illustrates the situation.

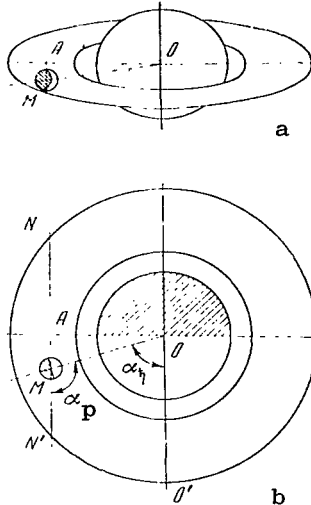


Figure 15. Calculation of the illumination of the dark side of the rings by the ball of Saturn [see Eq. (21.1)].

a - schematic view of the Saturn system with the dark side of the rings turned to the earth; M is a ring particle (the size of the particle is greatly exaggerated for clarity); b - view from a point above the north pole of Saturn.

The $1/2$ in Eq. (21.1) means that the observer of the rings sees only half of Saturn's disk ("half of the moon, half set," as Bond has put it). Russell placed his "test particle" at a point on the major axis of the ellipse of the rings at a distance measured from the center of Saturn equal to the polar diameter of the planet (we shall call it the Russell point"). This point is on the B ring at a distance of some 8,000 km from the ring's outer boundary, in the brightest zone of the entire ring system.

$P = 30^\circ$ at the Russell point. Taking $p = 9''.07$, $m_\odot - m_\gamma = -26^m.60 - 0^m.88 = -27^m.48$ [from whence $(I_\gamma/I_\odot) = 1.02 \cdot 10^{-11}$], $(R/r) = 9.539$, $\alpha_\gamma = \alpha_p = 90^\circ$, $f_\gamma(90^\circ) = 2/7$, $f_p(90^\circ) = 1/3$, and putting $2/7 \cdot 1/3 \approx 1/10$, approximately, Russell obtained

$$(b'_d/b_1) \approx 1/160. \quad (21.2)$$

The author of this book reviewed the work done by Russell. He took into 56 consideration the present day values for the magnitudes contained in Eq. (21.1), and verified the correctness of the basic assumptions. The intensity of the illumination of the dark side was calculated for a series of points along the major axis of the rings, and along a secant normal to the major axis and intersecting it at the Russell point, as well as for the Russell point. The results of the review can be formulated as follows.

1. The $\alpha_p = 90^\circ$ value for the Russell point is inaccurate. It would be more correct to measure α_p from the direction to the photometric center of gravity of the planet's crescent, rather than from the direction to the center of Saturn's disk. This will give a correction factor of $\Delta\alpha = 14^\circ$ for the Russell point. The corresponding b'_d/b_1 value will then be 40% greater than it is in Eq. (21.2). Analogous correction factors can be introduced for all the other points.

2. Present day values of m_{\odot} and p are $-26^m.73$ (Allen, 1950), and $8''.80$ (Rabe, 1928). When they are substituted into Eq. (21.1) in place of the values accepted by Russell, the result is changed by 6% in all (on the lower side).

3. Russell's assumption that $f_{\gamma}(0^{\circ}) \cdot f_p(90^{\circ}) = 1/10$ is equivalent to adopting Lambert's scatter law for Saturn, and for the particle. According to Lambert's law $f(90^{\circ}) = 0.318$, so that $f(90^{\circ}) \cdot f(90^{\circ}) = 0.101$. Contemporary research (see Harris, 1963, section 8.5) indicates that the phase functions of large planets are, in all probability, intermediate between the Lambert functions and Rayleigh /57 scattering. The latter yields $f(90^{\circ}) = 0.24$. $f(90^{\circ})$ for Venus has precisely this value (Danjon, 1949; the phase function of Venus observed by him practically coincides with the phase function of the Rayleigh scattering right up to $\alpha = 100^{\circ}$). So far as the phase function of particles of Saturn's rings is concerned, it should be near the phase function of the moon, and then $f(90^{\circ}) = 0.08$ (Rougier, 1933). However, this value is valid only when the angular dimensions of the light source are small. In the case under consideration the half-crescent visible from the Russell point is 30° in altitude and somewhat in excess of that in azimuth. A wide-angle source such as this will greatly reduce the shadow on the surface of the particle, and the resultant $f_p(90^{\circ})$ will be much larger than 0.08.

With all of this in mind, we calculated the behavior of the dark side brightness in the eyes (along the major axis, and along the normal secant through the Russell point), using two assumptions

$$1) \quad f_{\gamma}(\alpha) = f_p(\alpha) = f_L(\alpha) \quad \text{and} \quad 2) \quad f_{\gamma}(\alpha) = f_p(\alpha) = f_{\odot}(\alpha),$$

where $f_L(\alpha)$ and $f_{\odot}(\alpha)$ are the phase functions of the Lambert scattering and of Venus, respectively. Figure 16 is a plot of the results for the "Russell secant."

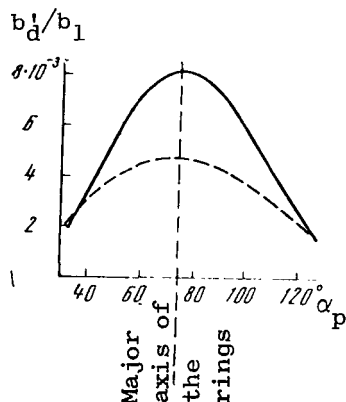


Figure 16. Theoretical distribution of the brightness of the dark side of Saturn's rings along the secant passing through the Russell point normal to the major axis of the rings.

The solid curve is for the assumption that Saturn's ball and the particle reflect in accordance with Lambert's law. The dashed curve is for the assumption that they reflect in a manner similar to that for Venus.

As will be seen, the brightness of the dark side diminishes with distance from the Russel point along the secant. The mean magnitude of the b_d'/b_1 ratio is $5.4 \cdot 10^{-3}$ for the Lambert phase function, and $3.6 \cdot 10^{-3}$ for the phase function of Venus.

The b_d'/b_1 ratio changes along the major axis in the case of the Lambert phase function from $5 \cdot 10^{-3}$ at the outer boundary of the A ring, to $13 \cdot 10^{-3}$ at the inner boundary of the B ring.

(b) Component of the brightness attributable to diffusely transmitted solar radiation. This component can be estimated through formulas and tables that are part of the theory of multiple scattering. Table 6 lists the results of our calculations for the A and B rings. The calculations were made for a spherical indicatrix. Because the indicatrix for the scattering of the ring material is in fact very aspherical, and has backward elongation, the actual brightnesses should be lower than those calculated.

TABLE 6

Ring	τ_0	A'	A	Sign A'	Sign A	α	$(b_d''/b_1)_{true}$	$(b_d''/b_1)_{app}$
A	0,5	2°20'	0°35'	0,04	0,01	1,0	$4,5 \cdot 10^{-3}$	$3,3 \cdot 10^{-3}$
						0,8	2,4	1,8
						0,5	0,8	0,6
	0,5	0 35	2 20	0,01	0,04	1,0	18,4	5,3
						0,8	9,6	2,8
						0,5	2,9	0,8
B	1,0	2 20	0 35	0,04	0,01	1,0	2,9	2,1
						0,8	1,3	1,0
						0,5	0,4	0,3
	1,0	0 35	2 20	0,01	0,04	1,0	11,8	3,4
						0,8	5,1	1,5
						0,5	1,4	0,4

In Table 6, b_d'' is the component of dark side brightness created by the diffusely transmitted solar light. The subscripts "true" and "app" designate true and apparent brightness. Apparent brightness is understood to mean the brightness attenuated by atmospheric and instrumental wash out for the case of visual observations made in a telescope with an aperture of between 0.6 and 1.0 meter when image quality is good. We used the contour of brightness distribution in the image of a star obtained by Meinel (1963) for the reduction, taking

it that the central peak contains 30 percent of the total luminous flux from the star and that the telescope can resolve a dual system with components of equal brightness distant from each other by $0''.375$. Graphical integration was used to make the transition from a point source of light to a line, and to a band.

The magnitude of $(b''_d/b_1)_{app}$ was calculated for equal pupillary magnification, and was not reduced for atmospheric and instrumental absorption.

As will be seen from Table 6, when $\alpha \sim 0.5$, the b''_d component is somewhat smaller than b'_d , and this is true in all cases. This difference is even greater for the backward elongated indicatrix.

(c) Solar radiation diffusely transmitted through the Cassini division; optical thickness of the division. Let us suppose that the scattering properties of the particles filling the Cassini division are identical with those of the particles filling the B ring. The problem is to find that value of the optical thickness of the Cassini division (τ_{oCd}) that will satisfy the following observational data: /59

- (1) visibility of the external bright condensation on the dark side when $A \gtrsim 1 - 2^\circ$;
- (2) visibility (at sites of external bright condensations) of dark spots when the ring has its illuminated side turned toward the earth and A is of the order of 2° ;
- (3) non-visibility of the double bright line of the Cassini division on the dark side of the rings between the external and internal condensations;
- (4) the significant excess of the brightness of the outer condensations over the brightness of the dark side. Specifically, when $A' \sim 0^\circ 40'$, the external condensations visually are 6 to 8 times brighter than the dark side (Barnard, 1908a).

Our calculations revealed that we can obtain satisfactory concordance with all of these points when $\tau_o \sim 1.5 \cdot 10^{-3}$. Because τ_{oCd} is exceptionally small, the value of the brightness can be calculated with only the first order scattering taken into consideration. Figures 17 and 18 show some of the results in graphic form. They confirm Barnard's assumption that the outer condensations can be attributed to the light diffusely transmitted through the Cassini divi-

sion. Let us add that the inner condensations (coinciding in terms of position with the C ring) evidently can be attributed to the like diffusion of light through other optically thin zones, specifically through the division between the B and C rings, and through the zone near the inner part of the C ring where τ_{oC} can be quite small too (Cook and Franklin, 1958). This assumption is strengthened by the fact that some observers with good images (Aitken, 1907; Barnard, 1908b) saw each of the inner condensations twice.

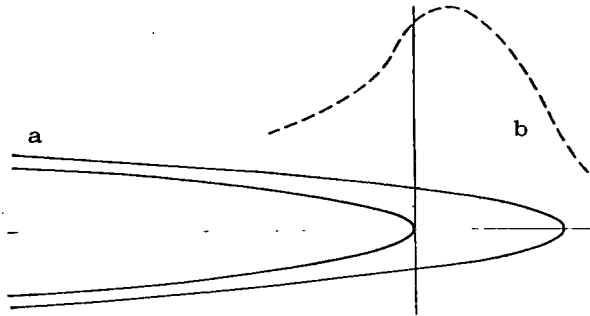


Figure 17. a - the Cassini division as seen from the earth when $\sin A' = 0.04$; b - theoretical distribution of apparent brightness (excess over dark side brightness) along the major axis of the rings (telescope with aperture $\sim \sim 0.6$ to 1.0 meter, resolution $0''.375$; central peak of star image contains 30 percent of total luminous flux).

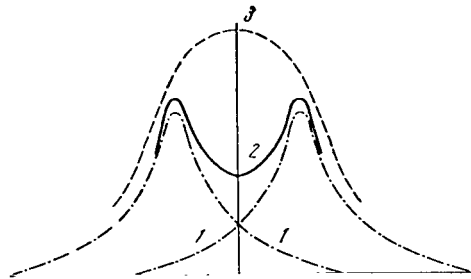


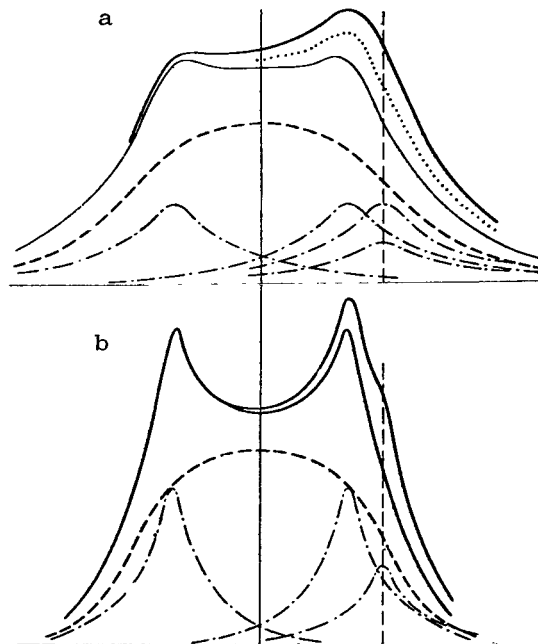
Figure 18. Theoretical distribution of the apparent brightness in the image of the dark side of the rings along a secant normal to the major axis at a distance of $12''.9$ from the center of Saturn (observation conditions the same as those in the preceding figure).

1 - component of brightness from diffusion of light through the north and south branches of the Cassini division; 2 - summed brightness from both branches; 3 - component of brightness from dark side of A and B rings when the Cassini division was missing.

/60

#22. Analysis of Observations for Estimating the Physical Thickness of the Rings

(a) Observations of dark side. The presence of a fully illuminated edge of the rings at the boundary of the ellipse closest to the earth evidently should result in asymmetry in the distribution of brightness along the secants of the eyes normal to the major axis. Once again, assuming that the resolution of point sources of light is $0''.375$, and that the central hump of the star image includes 30 percent of the total luminous flux from the star, we obtain the brightness distribution shown in Figure 19a for a secant $14''.0$ from the center of Saturn when $z_0 = 20$ and 10 km. When $z_0 = 10$ km, the brightness of the right maximum on the resultant curve is 9 percent higher than the brightness of the left. It is probable that this is close to the lower limit of detection by visual methods. Further, if it is assumed that the resolution is double the above ($0''.187$), the distribution of the brightness of this same secant will be that shown in Figure 19b ($z_0 = 10$ km). The peaks created by the Cassini division have much greater intensity in this case than they do in the previous one. The result is that the contrast between the right and the left maxima remains almost the same (10 percent).



/61

Figure 19. Influence of z_0 on the distribution of apparent brightness in the dark side image (along a secant normal to the major axis at a distance of $14''.0$ from the center of Saturn).

a - resolution $0''.375$. The bold face and dashed curves are the theoretical contours for $z_0 \approx 20$ and 10 km; b - resolution $0''.187$, $z_0 \approx 10$ km.

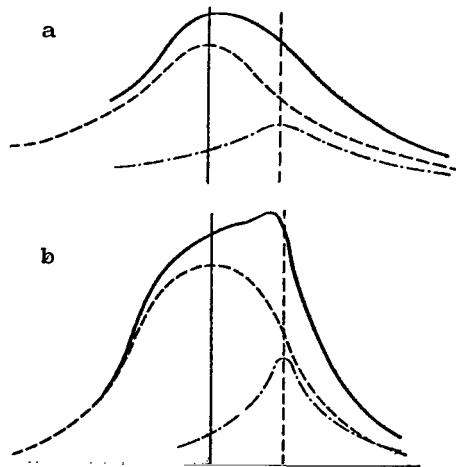


Figure 20. Same as in Figure 19, but for a secant passing through the A ring (distance from the center of Saturn $19''.1$); $z_0 \approx 10$ km.

a - resolution $0''.375$; b - resolution $0''.187$.

Conditions are more favorable along the secant passing through the A ring /62 eye, that is, outside the Cassini division. Figure 20 shows the corresponding brightness distribution. Evidently, asymmetry in the distribution of brightness can be detected visually in this case, even when $z_0 = 5$ km. However, this effect was not noted at the time the old observations were made (1907-1908, 1920-1921), nor was it noted during the international patrol observations made of Saturn in 1966.

(b) Observations of edge. The rings transmit a luminous flux to the earth from the edge only when A' is precisely equal to zero. If the receiver is sensitive enough to detect the line of the rings beyond the ball of Saturn, we obtain data on which to base an estimate of the low limit of z_0 . Up to 1966, there had been no success in obtaining a positive effect.

This author found that when $A' = 0$, the expected brightness of the ring image (beyond Saturn's ball) was so low that Saturn's atmospheric aureole can prevent detection. High mountain observatories therefore offer the best results. Reflectors (since they do not have chromatic aberration) are preferable to refractors.

The 1966 observations showed that in general our calculations were correct. This can be seen from Figure 21a, which shows a positive print from one of the

plates obtained by Dollfus on Pic du Midi, and which led him to the discovery of Saturn's tenth satellite. The brightness of the planet's disk was attenuated artificially by approximately two orders of magnitude by a band of absorbing material. The intense aureole of Saturn, the brightness of which diminishes with distance from the limb, will be seen outside the band. The rings (dark side turned toward the earth and visible almost from the edge) can be distinguished against the background of the aureole with difficulty. But it must be remembered that the situation is somewhat more favorable for visual or photoelectric observations because the widening of the line of the ring is less in cases such as these.

Let us assume we observe the passage of the earth through the plane of Saturn's rings under ideal conditions, when only the diffraction aureole plays any significant role. The calculations made to determine the intensity of this component of the aureole yield brightnesses of 7.4, 1.8, and $1.2 \cdot 10^{-4} b_c$, respectively, for distances from the center of Saturn of $r = 14''.4$, $18''.0$, and $19''.6$ (telescope aperture $D = 60$ cm and magnification $G = 220$). b_c is the brightness of the center of Saturn's disk. Moreover, it can be shown that for our "standard" image quality (resolution $0''.375$, concentration 30 percent of total luminous flux at the central hump or the star image) brightness b_a along the axis of an extremely narrow bright band is

$$b_a = (\varphi/0''.37) b_{\text{true}}, \quad (22.1)$$

where φ is the angular width of the band (in seconds of arc) and b_{true} is the 63 true brightness of the band. Finally, the linear width, h , of the band at the mean distance of Saturn is

$$h_{\text{km}} = 6.91 \cdot 10^3 \varphi \text{ sec arc} \quad (22.2)$$

Then, taking $b_{\text{true}} = b_c$, and $b_a = 5 \cdot 10^{-5} b_c$ (contrast with the brightness of the aureole is $\epsilon \sim 25\%$), we obtain

$$h = 0.26 \text{ km} \quad (22.3)$$

The order of z_0 should be such that it can still be detected by a high-mountain observatory. Consequently, the sensitivity of this method is at least an order of magnitude greater than the sensitivity of the method described in section (a).

The procedure for estimating z_0 from observations when $A' = 0$ is simple, at least at first glance. All that need be done is to select a high-mountain observatory where, at time $A' = 0$, computed in advance, it will be astronomical night and Saturn will be high enough above the horizon to observe (visually or photo-electrically) whether or not the lines of the rings disappear, after which Eq. (22.1), or one similar to it, is used for the calculation. Unfortunately, the position of the plane of Saturn's rings was not known accurately enough until recently. According to Slipher (1922), the actual time $A' = 0$ can differ from the computed time by as much as ± 1 day.* Consequently, successful observations required the conduct of an international patrol of Saturn by personnel in many observatories covering a sufficiently wide range of longitudes. Let us emphasize the fact that the observer's task should include not only establishment of the fact of visibility, or non-visibility of the rings on the critical night, but also the obtaining of evidence of the fact that his eyes observed transit of the earth through the plane of the rings.

The author, together with Dollfus, made the first attempt to organize a patrol such as this in 1966 (within the framework of the Commission on Physics of Planets of the International Astronomical Union). It was possible to observe two transits of the earth, and one transit of the sun through the plane of the rings, as well as two quite long periods of visibility of the dark side of the rings (see Figure 3).

More than ten first-class observatories in the eastern and western hemispheres participated in this cooperative venture. The program distributed to the observers (Bobrov, 1966) envisaged not only observations designed to solve the main problem, that of estimating the thickness of the rings, but doing other work as well, the /64 desirability of the imposition of which was determined by the special location of the rings relative to the earth in 1966. Recommendations included making photometric, spectroscopic, and spectrophotometric observations of the light and dark sides of the rings, to attempt to obtain the dependence of brightness of

* The results of the international cooperative observations of Saturn in 1966 showed that in fact the correction factor for the ephemeris time $A' = 0$ is some 5 hours (Dollfus and Focas, 1968; Kiladze, 1968). The sign of the correction factor is positive for passage of the earth on the south side of the plane of the rings and negative for passage on the north side. The error of the correction factor for the observer is estimated at ± 2 hours.

the rings on the phase angle and on the angle of elevation of the sun above their plane, to detect the presence of a feebly luminous "atmosphere" (dust or gas) that, according to Maggini (1937), is entrained in the plane of the rings, to check the existence of the so-called D ring, more distant from Saturn than the A ring, and others. Further, it was emphasized that the practical absence of the disturbing influence of light scattered by the rings (particularly in the period of their dark side visibility) made many types of observations of Saturn's disk and satellites favorable, including determination of the integral stellar magnitude of the disk, and its dependence on the phase angle, photometry, spectrophotometry, spectroscopy of the disk and of details of the disk, and of observations of the covering of the satellites by the atmosphere and by the edge of Saturn's disk, as well as observations of the eclipse of the satellites.

The majority of the observatories that took part in the 1966 patrol observations obtained a wealth of material, much of it unique in many ways, that helps explain many of the questions concerned with the physics of the Saturn system, particularly its rings. The primary processing is completed and results obtained by the Pic du Midi, Meudon (Dollfus and Focas, 1967) observatories have been published. In processing are a number of the observations obtained by the University of New Mexico observatory (140 plates, covering 64 nights), and a similar series obtained in the Kuiper Lunar-Planetary Laboratory.

Frantz and Johnson (1967) attempted photoelectric scanning of the line of rings in the Lowell Observatory for 14 nights. Unfortunately, the equipment was not good enough to obtain any definitive results (Hall, 1968).

Texereau (1967) published a short report on his photographic photometry of Saturn's disk and rings, made with a 2 meter telescope in the McDonald Observatory, November 1966. If his data are to be trusted, the intensity of the rings continued to diminish within two or three days after the transit of the earth through the plane of the rings. This is clearly in error. Texereau himself notes that the measured intensities were greatly distorted by diffused light from Saturn's disk (the brightness of which Texereau failed to attenuate), and that the image quality changed greatly from night to night.

These isolated failures are recognized as being inevitable, to some extent, /65 because the measurements required were very delicate, and involved many difficulties.

Figures 21a through e illustrate the most important results of the patrol observations of Saturn (other than the work done by Kozyrev, more about which in #23).

Figure 21a reproduces the photography on which, for the first time, there was detected the previously unknown tenth satellite of Saturn (Dollfus, 1967). This satellite, called Janus, rotates around the planet at a distance of three earth radii from the outer limit of the A ring, and has a stellar brightness of 14. The nearness to the rings, and the weakness of the satellite, in terms of brightness, result in its being seen only at times when the rings have their dark side turned to the earth. Beyond this, at the time of observation, Janus should be near the position of maximum elongation (east, or west). All of this makes Janus an extremely difficult object to detect. Dollfus discovered it by basing his efforts on his own idea that the Cassini division by its very existence was responsible for the resonance perturbations, not of Mimos, but of a body closer to Saturn, a conclusion arrived at as a result of new, more precise micrometric measurements made of Saturn's rings in the Pic du Midi Observatory (Figure 1c).

Figures 21b and c are the curves for the intensity of the line of the rings (in terms of time) during the October and December transits of the earth through their plane. These curves, obtained by the photographic photometry method by Kiladze, and Dollfus and Focas, respectively, are an important step forward in the investigation of Saturn's rings. They made it possible for the first time to find the orders of the physical thicknesses of the rings. We will discuss these curves in detail at the end of this section.

Figure 21 d has been taken from Feibelman (1967), and demonstrates the successful effort to confirm the existence of the so-called D ring (of the extension of the ring system beyond the limits of the A ring). It was so dim that it could be seen only near the position on the edge, and then only when conditions were such that the entire ring system had its dark side turned to the earth. As will be seen from the figure, the D ring line extends for a distance exceeding the apparent diameter of the ring system by a factor greater than two (so that Janus is revolving around Saturn, inside this ring!). Feibelman's estimate of D ring brightness is 15 stellar magnitudes/square second of arc, or less.

Figure 21e shows one more result of Dollfus and Focas' photometry, measurements of the luminance of the dark side of the rings as a function of the elevation of the sun above their lighted side. These are the first, and as yet the only, quantitative measurements of dark side luminance. Prior to 1966, estimates of dark side brightness were based on old, visual observations made by Barnard, Slipher, and Graff, as well as by an approximate calculation of the illumination of the night side by light reflected by the ball of Saturn, and by light diffusely transmitted through the thickness of the rings from the day side (#21). The observations made by Dollfus and Focas now make it possible to check these calculations. Agreement seems to be completely satisfactory.

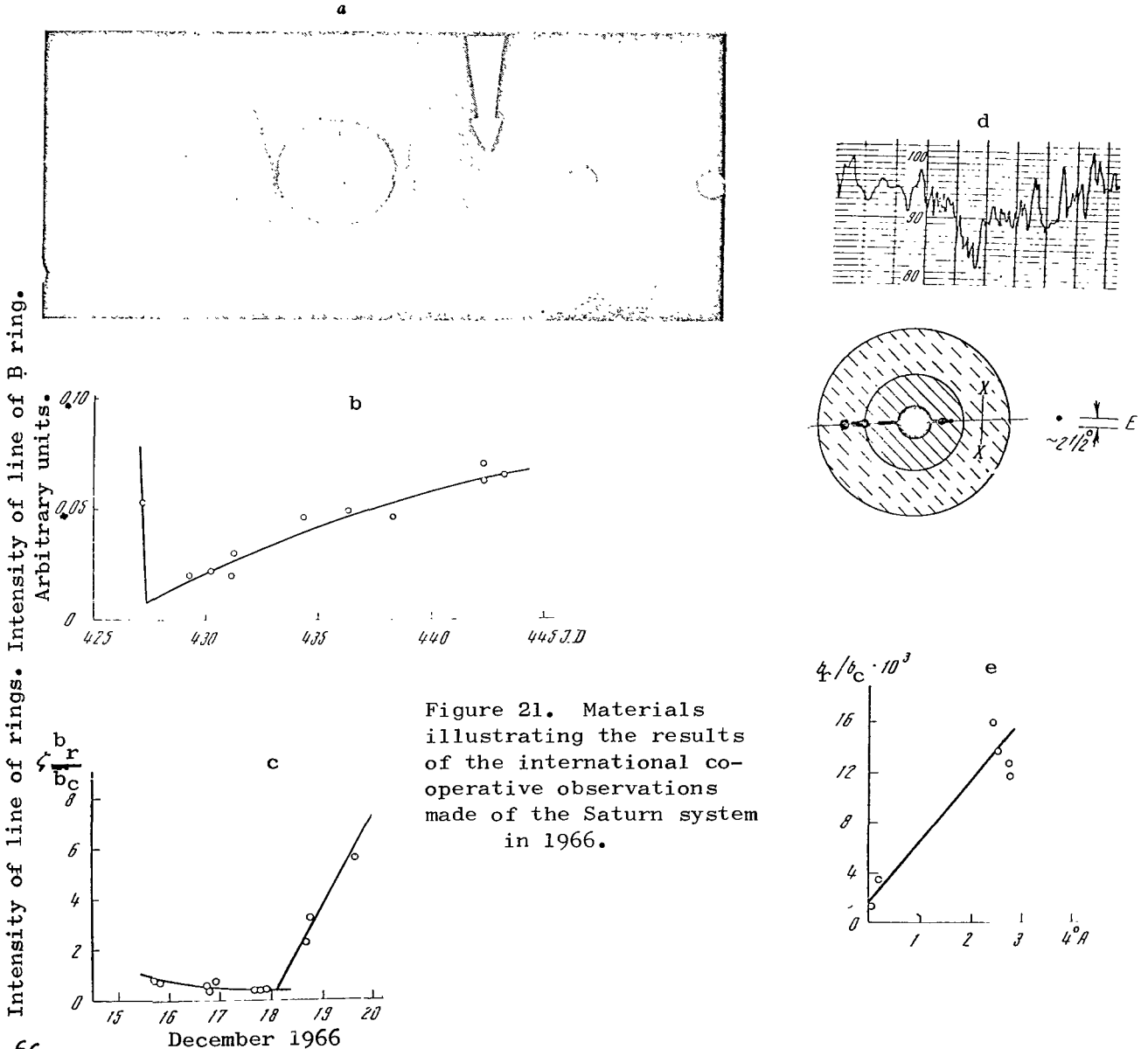


Figure 21. Materials illustrating the results of the international co-operative observations made of the Saturn system in 1966.

Intensity of line of rings. Intensity of line of B ring. Arbitrary units.

$\frac{b}{b_c} \frac{r}{r_c}$

a - Print from a plate obtained by Dollfus on Pic du Midi on 15 December 1966. The luminance of Saturn's disk was artificially attenuated by a factor of 140 by an absorbing band. The rings have their dark side turned to the earth and are almost edge-on ($A' = 0^{\circ}2'.5$). The inside parts of the image of the rings sink into the intensive aureole of Saturn's disk. The arrow points to the new, tenth satellite of Saturn, discovered by Dollfus; b - Change in the intensity of the rings during the transit of the earth through their plane in October 1966, in the direction from the lighted side to the dark (photometric measurements made to estimate ring thicknesses; Kiladze, 1968); c - Similar measurement of intensity of rings in December 1966, when the earth intersected the plane of the rings in the opposite direction (Dollfus, Focas, 1968); d - Bottom - View of Saturn on 14 November 1966; Top - Microdensitogram along the line X-X. The decay in the center corresponds to the position of the visible thin line of the D ring (Feibelman, 1967); e - Luminance of the dark side of the rings as a function of the angle of elevation of the sun over their lighted side (Dollfus, Focas, 1968).

Let us add that the Dollfus and Focas photometry also contains data on the luminance of the lighted side of the rings in terms of the phase angle when the ring openings are extremely small. This is the first time for such observational material as well. Later on its analysis can be used to check existing theories of ring structure (#34).

Let us now turn to the curve for the intensity of the line of the rings as a function of A' near the time of transit of the earth through the plane of the rings (Figure 21b and c). The December curve (Dollfus and Focas) is very similar to the October one (Kiladze), differing from it only by the order of movement in terms of time of the steep and flat branches (corresponding to the bright and dark sides of the rings). The intensity within the limits of each branch near $A' = 0$ changes monotonically, and is practically linear. Significant inadequacies in both series are lack of measurements at the intensity minimum, and in direct proximity to it. This results in the shape of the curves over the section of the transit from the steep branch to the flat one remaining unknown. At the same time, it is apparent that the shape of the transition section should have a significant dependence on the shape of the ring cross-section. For example, plane-parallel rings should yield a linear intensity curve, with a minimum coinciding with the point of intersection of the branches. An elliptical /68 section gives a rounded minimum. If the thickness increases toward the outer edge of the ring system, the minimum will be flat. The presence of an absorbing

ring outside the visible ring system will cause a nonlinear decay in intensity to the minimum, and so forth. (Moreover, the intensity of the line of the rings will depend on the phase angle, α , and on the angle of elevation of the sun over the plane of the rings, A , but analysis of existing observational data shows that near $A' = 0$, the influence of α and A is slight compared with the influence of A').

Kiladze, as well as Dollfus and Focas, assumed that the ring intensity minimum occurs at the intersection of the two branches. We have seen that this applies with equal force to the plane-parallel rings hypothesis. Based on this assumption, the October series of measurements (Kiladze, in blue light) provides $z_0 = 1.6$ km, and the December ones (Dollfus and Focas, in yellow light) $z_0 = 2.8$ km, with a root-mean-square error of the order of 25 to 50 percent. At the same time, as in the case of the #21 calculations, it is assumed that the surface brightness of the edge is equal to the brightness of the most intense zone of the B ring at large openings.

Since the true behavior of the intensity in the transit section is unknown, strictly speaking we have no right to assume in the case of the ring thickness calculations, that they are plane-parallel. In that case, though, estimates of ring thickness can be purely formal in nature. So we must find z_0 by taking an approach that will be as free as possible from arbitrary hypotheses.

This calculation can be made if we use the results of the measurements Dollfus and Focas made of the intensity of the dark side image very close to $A' = 0$ (Figure 21c) on 17 December 1966. Three images were obtained on that night. The midpoint of the observations occurred at $t = 1966$ December $17^d 19^h .2$ UT, when $A' = 0$ in the "plane-parallel" approximation was $t_0 = 1966$ December $18^d 03^h .0$, from whence $t_0 - t = 7^h .8$ (at the end of the calculation we can consider the effect an error in t_0 , random or systematic, occurring as a result of the divergence of the figure of the rings from plane-parallel, has on the z_0 estimate). The mean of intensities measured on 17 December is $\bar{I}(t) = 0.39 \cdot 10^{-3}$ (in $\zeta b_r/b_c$ units, where ζ is the width of the eye of the rings on the microphotometer scanning line in seconds of arc, and b_r/b_c is the ratio of surface brightness of the rings to surface brightness of the center of Saturn's disk).

Let us compare $\bar{I}(t)$ with the contribution made to total intensity of the line of the rings by the dark side luminous flux. Let us designate this magni-

tude by $I_d/(t)$. It is obvious that $I_d(t) = \zeta b_d/b_c$, where b_d is the dark side brightness. The magnitude of the b_d/b_c ratio can be found from the graphic in Figure 21e, remembering that t corresponds to $A = 2^\circ.750$. This yields $b_d/b_c = 15.3 \cdot 10^{-3}$. With respect to ζ , $t_0 - t = 7^h.8$ corresponds to $\zeta = 3.4 \times 10^{-3}$ second of arc. The dark side contribution to total intensity then is $I_d(t) = 3.4 \cdot 10^{-3} \cdot 15.3 \cdot 10^{-3} = 0.052 \cdot 10^{-3}$, that is, 0.13 the measured intensity $\bar{I}(t)$. This important result indicates that at time t the luminous flux from the dark side was low compared with the total luminous flux. The 0.87 remainder of intensity evidently was contributed by the luminous flux from the edge of the rings, and this makes it possible to find the value of ring thickness without resort to the estimates made by Kiladze and Dollfus and Focas. Putting ring edge brightness, b_e , equal to the brightness of the lighted side of the rings during large openings, as above, we will have

$$z_0 = \frac{0.87 \zeta b_d}{0.13 b_e} = \frac{0.87 \cdot 3.4 \cdot 10^{-3} \cdot 15.3 \cdot 10^{-3}}{0.13 \cdot 0.673} = 0.52 \cdot 10^{-3} \text{ sec of arc} = \quad (22.4)$$

$$= 0.52 \cdot 10^{-3} \cdot 6.94 \cdot 10^3 = 3.6 \text{ km}$$

The random error in t_0 (estimated by the observers as $\pm 2^h$) has almost no effect on this result. In fact, if we take the extreme values of $5^h.8$ and $9^h.8$ for $t_0 - t$, we obtain z_0 equal to 3.2 and 3.5 km, respectively. Nor does the value used for b_d/b_c have much effect on z_0 . For example, if we take $12.0 \cdot 10^{-3}$ for b_d/b_c , rather than $15.3 \cdot 10^{-3}$, as we did above, (the figure is from Dollfus' observations on the night preceding the December transit of the earth through the plane of the rings), we will have $z_0 = 3.7$ km when $t_0 - t = 7^h.8$. Hence, we can take the Eq. (22.4) estimate as quite reliable.

This method provides a mean of $z_0 = 3.4$ km, which is 22 percent higher than the value obtained by Dollfus and Focas, and double that of Kiladze. The discrepancy can be explained simply by the systematic errors in the photometry, but at the same time the fact that what is suggested here is some deviation of the figure of the rings from plane-parallel cannot be precluded. This raises the question of whether or not the t_0 we found by assuming the rings to be plane-parallel ought to be corrected for the corresponding systematic error.

The reply must be in the negative. As a matter of fact, the approximately linear behavior of the branches, of the decay and the rise in the intensity, as shown in Figures 21b and c, reveals that photometrically the rings conduct them-

selves as a plane-parallel system when they are not very close to t_0 , so that their intersection with the mid-plane of the earth ought to take place very close to the time of intersection of the branches. Something else again is the fact that t_0 found in the plane-parallel approximation will not, generally speaking, be the time of the intensity minimum for the line of the rings, but /70 this is a question that more properly belongs to refinement of the ring thickness concept, rather than to the first plausible estimate of the order of the thickness. We should point out that during a more precise consideration it will be necessary to remember the poor definition of the boundaries of the figure of the rings, that is, the gradualness of the reduction in the volumetric density of the ring material with approach to the boundaries, as well as the gas-dust "atmosphere" of the rings (#23). But this consideration will require photometric data in the direct proximity of t_0 , and since there are no such data as yet, all possible considerations in this regard can be nothing more than speculative.

Summing up, it can be said that one of the main goals of the international patrol observations of Saturn in 1966, has been achieved. The thickness of the rings, a parameter that for many years had escaped observational estimation, has been established. It is of the order of 3 to 4 kilometers.

#23. "Atmosphere" of the Rings.

The first evidence of the existence of evacuated material enveloping the rings was the effect of some residual brightness in the space between the inner boundary of the C ring and the ball of Saturn, discovered in blue light by Barabashov and Semeykin (1933; see #3 of this book). Maggini (1937; see #13, Figure 11) discovered two other effects: (1) a gradual darkening of the rings with reduction in the angle of elevation of the sun, A , above the plane of the rings, wherein reduction in A from $2^{\circ}.06$ to $1^{\circ}.01$ resulted in a decay in the brightness of $1^m.2$ for $\lambda = 5300 \text{ \AA}$, and of $1^m.6$ for $\lambda = 4200 \text{ \AA}$; (2) a simultaneous increase in the ring color equivalent. These results certainly point to the presence of some evacuated material above the plane of the rings (Maggini even reports that he was able to observe it visually, and that it blanketed the plane of the rings on both sides. This has not been confirmed by other observers, however). In 1966, Kozyrev, using the 122-cm reflector in the Crimean Astrophysical Observatory of the Academy of Sciences of the USSR, made spectrographic

observations of the shadow of the rings on the ball of Saturn (see Kozyrev, 1968). The direction of the solar rays was almost parallel to the plane of the rings, so the path of the solar radiation inside the suspected "atmosphere" of the rings was long enough for it to be observed. The observer found the NH_3 band to be stronger in the shadow of the rings, and the CH_4 weaker, than outside it (indications of the hothouse effect created by the "atmosphere" of the rings). He also noted the presence of H_2O vapors, and estimated the thickness of the shell to be between 5,000 and 10,000 km. There is reason to think that the processing of materials obtained by other observatories in 1966, will even further enrich our information on the shell of the rings.

VI. Ring Dynamics

#24. Ring Rotation Law

One of the most important dynamic features of Saturn's rings is that their mass (M_r) is extremely small compared with the mass of Saturn (M_h). This is shown by the observed fact (#8) that the speed of rotation for any ring zone is almost precisely equal to the Keplerian circular velocity. This would be the ring rotation law for the condition that there is little disappearance of M_r as compared with M_h . The contrary, extreme case is a homogeneous disk without central condensation. It would rotate as would a solid body. If the M_r/M_h ratio were not very small, the ring rotation law would be somewhere between these two extreme cases. But the spectroscopic data on ring velocity as a function of r (#8, Table 2) fail to show systematic deviations of the rotation law from the Keplerian law.

H. Struve (1898) attempted to estimate (M_r/M_h) from the observed movements of the pericenters and nodes of the internal satellites of Saturn. But these movements are mandatory not only for the rings, but for the flattening of Saturn as well. It is very difficult to separate the effects. In fact, a more or less valid solution to the problem requires a knowledge of the density distribution law in the ball of the planet, as well as the precise value for the flattening of Saturn. Actually, knowledge of both these magnitudes (and particularly of the first) is only approximate. Consequently, Struve's estimate of $M_r/M_h = 1/27000$, cited in all the handbooks, is viewed as without foundation by Brower and Clemence (1963), as well as by Yabushita (1966). Yabushita adds that it is his view that the observed estimate of M_r/M_h cannot be arrived at other than by optical observations. The author (Bobrov, 1956b, 1961) made several attempts of this type, based on the theory of the effect of mutual shading, as did Franklin and Cook (1965) later on. We shall discuss this question in Chapter VII.

At the same time, it seems that a comparison of the Keplerian rotation law /72 with the actual ring rotation law (obtained from extremely accurate spectrographic observations which should be made especially for this purpose) would, in principle, make it possible to estimate the upper limit of M_r/M_h from dynamic considerations.

#25. Differential Rotation and Its Consequence

Correctness of a Keplerian rotation law for Saturn's rings implies differential rotation. This effect is very great and is capable of destroying any condensation (or evacuation) that could occur in the ring material in a very short period of time.

In fact, the Keplerian circular velocity for a narrow zone of the rings at distance r from the center of Saturn is

$$v_{\text{km/s}} = 6.16 \cdot 10^3 / r_{\text{km}}^{1/2}, \quad (25.1)$$

whence

$$\left| \frac{\Delta v}{v} \right| = \frac{1}{2} \frac{\Delta r}{r}, \quad (25.2)$$

where Δr is the width of the zone; Δv is the corresponding difference in velocities. We also can write $\Delta s(t) = \left| t \Delta v \right| = 1/2 \omega t \Delta r$, where ω is the angular velocity of the inside edge of the zone; Δs is the relative displacement in the two points, which, at time $t = 0$, have identical azimuths and are located at distance Δr from each other. Let us use T and n to designate the period of rotation and the number of revolutions of a point on the inside edge of the zone.

$$\Delta s(nT) = \pi n \Delta r. \quad (25.3)$$

If, for example, $\Delta r = 1000$ km, and $n = 1$

$$\Delta s = 3140 \text{ km}. \quad (25.4)$$

Such is the displacement of points of the inner boundary of a zone 1000 km wide with respect to points on its outer boundary during one revolution (regardless of r).

Here a few words need be said about the so-called Roche limit and its relationship to ring dynamics. According to Roche, (1850), the homogeneous, unflattened, liquid satellite would be torn by tidal forces if it approached the central body at distance

$$r_s = 2.45 \sqrt[3]{\delta_p / \delta_x} r_p, \quad (25.5)$$

where r_p is the radius of the central body (the planet, in this case); δ_s and δ_p are the densities of satellite and central body, respectively. Note that only the gravitational forces (the molecular cohesion is ignored) are considered in Eq. (25.5). /73

Some authors raise the question of whether Saturn's rings lie inside the Roche limit, or whether they are, in part, beyond that limit, and then they proceed to discuss the physical and cosmogonic consequences of this fact. As will be seen from Eq. (25.5), the reply to the first question depends on the value of δ_s . Specifically, if it is taken that $\delta_s = 3$ (stony particles), it will seem that Saturn's rings lie inside the Roche limit, but only in part. But if it is taken that $\delta_s \sim 1$ (ice particles), the rings will lie almost entirely inside the limit. This sometimes leads to the conclusion that (I) Roche's formula indicates a preference for ice particles, and (II) that inside the Roche limit the tidal forces hamper the gravitational condensation of the particles.

So far as conclusion (I) is concerned, it should be pointed out that according to Jeffreys (1947a), who considered not only the gravitational forces, but molecular cohesion as well, the ice ball, which is inside Roche's limit, will be torn by tidal forces only if its diameter is in excess of 200 km. Yet observations show that ring thickness is between 3 and 4 km. Thus, the question of the nature of the particles has no relation to Roche's limit (providing it is not assumed that the rings were formed as a result of the explosion of a comparatively large satellite that approached the planet to a distance less than Roche's limit, a hypothesis that has no confirmation in contemporary cosmogony).

Conclusion II lacks persuasion as well because Eq. (25.3) and (25.4) show that in the case of Saturn's rings, any condensation of the particles will be disrupted in a very short period of time simply because of differential rotation.

#26. The Physical Condition of the Ring Material

It is completely evident to modern astronomy that Saturn's rings consist of a multiplicity of individual solid particles, but it still is useful to review here the arguments advanced to preclude any other possibilities.

The Keplerian rotation law evidently precludes the possibility that the A, B, and C rings can be monolithic, solid bodies. Liquid rings would reflect Saturn's ball, an effect that never has been observed. The rings would have low reflectivity, and the A and B rings would be substantially less bright than they in fact are. They could be made up of just hydrogen and helium. Other substances cannot remain liquid at $T \sim 65^\circ\text{K}$ (#15) and at very low pressure. Yet ring spec- /74

trometry (#10) has detected the presence of solid H_2O , and not liquid hydrogen, or helium. Also completely evident is the fact that the rings are not gaseous.

So the rings can be made up of nothing other than solid material. However, because the rings have differential rotation, they can be a system of many narrow, concentric, ring-like zones, or a flat cloud made up of many tiny satellites. Laplace (1802) eliminated the first possibility. He proved that a narrow, homogeneous ring, rotating with constant angular velocity around a gravitating center, will be unstable. Kowalewsky (1885) refined the shape of the cross-section of a ring such as this, and Maxwell (1859) showed that the stability of a ring such as this can be achieved only by the addition to it at one point of a satellite with mass corresponding to $4 \frac{1}{2} M_r$. The observations are not in favor of this model. Consequently, Saturn's rings should be clouds of independent, solid particles.

#27. Stability

The research that has been done on the problem of the stability of Saturn's rings is extensive. Of that research, that of Duboshin (1940) contains in addition an extremely complete critical review of the preceding results. Hagihara (1963) includes a list of later efforts. This section reviewed the problem of ring stability primarily from the physical side. Particular attention is devoted to an analysis of the role of the collisions between particles, and to questions concerned with an observational verification of the theory. Hence, we certainly will not be able here to discuss all of the available papers on the subject.

(a) Maxwell's stability criteria for a ring of collisionless particles.

Maxwell (1859) analyzed the case of the narrow, monolithic ring, as well as that of a ring consisting of independent particles. The first model Maxwell considered was an elementary ring of μ equal particulates. The mean positions of the particles will move around Saturn at equal distances in the same circular orbit, and at the same Keplerian velocity. Mutual gravitational perturbations of the particles will force them to oscillate near these mean positions. The oscillations will produce crowding and thinning in the elementary ring, propagating tangentially as waves of some kind. Maxwell notes that the wave, at a fixed moment in time, has what is, generally speaking, an arbitrary shape, but that it can be represented by the sum of the elementary waves through a Fourier series. Maxwell deduces the following condition for which the amplitude of the waves will remain finite

$$\lim_{\mu \rightarrow \infty} \mathfrak{M}_r < 2.298 (\mathfrak{M}_p / \mu^2). \quad (27.1)$$

This is the stability criterion for an elementary ring of equal particles. Eq. (27.1) shows that the ring is stable if its mass is small compared with Saturn's mass (the larger the number of satellites, μ , the smaller $\mathfrak{M}_r / \mathfrak{M}_p$ should be).

Of the other models considered by Maxwell, the one of greatest, significant interest is the ring-shaped cloud of independent particles rotating around Saturn as a whole, that is, at a single angular velocity. Using the same method here as he did for the elementary ring, Maxwell concluded that the ring would be stable if the condition

$$\delta_r < 1/300 \delta_p, \quad (27.2)$$

were satisfied. Here δ_r and δ_p are ring and Saturn densities, respectively. If the conditions of Eq. (27.2) were not satisfied, the ring would be destroyed by tangential waves because their amplitudes would rise to infinity.

It should be emphasized that Eq. (27.2) ignored differential rotation. But since the latter plays so important a role in the case of Saturn's rings (#25), it can be assumed that some system of crowding, or of waves, capable of destroying the rings, will in fact itself destroy the differential rotation before perturbation reaches a dangerous magnitude. If this is so, Maxwell's upper limit of permissible ring density, Eq. (27.2), is greatly underestimated.

This contradiction passed unnoticed until very recently, when Cook and Franklin (1964, 1966) reviewed Maxwell's investigations. They found that the critical density in fact is considerably in excess of $1/300 \delta_p$. We shall return to this question a little later on.

(b) The effect of collisions between ring particles. Maxwell discusses this at the end of his paper. He reviews a model one particle thick (a series of concentric elementary rings) and concludes that the resonance phenomena occurring in this system will cause the perturbations to increase exponentially and as a result the particles should begin to collide with each other. The collisions (not entirely elastic) will lead to the radial expansion of the ring,

or to the radial redistribution of its surface density. Maxwell also points to the tendency of the system to form short-lived, narrow zones with a reduced surface density between them.

It must be pointed out, however, that resonance phenomena can only occur /76 when there is no differential rotation. Since the latter cannot be ignored, what must be expected is not resonance, but long-period beats. Goldsbrough (1951) made a quantitative analysis of this case (for two elementary rings) and found that the system can be maintained stable, providing its mass is small enough as compared with Saturn's mass.

Jeffreys (1947b) took the next step in the discussion of the effects of collisions on Saturn's rings. He concentrated on the dissipation of energy attributable to the partially inelastic nature of the collisions, and concluded that the dissipation gradually should suppress the oscillations of the particles near the mean positions, and that, finally, the ring should be converted into a collisionless system one particle thick. Jeffreys estimated that this process should take place over a very short period of time, cosmogonically speaking.

Jeffreys assumed that the finite condition of the ring system he found did not contradict observational data, including the photometric data. This is not so, in fact. A one-particle thickness system with the brightness of the B ring cannot yield the observed "logarithmic" shape of the phase curve near opposition (see Chapter IV). In other words, observations show that factors exist that prevent the rings from reaching a state of complete flattening.

But then the system is not collisionless, the energy of the oscillations of the particles gradually is dissipated, and the only possibility of preventing complete flattening lies in a continuous replenishment of this energy by some source with adequate capacity. The possible mechanisms of such replenishment will be taken up in #28.

(c) Latest research. As we already have pointed out, Maxwell's work recently was reviewed by Cook and Franklin (1964, 1966). This was wide-ranging theoretical research in which the authors analyzed seven models of ring systems. They used Maxwell's method; that is, they reviewed the compression and expansion waves propagating in the rings, and assumed that if the amplitudes of the waves

rose without limit, instability would result. The opposite case would mean stability.

The authors pointed out, and eliminated, three of Maxwell's errors at the same time. The most important error (the one that led Maxwell to his great underestimation of the upper limit of permissible density) was closely associated with the fact that Maxwell ignored the effect of differential rotation. He considered two types of waves, one of which is the result of the tangential component of the oscillations of the particles in the azimuthal direction, the other the result of the radial component, and propagated radially. Retaining the terminology used by Cook and Franklin, we will call these two types the tangential /77 and radial waves. Maxwell noted, and Cook and Franklin confirmed, the fact that the tangential waves become unstable sooner than do the radial waves. This was the fact upon which Maxwell based his conclusion that ring stability depended solely on the tangential waves, and thus arrived at his density criterion in Eq. (27.2). In fact, the presence of differential rotation can very quickly convert a tangential wave into a radial wave (see our example in #25), and this led Cook and Franklin to conclude that it is not the tangential, but the radial waves that control ring stability. This opinion (whether it is, or is not, correct will be discussed later) is the authors' point of departure. They used their mode primarily to estimate the critical density of the rings satisfying the condition of stability for radial waves. Recognizing that the width to thickness ratio for Saturn's rings is very great, the authors ignored ring curvature and limb effects in all their models. Their final conclusion was that the ring system is gravitationally stable if the system's mean density is less than 0.18 g/cm^3 , and that it is unstable if the mean density is greater than 1.04 g/cm^3 . We should emphasize the fact that even the smallest of these values is larger than the Maxwellian upper density limit by a factor of approximately 80. The limits of the region in which the critical value of the $\mathbb{M}_r/\mathbb{M}_p$ ratio is contained can be obtained at once from these estimates. Actually

$$\left(\frac{\mathbb{M}_r}{\mathbb{M}_p}\right) = \pi(r_2^2 - r_1^2) z_0 \delta_r \quad (27.3)$$

where r_1 and r_2 are the internal and external radii of the ring system; δ_r is the mean density of the rings. Substituting $r_1 = 0.89 \cdot 10^{10} \text{ cm}$, $r_2 = 1.39 \cdot 10^{10} \text{ cm}$, $z_0 = 10^5 \text{ cm}$, and using the δ_r estimate cited above, we obtain

$$\frac{1}{88000} \leq (\mathfrak{M}_R/\mathfrak{M}_T)_{\max} < \frac{1}{15000}. \quad (27.4)$$

Yabushita (1966) is another who made a recent estimate of $(\mathfrak{M}_R/\mathfrak{M}_T)_{\max}$. He too investigated the stability of the rings in terms of axisymmetrical perturbations, but he took ring curvature, limb effects, and (somewhat arbitrarily) the radial distribution of the density, into consideration. His results differ even more from those of Maxwell

$$\frac{1}{480} \leq (\mathfrak{M}_R/\mathfrak{M}_T)_{\max} < \frac{1}{26}. \quad (27.5)$$

(d) Objections to the conception of wave-like perturbations. We shall not, here, seek the reasons for the striking lack of agreement between Eqs. (27.4) and (27.5), but will point out the following weak points in both investigations. /78 The authors proceeded on the assumption that azimuthal waves with a wave front extending over the entire width of the ring, and radial waves with a wave front extending over the entire circumference of the ring, could exist. Neither assumption has a physical basis. In fact, there is no physical reason for the creation in a ring with differential rotation of compression (expansion) of the order of 10,000 km in length extending in the radial direction, or of the formation of a radially propagating ring-like perturbation in which all particles would oscillate in identical phase over 360°. This is so because the criteria of stability, based on similar assumptions, cannot be trusted.

Here the question of the shape of the density perturbation that occurs when the ring approaches a state of gravitational instability is of much interest. The answer is as follows. The most probable answer is that increase in $(\mathfrak{M}_R/\mathfrak{M}_T)$ will create random fluctuations in density, rather than waves. The only shape for perturbations such as this is an ellipsoid with a density somewhat greater than its surrounding region. It should be greatly flattened with respect to the z coordinate because $(r_2 - r_1) \gg z_0$. The dimensions, and the life span, of the ellipsoid will depend on the differential rotation velocity, or in other words, on the value of $(\mathfrak{M}_R/\mathfrak{M}_T)$. We may recall that this presentation was analyzed in detail by Gurevich and Lebedinskiy (1950) for a protoplanetary cloud.

Let us point out as well that if $(\mathfrak{M}_R/\mathfrak{M}_T)$ were so large that the effect of differential rotation turned out to be small, the objection to wave-like perturbations would vanish. This is not so in the case of Saturn's rings, however, because spectroscopy of the rings has detected significant differential rotation.

(e) Observational indications that the rings are far from unstable. There is yet another shortcoming common to the work done by Cook and Franklin, and by Yabushita. This is that the problem of the stability of Saturn's rings was analyzed as if the rings were an object not susceptible to direct observations. In point of fact, during this century the rings have been thoroughly studied by Lowell, Barnard, Lyot, Dollfus, Camichel, Kuiper, and other very experienced observers under conditions providing good, and even excellent, images and high resolution. Not a trace of moving, heterogeneous ring material has been observed (in the form of radial or tangential waves, or in the form of ellipsoids). All observers report stable, ring-like divisions (Kirkwood's slits), attributable to resonancy with the internal satellites of Saturn (#1), and minor azimuthal differences in brightness, such as the nonuniform brightness of the eyes, and the like (#13). The causes of the azimuthal effects are unknown, but their definite orientation with respect to the sun indicates that they can be attributed to the influence of solar radiation. In any case, it would be extremely unjustified to say that they are connected with dynamic instability.

So far as the minimum nonuniformity that can be observed in the dimensions of Saturn's rings from a high mountain observatory (Pic du Midi, or Lowell, for example) is concerned, its magnitude is of the order of $0''.1$ to $0''.2$ for ring-like nonuniformities, and of the order of $0''.2$ to $0''.4$ for bright or dark spots (here we are assuming that the nonuniformities have adequate brightness contrast with their surroundings). It is between 700 and 1400 and 1400 and 2800 km, respectively. Comparing these numbers with Eq. (25.4), one can be persuaded that a spot from 1400 to 2800 km in diameter would be destroyed by differential rotation within one, or two, revolutions (one day, or less). A small nonuniformity with a diameter of 4 km would have a life span of the order of one year. In other words, long-term existence, even of such small condensation densities as 4 km, is not compatible with the observed magnitude of the differential rotation of the rings.

So, direct observations show that the rings are far from unstable. The mass of Saturn is many orders of magnitude in excess of the mass of the rings, and damps even small fluctuations in density in short order.

#28. Mechanisms That Possibly Prevent Complete Flattening of the Rings

Let us turn to the problem touched upon in #27, that of the former Jeffreys Conception, in accordance with which the rings are a one-particle thickness system, but which has been contradicted by observations. If this is so, collisions should occur between the particles, and there should be continuous dissipation of the particle oscillation energy. Just what mechanisms are there that can be involved in replenishing the energy capable of preventing the complete flattening of the rings during the life span of the solar system?

One obvious mechanism is that of gravitational perturbations of the particles by Saturn's satellites. The perturbations could be of several types: short-period, long-period, resonance, and the like. Resonance perturbations are effective only for narrow zones, within the limits of which there is commensurability of the periods of rotation of particles and satellites (that is, for the divisions). They cannot, therefore, prevent the complete flattening of the ring system as a whole. Short-period perturbations are of greatest interest in the case of frequent collisions (yet only the differential effects are important). There are no estimates of their effectiveness as yet. Long-period perturbations are important in the case of rare collisions. Calculations made at our request by the Shternberg State Astronomical Institute provided the following results. Perturbations from the accumulation of the orbits of particles of Mimas, Tethys, /80 and Titan create amplitudes of oscillation of particles along the z coordinate of 16, 47, and 106 meters, respectively, at the outer boundary of the ring system. The period of the perturbations is of the order of 400 revolutions of a particle. Long-period perturbations, therefore, can be effective only in very transparent zones of the rings (in the internal zones of the C ring, for example), where collisions are extremely rare.

Collisions should be frequent in the A and B ring regions. In order to show this, let us compute the l/z_0 ratio, which is the ratio of the mean length of the free path of a particle to the ring thickness. Let us assume that the particles have the same radius, ρ , and that they are distributed at random in a plane-parallel layer with thickness z_0 and optical thickness

$$\tau_0 = \pi \rho^2 N_{a0} / R, \quad (28.1)$$

where N is the number of particles in the ring; R is the volume of the ring. The mean length of the free path for the particle is

$$l = R/4 \sqrt{2\pi\rho^2 N}, \quad (28.2)$$

Comparing these expressions, we obtain

$$l/z_0 = 1/4 \sqrt{2}\tau_0. \quad (28.3)$$

When $\tau_0 = \tau_{OA} = 0.6$ and $\tau_0 = \tau_{OB} = 1$, the values 0.18 and 0.30 are obtained for l/z_0 , respectively. Thus, collisions in the A and B rings are frequent.

In this case the source of energy compensating for dissipation during collisions can be the energy of differential rotation of the ring. Actually, differential rotation creates transfer of the pulse moment in the direction of increase in the radius of the ring, r . Since the collisions are not central collisions, generally speaking (the probability of what would be central collision, strictly speaking, is zero), the transfer of pulse moment is accompanied by frequent conversions of differential rotation energy into random particle motion energy near their mean positions; into "heat." Dissipation of energy can be considered as "cooling" the ring, because of the less than complete elasticity of the particles. The two processes cancel each other in the stationary state. z_0 remains constant, but the total mechanical energy of the ring decreases steadily. The result is that all particles slowly approach Saturn.

Let us introduce a formula for z_0 as a function of the mean velocity of random motion, \bar{u} . We will assume that the reduction in energy attributable to the less than total elasticity during each collision is completely balanced by the above-indicated "heating." In fact, there is only a mean compensation, but if the collisions are frequent, the behavior of the system will be close to the case of completely elastic collisions. Specifically, velocity distribution will be close to Maxwellian.

Since the system is unusually flat, and since $\frac{M}{R^3}$ is extremely small, the random motion of a particle along the z coordinate (that is, normal to the plane of the ring) can be considered a harmonic oscillation in Saturn's gravitational field. Its amplitude then is

$$z_{\max} = (u_z/\omega), \quad (28.4)$$

where u_z is the component of the random velocity in terms of the z coordinate when $z = 0$; ω is the angular velocity of the circular Keplerian motion of the particle. In turn, the distribution of the particle concentration in terms of the z coordinate will be described by the Boltzmann equation

$$n(z) = n(0) \exp(-E_p/kT). \quad (28.5)$$

Substituting $E_p = 1/2 m \omega^2 z^2$ and $kT = 1/3 m \bar{c}^2 = 1/8 \pi m \bar{u}^2$ (where c and \bar{u} are the mean-square and the mean velocities, respectively), we obtain

$$n(z) = n(0) \exp(-4\omega^2 z^2 / \pi \bar{u}^2). \quad (28.6)$$

Let us introduce the effective physical thickness $z_{o \text{ eff}}$, satisfying the condition

$$n(z_{o \text{ eff}}/2) = n(0) \exp(-1). \quad (28.7)$$

A comparison of Eq. (28.6) with Eq. (28.7) will yield

$$\bar{u} = \omega z_{o \text{ eff}} / \sqrt{\pi}. \quad (28.8)$$

It can be shown that about 84 percent of all the particles can be contained between the $+z_{o \text{ eff}}$ and $-z_{o \text{ eff}}$ planes.

Now let us estimate the z_o value that can be maintained constant for time t of the life of the solar system attributable to the expenditure of mechanical energy by the particle, if the radius of the particle's orbit changes from r_o to r_t in that time.

According to the hydrodynamics of a viscous, incompressible medium, the amount of energy converted into heat (in a unit of volume in a unit of time) during the transfer of pulse moment is

$$-(dE/dt) = \eta r^2 (d\omega/dr)^2, \quad (28.9)$$

where $\eta = 1/3 \bar{u} \delta$, and is the coefficient of internal friction; (δ is density of the medium). Mindful of the fact that the mechanical energy of the particle is

$$E_p = \gamma m \frac{M_\gamma}{r^2}, \quad (28.10)$$

where γ is the constant of gravitation, and that

$$r^2 (d\omega/dr)^2 = 9/4 (\gamma M_\gamma / r^3), \quad (28.11)$$

and resorting as well to the use of Eqs. (28.3) and (28.8), in place of Eq. (28.9), we obtain

$$-r^{5/2} dr = (3 \sqrt{\frac{2\pi}{\tau_0}} z_{o \text{ eff}}^2 / 8 \sqrt{2\pi\tau_0}) dt, \quad (28.12)$$

implying

$$z_{o \text{ eff}}^2 = \frac{16}{27} \left(\frac{2\pi}{\tau_0} \right)^{3/2} \frac{r_0^7}{8} [1 - (r/r_0)^7]. \quad (28.13)$$

In order to use this equation to estimate $z_{o \text{ eff}}$, let us assume for example that a particle that now is located close to the center of the B ring ($r = r_t = 1.00 \cdot 10^{10}$ cm) was, at the beginning of the existence of the ring system, at distance $r = r_o = 1.37 \cdot 10^{10}$ cm (the present day outer boundary of the system). Then, setting $\tau_0 = 1$, and $t = 5 \cdot 10^9$ years = $1.58 \cdot 10^{17}$ seconds, we find

$$z_{o \text{ eff}} = 35 \text{ m} \quad (28.14)$$

The apparent physical thickness of the rings, $z_{o \text{ app}}$, is considerably more than this when the rings are viewed precisely edge-on. The judicious thing to do is to define $z_{o \text{ app}}$ as the thickness of a layer having an optical thickness along the plane of the rings at the boundaries equal to unity. In such case $z_{o \text{ app}}/z_{o \text{ eff}} \approx 3.5$. The just considered mechanism therefore is capable of sustaining

$$z_{o \text{ app}} \approx 120 \text{ m} \quad (28.15)$$

for $5 \cdot 10^9$ years. Since we have assumed that all the particles are of a size, this estimate is the low limit for $z_{o \text{ app}}$.*

Let us add that in accordance with Eqs. (28.8) and (28.14), the mean velocity of the random movement of the particles is about 0.4 cm/s. The impact force during collisions should not be great, therefore, and the Newtonian coefficient of restitution should be close to unity (see Goldsmith, 1965).

* * The observed thickness of the rings (established for the first time in 1966, and for which see #22) is of the order of 3 to 4 km.

* Equation is illegible in original text - Translation editor.

#29. Introductory Remarks

As soon as we have established that the mutual shading of the particles is the principal effect responsible for the observed shape of the phase curves for the rings (#18) we can estimate the volumetric density of the rings, D , from the theory of this effect. Then a knowledge of the order of thickness of the rings, z_o (#22) and of the particle density, δ_p , enables us to estimate the total mass of the rings, M_r , just as knowledge of z_o , and of the optical thickness, τ_o (#14), enables us to estimate the mean radius, ρ , of a particle of the ring.

The mechanism involved in the mutual shading effect is very simple, qualitatively speaking. Let us suppose that we have a plane-parallel layer of particles illuminated by the sun and observed from the earth (the angles of elevation A and A' , respectively). Let us take it that the thickness of the layer is many times that of ρ , that is, that we have a many-particle thickness system. Particles located closer to the sun cast their shadow on particles farther from it. But these shadows cannot be seen from the earth at the time of exact opposition ($\alpha = 0$), because every particle shields its own shadow. With increase in α , the shadows gradually emerge from the disks of the particles, and the mean brightness of the system diminishes.

We are indebted to Seeliger for this concept. He also was the first to develop the quantitative theory of this effect (Seeliger, 1887, 1893).

#30. The Seeliger Approximation

The reader should keep in mind that the theoretical research done by Seeliger on the phase function of Saturn's rings, and its association with the structure of this object, was carried out almost 80 years ago, before spectrographic observations were made of ring rotation (Belopol'skiy, Deslandres, /84 Keeler, #8), long before direct measurements were made of the surface brightness

* See the Appendix (pp. 118-119 for the notations used in the formulas in this chapter.

of the rings (Schoenberg, Hertzprung, #12), and much earlier than the formulation of the theory of the multiple scattering of light (Ambartsumyan, Sobolev, Chandrasekhar). Nor had Mie's diffraction theory been formulated.

The proximate cause of Seeliger's research evidently was the results of Müller's measurements (1893) of the integral brightness of the Saturn system as a function of A' and α . Müller found a value of 0.044 stellar magnitude/degree of phase for Saturn's phase coefficient, a value far in excess of Jupiter's phase coefficient (0.015) and of the phase coefficients of other planets. Seeliger showed that he was extremely perspicacious by postulating that this fact could be attributed to the "meteoritic" structure of Saturn's rings. The idea of the "meteoritic" structure was borrowed from Maxwell (1859).

Seeliger, in his theory, considered only first order scattering, dictated by the level of knowledge of the time. In his first paper he wrote of a ring made up of particles of identical size, but his second paper included generalization of a theory dealing with the case of particles not all of the same size. The sun was replaced by a point source of light at infinity, and it was taken that the particles were macroscopic, diffusely reflecting spheres. The natural phase function of the particle was taken into consideration by introducing a factor that was dependent on α . Seeliger, in this approximation, obtained formulas for calculating the phase function.

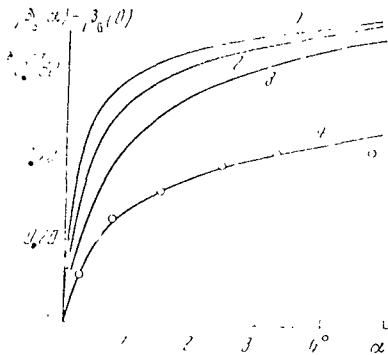


Figure 22. Discrepancy between Seeliger's phase curves and the observational curves.

1, 2, 3 - theoretical phase curves (Seeliger, 1887) for $D = 3.75 \cdot 10^{-3}$, $6.25 \cdot 10^{-3}$ and $1.25 \cdot 10^{-3}$, corrected for the natural effect of particle phase and for higher order scattering; circles are the means from Schoenberg's observations (1933); 4 - observed phase curve for B ring, constructed using these points [Eq. (12.1)].

Direct measurements of the surface brightness of the A and B rings as a function of α (Hertzprung, 1919; Schoenberg, 1921, 1933) detected a great discrepancy between Seeliger's theoretical phase curve and the observational data

(Figure 22). This author (see Bobrov, 1940, 1959, 1967) demonstrated that these discrepancies arose because Seeliger's approximation did not reproduce the condition of Saturn's rings accurately enough, in that (1) he disregarded /85 the angular dimensions of the solar disk ($\sim 3'.5$), (2) he did not consider multiple scattering, and (3) he assumed that all sizes of particles were equally probable.

We postulated that an approximation free of these limitation would satisfy the conditions for Saturn's rings incomparably better than would Seeliger's approximation. This approximation of the theory was constructed and was in extremely good concordance with observations. It will be reviewed in the sections that follow.

#31. The "Cone-Cylinder" Approximation, Without Variance in the Sizes of Particles Taken into Consideration

The shadow of a particle in Seeliger's approximation is an infinitely long cylinder, because of his limitation (1). The volume behind the particle, in which the ring material is shielded from the observer by the disk of the particle, too is an infinitely long cylinder. We can call this scheme the "cylinder-cylinder" approximation.

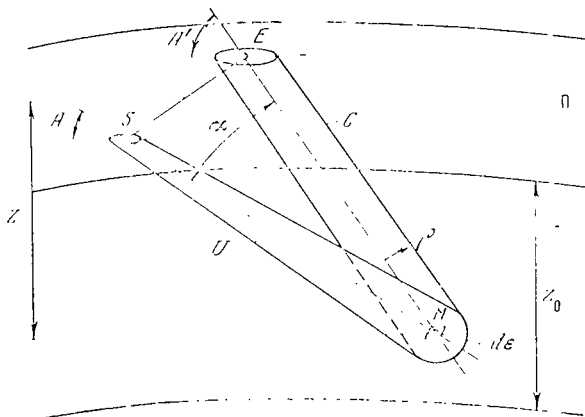


Figure 23. Schematic View of the eye of Saturn's rings.

The element de belongs to a particle arbitrarily selected at depth z , measured from plane Π (closest to the sun). The straight lines MS and ME are directed toward the sun, and toward the earth, respectively. C is the cylinder of shielding; U is the cone of shading; ρ is the particle radius; α is the phase angle; A and A' are the angles of elevation of the sun and earth over the plane of the rings.



Let us remove limitation (1), and let us say that at the mean distance of Saturn from the sun, the disk of the latter has an angular radius of

$$\varphi = 1'.676; \quad 1/\varphi \approx 2.0 \cdot 10^3. \quad (31.1)$$

The shadows of the particles then will be cones with a finite length of ρ/φ , /86 where ρ is the particle radius. But at the same time, the shielded volumes remain infinitely long cylinders. We obtain the "cone-cylinder" approximation.

(a) Amplitude of change in brightness with phase angle when penumbra is disregarded. Let us look at Figure 23. Some particle, striking the center of volume C, or U, shields element $d\epsilon$ from the earth, or from the sun, respectively. In the case of the former the element $d\epsilon$ will be shielded by the disk of the particle considered. In the case of the latter the particle will cast its shadow on $d\epsilon$. The shadow of the particle should be considered as black with an accuracy of within first order scattering, so that the element $d\epsilon$ will be seen from the earth only for the period of time when the centers of all the other $N-1$ particles of the rings (N is the number of all particles) will be outside the so-called volume of probability

$$V = C + U - W, \quad (31.2)$$

where W is part of V , the total of C and U .

The probability that $d\epsilon$ will be seen is

$$p := [(R - V)/R]^{N-1} \approx \exp(-VN/R), \quad (31.3)$$

where R is the volume of the ring. The mean luminous flux transmitted to the earth by element $d\epsilon$ when the latter is not shielded, and is not shaded. For the many-particle thickness system, all layers not too close to plane Π satisfy the condition

$$\rho \ll z. \quad (31.4)$$

Further, if the volumetric density is

$$D := \frac{4}{3} \pi \rho^3 (N/R) \quad (31.5)$$

which is small compared with unity, Eq. (31.4) can be satisfied by practically all particles that can be shielded, or shaded. This means that for all elements $d\epsilon$, the probability of no shielding, or shading, by the same particle is practically the same. Consequently, the light flux from this particle will be

$$F = pF_0 = I'(\chi) \exp(-VN/R), \quad (31.6)$$

where Γ is the value of F_0 when $\alpha = 0$ and $f(\alpha)$ is the particle's natural phase function.

We can, therefore, write the following expression for the amplitude of the change in ring brightness when α changes from 0 to $\alpha_{\max} \approx 6^\circ.5$:

$$\frac{b_1(\alpha_{\max})}{b_1(0)} = \frac{f(\alpha_{\max})}{f(0)} \frac{\int_0^{\alpha_{\max}} \exp[-(N/R)V(\alpha)] d\alpha}{\int_0^{\alpha_{\max}} \exp[-(N/R)V(0)] d\alpha}. \quad (31.7)$$

Since, when $\alpha = \alpha_{\max}$

$$W \ll C + U, \quad (31.8)$$

(see Bobrov, 1960, p. 314), we can set

$$V(\alpha_{\max}) = C + U, \quad (31.9)$$

while

$$V(0) = C. \quad (31.10)$$

The volume of C is a function of A' , and the volume of U is a function of A . But if the ring opening is not very small A and A' will be close in value, and we can take it that

$$A' = A. \quad (31.11)$$

It is convenient to introduce a new variable

$$x = (\varphi z / \rho \sin A). \quad (31.12)$$

Then

$$(CN/R) = \frac{3}{4} (D/\varphi) x \quad (31.13)$$

and

$$(UN/R) = \begin{cases} \frac{3}{4} (D/\varphi) \left(x - x^2 + \frac{1}{3} x^3 \right); & 0 \leq x \leq 1 \\ \frac{1}{4} (D/\varphi); & 1 \leq x \leq x_0. \end{cases} \quad (31.14)$$

In place of Eq. (31.7), we obtain

$$\frac{b_1(\alpha_{\max})}{b_1(0)} = \frac{f(\alpha_{\max})}{f(0)} \left\{ \frac{3}{4} \frac{D}{\varphi} \int_0^1 \exp \left[- \left[\frac{3}{4} \frac{D}{\varphi} \left(2x - x^2 + \frac{1}{3} x^3 \right) \right] dx + \right. \right. \quad (31.15)$$

$$\left. \left. + \exp \left(- \frac{D}{\varphi} \right) - \exp \left(- \frac{D}{4\varphi} + \frac{\tau_0}{\sin A} \right) \right] \right\} \left/ \left[1 - \exp \left(- \frac{\tau_0}{\sin A} \right) \right] \right.;$$

and the integral in this equation is readily evaluated by numerical integration.

In Eqs. (31.13) - (31.15), τ_0 is the optical thickness, previously determined through Eq. (28.1), and

$$x_0 = (\varphi z_0 / \rho \sin A) = \frac{4}{3} \frac{\tau_0 \varphi}{D \sin A}; \quad (31.16)$$

where b_1 is the brightness created by first order scattering. As already has been indicated by Eq. (17.11), the total brightness, with higher order scattering taken into consideration, is

$$b = b_1 + \Delta b. \quad (31.17)$$

Since the interval of change in α for Saturn is very small, it can be taken that

$$\Delta b(\alpha_{\max}) = \Delta b(0). \quad (31.18)$$

Then we can use the following equation to make the transition from $b_1(\alpha_{\max})/b_1(0)$ to $b(\alpha_{\max})/b(0)$

$$\frac{b(\alpha_{\max})}{b(0)} = \frac{b_1(\alpha_{\max}) + \Delta b(0)}{b_1(0) + \Delta b(0)}, \quad (31.19)$$

where $\Delta b(0)$ can be computed through formulas and tables for the theory of multiple scattering of light. The results of the calculations of the $\Delta b(0)/b(0)$ ratio for Saturn's rings have already been presented in #17 (see Table 5). $\Delta b(0)/b(0)$ is of the order of 10 percent, or less, for particles with a ~ 0.6 , and the phase function is similar to that of the moon, and this is extremely close to actual conditions. /88

The factor $f(\alpha_{\max})/f(0)$ can be computed as follows. Since the spherical albedo of a typical ring particle is now low, the natural effect of opposition of the particles (the Gehrels-Hapke effect) is slight. Consequently, the natural phase curve for a particle in limits ($0 \leq \alpha \leq 6^\circ.5$) should be practically linear, so that

$$[f(\alpha_{\max})/f(0)] = 2.512^{-p_p \alpha_{\max}}, \quad (31.20)$$

where p_p is the particle phase coefficient.

Eqs. (31.15), (31.19), and (31.20) solve this problem. They make it possible to compute the amplitude of the effect of mutual shading when the penumbra is ignored.

The results of the calculations converted to stellar magnitudes are shown in Figure 24 (the solid curve). The dashed curve shows similar results obtained when the penumbra was taken into consideration (see the next section). We used $\tau_0 = 1$, $A = A' = 25^\circ$ (wide open rings), $(\Delta b/b) = 0.10$, and $p_p = 0.024$. The only free parameter now is D . As will be seen from Figure 24, the amplitude is heavily dependent on D , a fact not included in the Seeliger approximation.

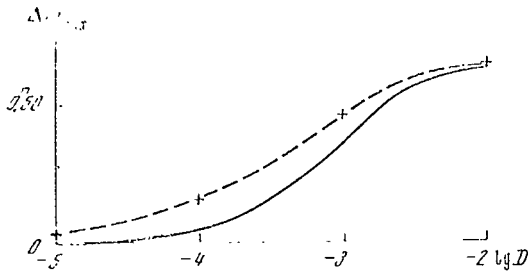


Figure 24. Theoretical amplitude, Δm_{\max} , of the effect of mutual shading in stellar magnitudes as a function of $\log D$.

The solid curve was computed with the penumbra ignored; the dashed curve with the penumbra taken into consideration. The amplitude is greatly dependent on D . The influence of the penumbra is slight.

to Figure 24, in order to obtain a significant amplitude from the effect of mutual shading. Setting $\tau_0 = \tau_{0B} = 1$, and $\sin A = \sin 25^\circ = 0.4225$, in Eq. (31.16), we find that $x_0 = 1$ corresponds to $D = 1.58 \cdot 10^{-3}$. The observed $\beta_B(\alpha_{\max}) - \beta_B(0)$ is of the order of $0.^m5$ (#12), a value corresponding to $x_0 \approx 1/3$ and $D \approx 5 \cdot 10^{-3}$. Thus, the strong effect of mutual shading can only be achieved when the condition is $x_0 \lesssim 1$. Turning now to Eq. (31.15), we can see that this latter condition means that only the first term in the numerator is present. This term describes the photometric properties of those layers of the ring where all shadow cones are truncated. Let us call them the "surface layers." The second and third terms in the numerator of Eq. (31.15) are the "deep layers," where, as before, some of the shadow cones are truncated, but some already have reached completion. The presence of completed cones reduces the probability of mutual shading; that is, the intensity of the effect is stronger the thicker the deep layers as compared with the thickness of the surface layers. Accordingly, the condition for intensive effect of mutual shading is absence of deep layers.

The physical implication is quite clear. Since the cones of the shadows cast by the particles have a finite length, the probability of mutual shading diminishes with increase in the mean distance between adjacent particles. But the mean distance can only increase when there is a reduction in D . As opposed to this, the shadows in Seeliger's approximation are infinitely long cylinders, and, as a result, the probability of the mutual shading does not depend on the mean distance between particles.

Let us point out that Eq. (31.16) demonstrates the dependence of x_0 on D . It is necessary that $D \gtrsim 10^{-3}$, according

/89

Now, in place of Eq. (31.6),

$$F = (p_0 K_0 + p_1 K_1 + p_2 K_2 + \dots) F_0, \quad (31.22)$$

where p_0, p_1, p_2, \dots are the probabilities of 0, 1, 2, etc., particles hitting volume V ; K_0, K_1, K_2, \dots are the mean relative illuminations of the element dS corresponding to these events. $K_0 = 1$.

Ignoring all terms in Eq. (31.22) with subscripts larger than one, we obtain

$$F = (p_0 + p_1 K_1) F_0, \quad (31.23)$$

which gives the approximation for the effect of mutual shading with excess. Actually, the coefficients K_n and the probabilities p_n are positive. By ignoring the terms with subscripts larger than one we underestimate the mean luminous flux, F ; that is, we overestimate the effect of mutual shading. On the other hand, disregard for the penumbra (see "a" this section) underestimates the effect of mutual shading. Thus, the true amplitude of the effect will fall between these two extremes.

The probabilities p_n can be calculated by using the formula for the problem involving fluctuations (see Timiryazev, 1956, for example)

$$p_n = \frac{v^n \exp(-v)}{n!}, \quad (31.24)$$

where v is the mean number of particles in volume V . Eq. (31.24) is valid providing v and n are small compared with N . This condition is satisfied in our case because $V \ll R$. Since $v = (N/R)V$, we can replace Eq. (31.23) by

$$F = [1 + K_1 (N/R)V] \exp[-(N/R)V] F_0 = F_0 \{1 + K_1 (N/R)V\} \exp[-(N/R)V]. \quad (31.25)$$

Let us take it that, as in the case when the penumbra was ignored, $W = 0$ when $\alpha = \alpha_{\max}$.

Then

$$V(x_{\max}) = C + U + P \quad (31.26)$$

and

$$V(0) = U + P, \quad (31.27)$$

from whence

$$(N/R)V(x_{\max}) = \frac{3}{4} (D/\varphi) \left(2x + x^2 + \frac{1}{3} x^3 \right) \quad (31.28)$$

and

$$(N/R)V(0) = \frac{3}{4} (D/\varphi) \left(x + x^2 + \frac{1}{3} x^3 \right). \quad (31.29)$$

The general expression for the coefficient K_1 has the form

$$K_1 = (1/V) \int_P \left(1 - \frac{\sigma}{S_\odot}\right) dV, \quad (31.30)$$

where S_\odot and σ are solid angles at which the solar disk, and that part of it shielded by the particle, can be seen from point M.

The nature of the solar eclipse at point M attributable to the particle with its center in volume P will depend on the position of this center in terms of M. The eclipse can be partial, annular, or "partial annular."

All layers of the ring can be broken down into surface (subscript "S"), middle ("M"), and deep ("D"), depending on the nature of the eclipse. /91

Then

$$\begin{aligned} [b_1(\alpha_{\max}, \alpha) / b_1(0)] = 2,512^{-\alpha_{\max}} \times & \left\{ \int_0^1 [1 + K_1 S_{\max}(V_{\max}/R) N] \exp \dots \right. \\ & \dots [(V_{\max}/R) N] dx + \int_1^{\infty} [1 + K_{\mathbf{M}\max}(V_{\max}/R) N] \exp \dots \\ & \dots [(V_{\max}/R) N] dx \left. \right\} : \left\{ \int_0^1 [1 + K_1 S_0(V_0/R) N] \exp \dots \right. \\ & \dots [(V_0/R) N] dx + \int_1^2 [1 + K_{\mathbf{M}0}(V_0/R) N] \exp \dots \\ & \dots [(V_0/R) N] dx + \int_2^{\infty} [1 + K_{\mathbf{D}0}(V_0/R) N] \exp \dots [(V_0/R) N] dx \left. \right\}, \end{aligned} \quad (31.31)$$

where, for brevity, the values of K_1 and V when $\alpha = \alpha_{\max}$ and $\alpha = 0$, are shown by the subscripts "max" and "0." The approximate formulas for the coefficients have the forms

$$\begin{aligned} K_1 S_{\max} & = \left(x^2 + \frac{2}{9}x^3\right) / \left(2x + x^2 + \frac{1}{3}x^3\right), \\ K_1 \mathbf{M}_{\max} = K_1 \mathbf{D}_{\max} & = \left(\frac{1}{3}x^{-1} + x^2 + \frac{1}{3}x^3 - \frac{4}{9}\right) / \left(2x + x^2 + \frac{1}{3}x^3\right), \\ K_1 S_0 & = \left(\frac{3}{4}x + \frac{5}{18}x^2\right) / \left(x + x^2 + \frac{1}{3}x^3\right), \\ K_1 \mathbf{M}_0 & = \left(-\frac{1}{2}x + \frac{11}{12}x^2 + \frac{1}{3}x^3 + \frac{5}{18}\right) / \left(x + x^2 + \frac{1}{3}x^3\right), \\ K_1 \mathbf{D}_0 & = \left(-\frac{2}{3}x^{-1} - x + x^2 - \frac{1}{3}x^3 + \frac{28}{18}\right) / \left(x + x^2 + \frac{1}{3}x^3\right). \end{aligned} \quad (31.32)$$

Eqs. (31.31), (31.32), and (31.19) solve the problem. The results are shown by the dashed curve in Figure 24. As we see, it passes very close to the curve obtained when the penumbra was ignored. This reflects the rapid decay in the intensity of the penumbra with increase in the distance between the center of the particle and the full shadow cone. The error introduced by ignoring the penumbra is less than $O^m .1$. Now we can ignore the influence of the penumbra in all future formulas in the theory of the effect of mutual shading.

(c) Phase function. The original formula for $b_1(\alpha)/b_1(0)$ is obtained from Eq. (31.7) by replacing α_{\max} by α . W is not considered small as compared with $C + U$.

Since the form of the functions U and W changes with z , the interval of integration of the expression in the numerator must be broken down into parts corresponding to the "surface" (subscript S), "shallow" (Sh), "middle" (M), and deep (D) layers of the ring /92

$$\begin{aligned}
 [b_1(\alpha)/b_1(0)] = [I(\alpha)/I(0)] & \left\{ \int_0^{S_{\max}} \exp[-(N/R)(C+U_S+W_S)] dz + \right. & (31.33) \\
 & + \int_{z_{S_{\max}}}^{z_{Sh_{\max}}} \exp[-(N/R)(C+U_{Sh}+W_{Sh})] dz + \\
 & + \int_{z_{Sh_{\max}}}^{z_{M_{\max}}} \exp[-(N/R)(C+U_M+W_M)] dz + \\
 & \left. + \int_{z_{M_{\max}}}^{z_0} \exp[-(N/R)(C+U_D+W_D)] dz \right\} : \\
 & \int_0^{z_0} \exp[-(N/R)U] dz .
 \end{aligned}$$

As we have noted in the foregoing, the case that is of practical importance is the one in which there are no deep layers ($x_0 < 1$, or $z_0 < (\rho/\phi)$). For this case, setting $A' = A$, changing from the variable z to x , and taking cognizance of Eq. (31.20), in place of Eq. (31.33) we obtain

$$\begin{aligned}
 [b_1(\alpha)/b_1(0)] = 2.512 \frac{\rho^2}{p^2} & \left\{ \int_0^{1/(\alpha \sin \theta)} \exp\left[-\left[\frac{3}{4} - \frac{D}{\phi}\right](2x+x^2 + \right. & (31.34) \\
 & \left. + \frac{1}{3}x^3 - w_S)\right] dx + \int_{1/(\alpha \sin \theta)}^{2/(\alpha \sin \theta)} \exp\left[-\left[\frac{3}{4} - \frac{D}{\phi}\right](2x+x^2 + \frac{1}{3}x^3 - w_{Sh})\right] dx + \right. \\
 & \left. + \int_{2/(\alpha \sin \theta)}^{z_0} \exp\left[-\left[\frac{3}{4} - \frac{D}{\phi}\right](2x+x^2 + \frac{1}{3}x^3 - w_M)\right] dx \right\} : [1 - \exp(-\alpha_0/\sin \theta)] ,
 \end{aligned}$$

where

$$w = (\varphi/\pi\rho^3)W \quad (31.35)$$

and

$$v = \alpha/\varphi. \quad (31.36)$$

Let us remember that W designates the common part of the volumes C and U [see Eq. (31.2)]. The phase angle, α , also is the angle between the axes of the volumes C and U (Figure 23). When α increases, C and U move with respect to each other, in much the same fashion as the halves of a scissors, and W decreases quickly. Consequently, w is greatly dependent on α , since it is, in the final analysis, the reason for the "logarithmic" shape of the theoretical phase curve.

The precise expression for $w(\alpha)$ is very cumbersome. The reader can find it in our article (Bobrov, 1960), which contains simple, approximate, expressions as well.

The natural phase function of the particle (taken as linear on the stellar /93 magnitude scale) is represented by the factor $2.512^{-p_p \alpha}$. The reduction for scattering of higher orders is accomplished as for amplitude [see Eq. (31.19) and the explanatory text accompanying this expression].

Overall, $b(\alpha)/b(0)$ depends on the variables α , A , A' , and on the parameters D , τ_0 , $\Delta b(0)/b(0)$, p_p . The dependence of A and A' is slight. Beyond this, $A' \approx A$ for widely, or even moderately opened rings. The parameter τ_0 /94 is known from observations (#14) and its accuracy is satisfactory. The value of the parameters $\Delta b/b$ already has been calculated (#17), and is not in excess of 0.10. The anticipated value of p_p , according to the conclusion we reached in #17, should be close to that for the moon ($p_p \approx 0.027$ stellar magnitude/degree of phase). We can consider this parameter to be known from observations. The only free parameter is D , and the only variable (for fixed A) is α .

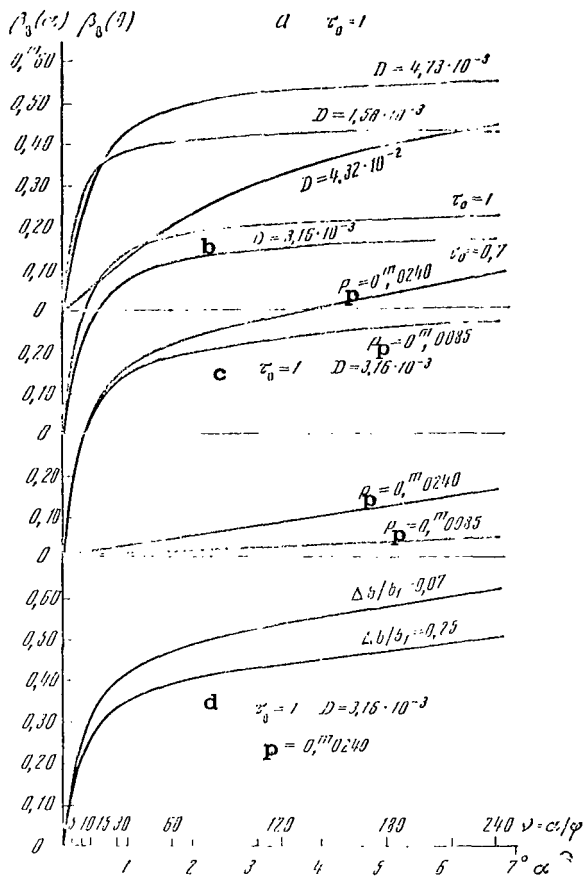


Figure 26. Shapes of theoretical phase curves in terms of parameters D , τ_0 , p_p , and $\Delta b/b$ (dispersions in sizes of particles ignored). The angles of elevation have the fixed value $A = A' = 25^\circ$ in all cases (widely opened rings), z_0 is taken as equal to 1 km. The values of the other parameters are shown near the curves.

Figure 26 shows the shapes of the theoretical phase curves in terms of D , τ_0 , p_p , and $\Delta b/b$ for fixed A , A' , and z_0 .

Figure 27 is a comparison between the theoretical phase curves and data /95 from observations made by Hertzprung (1919), Schoenberg (1933), and Lebedinets (1957). The Franklin and Cook data (1965) are very close to Schoenberg's (but are not plotted in Figure 27 in order to avoid clutter). We shall compare these data with the theoretical data a little later.

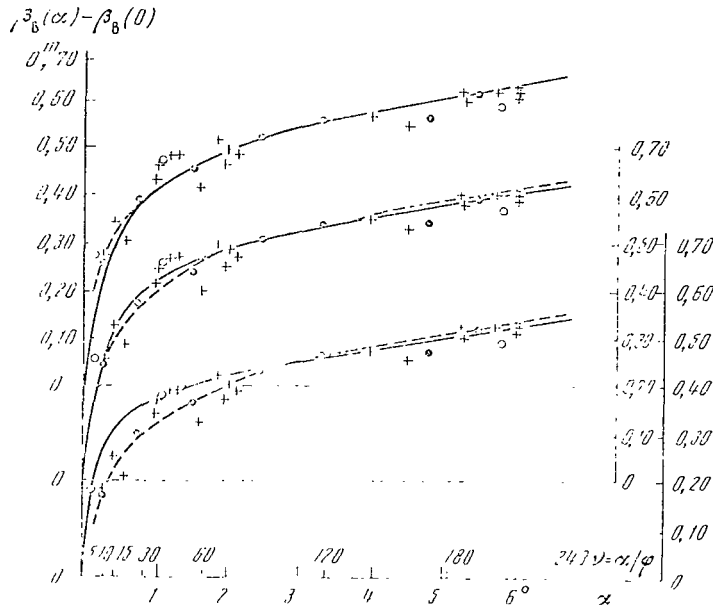


Figure 27. Comparison of theoretical phase curves (solid lines) with the observations made by Hertzsprung (open circles), Schoenberg (filled circles; mean weighted values for all of his filters), and Lebedinets (crosses). The lower, middle, and upper curves were computed for $D = 1.6 \cdot 10^{-3}$, $3.2 \cdot 10^{-3}$, and $4.7 \cdot 10^{-3}$. The corresponding values for $\beta_B(0) - \beta_C$ are $0^m.053$, $0^m.128$, and $0^m.145$. In all cases $A = A' = 25^B$, $\tau_0 = \tau_{QB} = 1$, $\Delta b/b_1 = 0.07$, and $p = 0.024$ stellar magnitude/degree of phase. The dashed curves were constructed through the empirical equation, Eq. (12.1), from Schoenberg's mean values, with the same changes in $\beta_B(0) - \beta_C$ as above.

As will be seen from Figure 27, the concordance between theory and observations is extremely good for the middle and upper curves. $D = 4.7 \cdot 10^{-3}$ is the more preferable, but the corresponding value for $\beta_B(0) - \beta_C$, $-0^m.145$, seems excessive (see note accompanying the figure). Also to be suspected is some small, albeit systematic, discrepancy between the upper curve and the observations in the region of extremely small α (the dashed curve plots above the solid one). Then too, we see that the Franklin and Cook observations confirm this assumption and that the discrepancy noted, just as is the case for too large $\beta_B(0) - \beta_C$, can readily be eliminated if the variance in the sizes of the particles is taken into consideration.

The values of the other parameters and variables used to compute the theoretical phase curves (see the note accompanying Figure 27) were taken from observations, for the most part, and evoke no real objections. Thus, even a simple model that ignores dispersions in particle sizes evidently quite satisfactorily reflects the Saturn ring structure.

#32. The "Cone-Cylinder" Approximation with Variances in Particle Size Taken into Consideration

(a) General expression for amplitude. The formulas set forth in the preceding section can quite easily be generalized for the case when the radii of the particles have variance in the interval (ρ_1, ρ_2) . The most interesting case is that when the interval of variance is broad. If it is narrow, the results will be close to those already obtained above, when variances are ignored.

Unfortunately, there are no observational data on the type of particle size variance law applicable to Saturn's rings. In the next deduction we will, for this law, take the expression ordinarily used in meteor astronomy

$$dN = K\rho^{-s}d\rho, \quad (32.1)$$

where ρ is the particle radius; K is a constant; s is a distribution parameter.

Let us take it that when ρ is sufficiently small, penetration of light into the region of the geometric shadow of the particle will occur because of diffraction. Arkad'yev's experiments (1912) lead to the conclusion that there is a significant shortening of the geometric shadow cone when the number of Fresnel zones, n , covered by the disk of a particle (reckoned from the apex of /96 the shadow cone) is 0.1 to 0.5. On the other hand, when $n = 3.5$, there is practically no washing away of the shadow cone. The value $n = 2$ is a judicious compromise. Then, when $(1/\varphi) = 2000$, the boundary value for ρ , at which the shadow cone still is not significantly shortened, is (for visual rays)

$$\rho_* = 2 \cdot 10^{-1} \text{ cm}; \quad (32.2)$$

and in accordance with which we can take it that all particles with $\rho \geq \rho_*$ cast a shadow with length ρ/φ , and that particles with $\rho < \rho_*$ cast no shadows. In this approximation, the participation of particles with $\rho < \rho_*$ simply reduces to one of their falling within the shadows of larger particles, so far as the mutual shading effect is concerned.

Let us find the luminous flux transmitted to the earth by particles in the interval $(\rho, \rho + d\rho)$ when they are shielded and shaded by particles in the interval $(r, r + dr)$. We shall ignore the effect of the penumbra of the particles, in accordance with the proof in #31b.

The geometry of the volume of probability, V , remains as it was in the problem without variance (Figure 23). Only the radius of the cylinder, and the maximum radius of the cone, now should be set equal to r . The magnitude of the volume of probability now will be a function of r

$$V_r = C_r + U_r - W_r / \quad (32.3)$$

The probability that the element $d\epsilon$ (see Figure 23) will not be shielded, or shaded, by particles in the interval $(r, r + dr)$ is $p_r = \exp(-\frac{V_r}{R} dN_r)$, where dN_r is the total number of particles in the interval $(r, r + dr)$. Let us suppose, as we did in #31, that the volumetric density is so low that the inequality $\rho \ll z$ satisfies the shielding, or shading, of any particle with radius ρ . Then, for all practical purposes, the values of p_r for various elements, $d\epsilon$, of the same particles coincide, and further arguments can be advanced for all particles, as a whole.

Let a luminous flux $\Gamma f(\alpha) \rho^2$, in which Γ is a constant and $f(\alpha)$ is the particle's phase function, be transmitted to the earth by a particle in the interval $(\rho, \rho + d\rho)$, outside the shading, or shielding. This particle, periodically shaded and shielded by particles in the interval $(r, r + dr)$, will, after a sufficiently long period of time, transmit a mean luminous flux to the earth of

$$\Gamma f(\alpha) \rho^2 \exp\left(-\frac{V_r}{R} dN_r\right). \quad (32.4)$$

The flat layer of particles in the interval $(\rho, \rho + d\rho)$, with thickness dz , and at depth z , will transmit a luminous flux to the earth of

$$\Gamma f(\alpha) \rho^2 \frac{dz}{z_0} dN_\rho \exp\left(-\frac{V_r}{R} dN_r\right), \quad (32.5)$$

where dN_ρ is the total number of particles in the interval $(\rho, \rho + d\rho)$. Replacing the magnitudes dN_ρ and dN_r in this last expression by their values from Eq. (32.1), we obtain

$$\Gamma f(\alpha) \frac{dz}{z_0} K \rho^{2-s} d\rho \exp\left(-\frac{V_r}{R} - K r^{-s} dr\right). \quad (32.6)$$

In order to take into account the effect of shading and shielding of the particles in the $(\rho, \rho + d\rho)$ interval by particles of all sizes from ρ_* to ρ_2 , we must find the probability of a particle of radius ρ not being shielded or shaded by one of the particles in the (ρ_*, ρ_2) interval. For sufficiently small D , it can be taken that the unknown probability is equal to the product of the probabilities, equated to fixed r . From whence, the luminous flux transmitted to the earth by particles in the interval $(\rho, \rho + d\rho)$ when they are shielded and shaded by particles of all sizes from ρ_* to ρ_2 can be found through the expression

$$-\frac{K\Gamma'(z)}{z_0} dz \rho^{2-s} d\rho \exp - \int_{\rho_*}^{\rho_2} \frac{K}{R} V_r r^{-s} dr. \quad (32.7)$$

Integrating in terms of ρ from ρ_1 to ρ_2 , and in terms of z from 0 to z_0 , we obtain the total luminous flux transmitted to the earth for phase angle α by all ring particles, with the shadow effect of particles, the radii of which are in the interval (ρ_*, ρ_2) , taken into consideration

$$\Phi(z) = \frac{K\Gamma'(z)}{z_0} \int_{\rho_1}^{\rho_2} \rho^{2-s} d\rho \int_0^{z_0} \left\{ \exp - \int_{\rho_*}^{\rho_2} \frac{K}{R} V_r r^{-s} dr \right\} dz. \quad (32.8)$$

It now is easy to find the amplitude of the shadow effect of a model with variance of ρ in the same manner as that used in #31, that is, that when $\alpha = 0$, $V_r = C_r$, and when $\alpha_{\max} V_r = C_r + U_r$. We obtain

$$\frac{b_1(\alpha_{\max})}{b_1(0)} = \frac{f(\alpha_{\max})}{f(0)} \frac{\int_0^{z_0} \left[\exp - \int_{\rho_*}^{\rho_2} \frac{K}{R} (C_r + U_r) r^{-s} dr \right] dz}{\int_0^{z_0} \left(\exp - \int_{\rho_*}^{\rho_2} \frac{K}{R} C_r r^{-s} dr \right) dz}. \quad (32.9)$$

The integration of the numerator of this expression has practical complications stemming from the fact that in the interval $0 \leq z \leq (\rho/\varphi) \sin A$, the volume U_r is a truncated cone (for any r from ρ_* to ρ_2), and is a complete cone for all r satisfying the inequality $\varphi z / \sin A \leq r \leq \rho_2$ in the interval $(\rho/\varphi) \sin \varphi \leq z \leq z_0$. With this in mind, we should write the following in place of Eq. (32.9)

$$\begin{aligned} \frac{b_1(\alpha_{\max})}{b_1(0)} = & 2,512^{-2} p^{\alpha_{\max}} \left\{ \int_0^{(\rho_*/\varphi)\sin A} \left[\exp - \int_{\rho_*}^{\rho_2} \frac{K}{R} (C + U_S) r^{-s} dr \right] dz + \right. \\ & + \int_{(\rho_*/\varphi)\sin A}^{(\rho_2/\varphi)\sin A} \left[\exp - \left(\int_{\rho_*}^{\varphi z / \sin A} \frac{K}{R} (C + U_D) r^{-s} dr + \int_{\varphi z / \sin A}^{\rho_2} \frac{K}{R} (C + U_S) r^{-s} dr \right) \right] dz + \\ & + \int_{(\rho_2/\varphi)\sin A}^{z_0} \left[\exp - \int_{\rho_*}^{\rho_2} \frac{K}{R} (C + U_D) r^{-s} dr \right] dz \Big\} : \\ & : \left\{ \int_0^{z_0} \left(\exp - \int_{\rho_*}^{\rho_2} \frac{K}{R} C r^{-s} dr \right) dz \right\}, \end{aligned} \quad (32.10)$$

where U_r designates complete cones (the "deep" layers of the rings); U_s designates truncated cones (the "surface" layers); the subscript r is omitted from all volumes.

Eq. (32.10) is a general equation (that is, it is valid for any s) for the amplitude of the shadow effect with variance ρ taken into consideration (in the approximation of the shadow effect with a shortcoming). The general formulas must be added. These are

$$\tau_0 = \int_N \frac{\pi \rho^2 dN}{R/z_0} = \frac{\pi K z_0}{R} \int_{\rho_1}^{\rho_2} \rho^{2-s} d\rho \quad (32.11)$$

for the optical thickness of the ring, and

$$D = \int_N \frac{4}{3} \frac{\pi \rho^3 dN}{R} = \frac{4}{3} \frac{\pi K}{R} \int_{\rho_1}^{\rho_2} \rho^{3-s} d\rho. \quad (32.12)$$

for the volumetric density.

Eq. (32.10) considers only first order scattering. Eq. (31.19) is used to make the reduction for higher order scattering. Let us note in addition that the natural phase coefficient for the particle, p_p , is assumed not dependent on ρ .

(b) Comments relative to the interval and parameter of variance. As will be pointed out at the end of the section, the parameter s for the B ring should satisfy the condition

$$s < 3. \quad (32.13)$$

in the Eq. (32.1) variance law. So let us consider the connection between the magnitudes ρ_1 , ρ_2 , τ_0 , D when s changes in the interval $2.5 \leq s \leq 3.5$.

First let us point out that we can take

$$\rho_{1 \min} \sim 1 \cdot 10^{-4} \text{ cm} \quad (32.14)$$

and

$$\rho_{2 \min} \sim 3 \text{ cm}. \quad (32.15)$$

as the minimum values for ρ_1 and ρ_2 . Eq. (32.14) follows because the B ring scatters solar light almost non-selectively (#9), and Eq. (32.15) follows from the condition of the cosmogonically acceptable age of the ring [#17, Eq. (17.4)].

Eqs. (32.11) and (32.12) make it easy to obtain the following special formulas for τ_0 and D in the interval of interest to us

$$s = 2.5$$

$$\tau_0 = \frac{2\pi K z_0 [1 - (\rho_1/\rho_2)^{1/2}]}{R} \rho_2^{1/2}, \quad (32.16)$$

$$D = \frac{8}{9} \frac{\pi K [1 - (\rho_1/\rho_2)^{1/2}]}{R} \rho_2^{1/2}. \quad (32.17)$$

$$s = 3.0$$

$$\tau_0 = \frac{\pi K z_0}{R} \ln \frac{\rho_2}{\rho_1}, \quad (32.18)$$

$$D = \frac{4}{3} \frac{\pi K [1 - (\rho_1/\rho_2)]}{R} \rho_2. \quad (32.19)$$

$$s = 3.5$$

$$\tau_0 = \frac{2\pi K z_0 [1 - (\rho_1/\rho_2)^{1/2}]}{R \rho_1^{1/2}}, \quad (32.20)$$

$$D = \frac{8}{3} \frac{\pi K [1 - (\rho_1/\rho_2)^{1/2}]}{R} \rho_2^{1/2}. \quad (32.21)$$

As will be seen from Eq. (32.16) - (32.21), when $s < 3.0$, the optical thickness (and therefore ring reflecting surface) is determined primarily by large particles, and when $s > 3.0$, by small ones. The volumetric density (and the mass of the ring) over the entire interval of s values of interest to us is determined by large particles.

This obvious relationship must be added to these formulas

$$z_0 \geq 2\rho_2 \quad (32.22)$$

Strictly speaking, the model of the many-particle thickness system requires the observation of the more rigid condition that

$$z_0 \gg \rho_2 \quad (32.23)$$

but the Eq. (32.22) condition is adequate for majorizing the amplitude estimate. That Eq. (32.22) does just that, that is, that it exaggerates the amplitude of the mutual shading effect, is clear from the following consideration. As will be seen from Figure 26, the section of expressed nonlinearity of the phase curve for the layer of particles with fixed ρ and z_0 covers a longer α interval the larger D may be, that is, the larger the ρ/z_0 ratio. If this ratio is large enough, the nonlinear section generally can prove to be outside the limits of the observed interval of phase angles, and the actual amplitude of the brightness of the layer with change in α from 0 to $6^\circ.5$ will be significantly below that computed through Eq. (32.10), in which it is assumed that $W = 0$,

that is, that when $\alpha = 6^\circ.5$, the nonlinear section of the curve has passed from ρ_1 to ρ_2 for all particles.

The application of the Eq. (32.22) condition to the ring model limits the range of possible D values from above. In fact, substituting Eq. (32.22) in Eqs. (32.16) - (32.21), and expressing D in terms of τ_0 , it will be found quite easily that when $\tau_0 = 1$, $\rho = 1 \cdot 10^{-4}$ cm, and $z_0 = 10^5$ cm. D_{\max} is 0.21, $3.3 \cdot 10^{-2}$, and $3.0 \cdot 10^{-5}$ for $s = 2.5, 3.0$ and 3.5 , respectively. The latter of these values is so small that there is no assurance that the amplitude of the change in brightness of the B ring can be observed, even when there is no dispersion, ρ (see Figure 24). But from what follows, we shall see that achievement of that amplitude requires a model with higher D values when there is variance of ρ , than when a model without variance is used. Consequently, when the interval of variance is a broad one, the value $s = 3.5$ is extremely high.

There is yet another distinctive feature of the model under consideration, and that is that since it includes a component in which $\rho \ll 3$ cm, the effect of the light pressure no longer can be taken as negligibly small. Specifically, radiative braking will play a significant role. It will sweep out the slightly-dispersed component of the ring material within the volume of the rings over a period of time that is short compared with $5 \cdot 10^9$ years. It is true enough that large particles approaching Saturn very much more slowly will shield the 100 planet from the small particles, and, at the same time, will interfere with the sweeping out process. As will be seen from Eqs. (32.16) - (32.21), the shielding is particularly strong when $s < 3$, when the optical thickness of the ring is fixed primarily by large particles. A ray penetrating the ring radially causes an optical thickness of tens of thousands because $\tau_{OB} \sim 1$. From this it follows that the effect of radiative braking on particles with $\rho \ll 3$ cm should lead to their settling on the surfaces of large particles. The subsequent fate of a small particle is a strong bond between it and the surface of a large particle (by freezing to it, for example), or of its being torn away from this surface when two large particles collide.

If the former is the case, the number of small, free particles in the ring volume will decrease rapidly with time. Now let us realize the latter case. Here we no longer can speak of the time of the free path of a small particle, but of the time it takes to wash it out of the ring volume completely.

Generally speaking, this time increases with consideration of the periods of the linking of small particles to large ones. But if collisions between particles are not too rare (as obviously is the case; see #28) the time required to wash the particles out does not increase significantly. So, even in this latter case there will be quite a rapid reduction in the number of small free particles in the ring volume.

Accordingly, consideration of the question of extensive variance of ρ , including particles with $\rho \ll 3$ cm, leads us to the problem of the continuous filling of the ring volume with such particles. Without engaging in a detailed discussion, we shall simply note that the most probable source of replenishment can be the fractionation and the breaking away from the surface layer of large particles as a result of the action on the surface layer of solar corpuscular radiation and of micrometeorites, as well as because of collisions between large particles.

Let us take this assumption as a working hypothesis. It imposes the following limitation on the distribution of particles in terms of ρ : the total mass of ring particles for which $\rho \gtrsim 3$ cm should be of the order of, or greater, than the mass of all those small particles which, during the existence of the ring, were washed out of its volume by radiative braking

$$\int_{\rho_1}^{\rho_2} \frac{4}{3} \pi \rho^3 \delta \cdot dN = \int_{\rho_1}^{\rho_2} \frac{4}{3} \pi \rho^2 n \delta \cdot dN, \quad (32.24)$$

where ρ_0 is the radius of a particle, the time of existence of which in the volume of the ring is equal to the age of the ring; δ is the density of the particle material; n is the ratio of time of existence in the volume of the ring of a particle with radius ρ_0 .

In accordance with Eq. (17.4), the time of existence of a particle in the 101 volume of the ring is directly proportional to its radius. Therefore

$$n = \rho_0 / \rho. \quad (32.25)$$

Assuming that δ is not dependent on ρ , and replacing n and dN in Eq. (32.24) by their values as calculated through Eqs. (32.25) and (32.1), we obtain

$$\int_{\rho_0}^{\rho_2} \rho^{3-s} d\rho = \rho_0 \int_{\rho_1}^{\rho_2} \rho^{2-s} d\rho. \quad (32.26)$$

From whence we find the following expressions for the upper limit of ρ for three particular values of s

$$a) \quad s = 2.5, \quad \rho_2 = \rho_0^{2/3} (4\rho_0^{1/2} - 3\rho_1^{1/2})^{3/2}; \quad (32.27)$$

$$b) \quad s = 3.0, \quad \rho_2 = \rho_0 \left(\ln \frac{\rho_0}{\rho_1} + 1 \right); \quad (32.28)$$

$$c) \quad s = 3.5, \quad \rho_2 = \rho_0^2 / \rho_1. \quad (32.29)$$

Substituting $\rho_0 = 3$ cm, and $\rho_1 = 10^{-4}$ cm here, we obtain the values of 7.6, 102, and $9 \cdot 10^4$ cm, respectively, for ρ_2 when $s = 2.5, 3.0$ and 3.5 . These numbers show that the very fact of a comparatively small ring thickness (of the order of 3 to 4 km) imposes a significant limitation on s . The maximum permissible value that should be taken for s is 3.5, or even a somewhat smaller value.

Planetocentric radiative braking, the effect of which we have just reviewed, is not the only effect light pressure has on the ring material. The component of the light pressure normal to the plane of the rings for example, causes a depression in the plane of the orbit of the particles; that is, it forces the particles to move in planes that do not pass through the center of the mass of Saturn. The smaller ρ , the deeper the depression, and it is of interest to estimate its magnitude for $\rho = 10^{-4}$ cm.

The pressure of direct solar radiation on an absolutely absorbing particle at a distance of 1 AU from the sun is of the order of $5 \cdot 10^{-5}$ dyne/cm². Considering the mean distance of Saturn from the sun (9.54 AU), the inclined incidence of light on the ring ($A \leq 26^\circ.7$), and the fact that almost one-third of the ring is in the shadow of Saturn, we obtain the following value for the component of the light pressure normal to the plane of the ring

$$p_n \leq 1.5 \cdot 10^{-7} \text{ dyne/cm}^2. \quad (32.30)$$

Actually, the particles are not absolutely black, but are light gray (the albedo is of the order of 0.5 to 0.6), diffusively scattering. p_n therefore is somewhat increased. But when it is remembered that solar radiation is attenuated substantially upon passage through the thickness of the ring, because of the large particles, the p_n value obtained through Eq. (32.20) will /102 be overestimated much more quickly than it will be underestimated.

We find the magnitude of the depression, H , by equating the normal component of the force of the light pressure to the corresponding component of the attractive force

$$H = \frac{3}{4} \frac{p_n r^3}{\gamma M \rho \delta}, \quad (32.31)$$

where r is the radius of the orbit of the particle; γ is the gravitational constant; M is the mass of Saturn; ρ and δ are the particle radius and density.

Setting $r = 10^{10}$ cm (the mean radius of the B ring), $\rho \geq \rho_1 = 10^{-4}$ cm, $M = 5.7 \cdot 10^{29}$ grams; and $\delta = 1$ (the particles consist of ice for the most part), we find that when $p_n = 1.5 \cdot 10^{-7}$ dyne/cm²

$$H \lesssim 300 M. \quad (32.32)$$

If z_0 is significantly larger than this number, the depression is not deep enough for spatial separation of small particles from large ones, even when $\rho = 10^{-4}$ cm. An estimate of the order of z_0 , based on 1966 observations (#22) shows that this is so.

The pressure of scattered solar radiation, and of infrared radiation from Saturn, also have an effect on small particles. The first of these factors is weaker than the direct radiation from the sun by approximately two orders of magnitude (#21), and the second is weaker by even many more orders of magnitude. The effects they create are slight, and we will not consider them.

TABLE 7

Model	Particle sizes, cm			$\frac{b_1(\alpha_{\max}) - b_1(0)}{b_1(0)}, \%$	D
	ρ_1	ρ_0	ρ_2		
Without variance	$2.4 \cdot 10^3$	$2.4 \cdot 10^2$	$2.4 \cdot 10^2$	39	$3.16 \cdot 10^{-3}$
$s = 2.5$	$1.0 \cdot 10^{-4}$	$2.0 \cdot 10^{-1}$	$7.0 \cdot 10^2$	33	$3.16 \cdot 10^{-3}$
	$1.0 \cdot 10^{-4}$	2.0.10	$7.1 \cdot 10^3$	41	$3.16 \cdot 10^{-3}$
$s = 3.0$	$1.0 \cdot 10^{-4}$	$2.0 \cdot 10^{-1}$	$4.2 \cdot 10^3$	14	$3.16 \cdot 10^{-3}$
	$1.0 \cdot 10^{-4}$	$2.0 \cdot 10^{-1}$	$4.7 \cdot 10^4$	<21	$3.16 \cdot 10^{-3}$
	$2.7 \cdot 10^1$	$2.7 \cdot 10^1$	$1.5 \cdot 10^4$	<39	$3.16 \cdot 10^{-2}$
$s = 3.5$	$1.0 \cdot 10^{-4}$	$2.0 \cdot 10^{-1}$	$5.0 \cdot 10^4$	< 1	$2.97 \cdot 10^{-5}$
	1.1	1.1	$5.0 \cdot 10^4$	< 9	$3.16 \cdot 10^{-3}$
	$1.1 \cdot 10^2$	$1.1 \cdot 10^2$	$5.0 \cdot 10^4$	<39	$3.16 \cdot 10^{-2}$

(c) Results of the amplitude calculations for $2.5 \leq s \leq 3.5$. The substitution of particular values $s = 2.5, 3.0$ and 3.5 in Eq. (32.10) readily supplies working formulas for amplitude calculation (see Bobrov, 1961). Setting $z_0 = 1.0 \cdot 10^5$ cm, $\tau_0 = 1$, $A = A' = 25^\circ$, we find the amplitude values

listed in Table 7. The "less than" sign is used when only the majorizing estimate of the amplitude can be obtained. Model data without variance are listed for purposes of comparison. The parameters of this model were selected in order to obtain concordance between the values of the magnitude $[b_1(\alpha_{\max}) - b_1(0)]/b_1(0)$ and the B ring observations. The observed value is 39 percent.

There is no need to reduce the data for multiple scattering, because ρ is equal to the amplitude value only when first order scattering is taken into consideration, and this is so for models with and without variance.

The following conclusions as to the nature of the variance in the sizes of B ring particles derive from consideration of the data listed in Table 7.

1. If the variance interval is a broad one, that is, if it includes macroscopic particles as well as fine dust with $\rho \sim 10^{-4}$ cm, concordance with the observations can be reached only when $s < 3$.

2. The estimate of the volumetric density of the B ring, obtained with variance ignored, should be reviewed. The new D value will be higher.

Let us point out that general considerations, as well as observed facts, impel the rejection of the preference for models with a broad variance interval; that is, models with $s < 3$. As a matter of fact, the effect on ring material of micrometeorites and of solar corpuscular radiation should result in a continuous formation of a fixed quantity of fine dust in the ring volume. Maggini (1937), observing a significant increase in the B ring color equivalent at small A angle values (#13), confirms the fact that dust such as this actually does exist in the B ring volume. At the same time, it is of interest to note that the relative dust content clearly is low, because it cannot be detected by observation when the rings are open half way, or wide open. This is yet another indication in favor of the models with $s < 3$, in which the dust content is low [see Eqs. (32.16), (32.18) and (32.20)].

(d) Phase function. The general expression for $b_1(\alpha)/b_1(0)$ is readily obtained from Eq. (32.9) by replacing α_{\max} with α and $C_r + U_r$ with $C_r + U_r - W_r$.

As in the case of finding the phase function of models without variance in the radii of the particles, ρ , we must distinguish between surface, shallow, middle, and deep layers of the ring (subscripts S, Sh, M, and D, see #31),

so the intervals of integration with respect to r and with respect to z can be broken down into parts, and there will be seven summands in the numerator of the expression for $b_1(\alpha)/b_1(0)$

/104

$$\begin{aligned}
 \frac{b_1(\alpha)}{b_1(0)} = & 2.512^{-1\alpha} \left\{ \int_0^{\rho_*/(\nu+1)\varphi} \exp - (C + U_S - W_S)_{\rho_*}^{\rho_*} d\eta + \right. \\
 & + \int_{\rho_*/(\nu+1)\varphi}^{2\rho_*/(\nu+1)\varphi} \exp - [(C + U_S)_{\rho_*}^{\rho_*} - (W_{Sh})_{\rho_*}^{(\nu+1)\varphi\eta} - (W_S)_{\rho_*}^{\rho_*} I] d\eta + \\
 & + \int_{\rho_*/\varphi}^{\rho_*/\varphi} \exp - [(C + U_S)_{\rho_*}^{\rho_*} - (W_M)_{\rho_*}^{(\nu+1)\varphi\tau/2} - (W_{Sh})_{\rho_*}^{(\nu+1)\varphi\eta/2} - \\
 & - (W_S)_{\rho_*}^{\rho_*} I] d\eta + \int_{\rho_*/\varphi}^{\rho_*/(\nu+1)\varphi} \exp - [(C)_{\rho_*}^{\rho_*} + (U_D)_{\rho_*}^{\varphi\eta} + \\
 & + (U_S)_{\rho_*}^{\rho_*} - (W_{D,M})_{\rho_*}^{(\nu+1)\varphi\tau/2} - (W_{Sh})_{\rho_*}^{(\nu+1)\varphi\eta/2} - \\
 & - (W_S)_{\rho_*}^{\rho_*} I] d\eta + \int_{\rho_*/(\nu+1)\varphi}^{\rho_*/\varphi} \exp - [(C)_{\rho_*}^{\rho_*} + (U_D)_{\rho_*}^{\varphi\eta} + \\
 & + (U_S)_{\rho_*}^{\rho_*} - (W_{D,M})_{\rho_*}^{(\nu+1)\varphi\tau/2} - (W_{Sh})_{\rho_*}^{(\nu+1)\varphi\eta/2}] d\eta + \\
 & + \int_{2\rho_*/(\nu+1)\varphi}^{\rho_*/\varphi} \exp - [(C)_{\rho_*}^{\rho_*} + (U_D)_{\rho_*}^{\varphi\eta} + (U_S)_{\rho_*}^{\rho_*} - (W_{D,M})_{\rho_*}^{\rho_*}] d\eta + \\
 & \left. + \int_{\rho_*/\varphi}^{\eta_0} \exp - (C + U_D - W_D)_{\rho_*}^{\rho_*} d\eta \right\} : \int_0^{\eta_0} \left[\exp - \int_{\rho_*}^{\rho_*} \frac{K}{R} C r^{-s} dr \right] d\eta, \quad (32.33)
 \end{aligned}$$

where

$$\eta = z/\sin A, \quad (32.34)$$

$$\nu = \alpha/\varphi \quad (32.35)$$

and designations of the type

$$(U_D)_{\rho_*}^{\varphi\eta} = \int_{\rho_*}^{\varphi\eta} \frac{K}{R} U_D r^{-s} dr \quad (32.36)$$

and the like are introduced. It is accepted that $A' = A$, and that the influence of the penumbra is negligibly small. The superscript r has been omitted from all volumes.

Eq. (32.33) is a general formula for the phase function of the effect of mutual shading, with variance in the particle radii, ρ , taken into consideration. The working formulas for certain special values of s can be obtained by substituting these special values in Eq. (32.33). We used Eq. (32.33) to calculate theoretical phase curves for the following two models

$$\begin{aligned}
s &= 2 & \rho_1 &= 1 \cdot 10^{-4} \text{ cm}, \\
\tau_0 &= \tau_{0B} = 1, & \rho_* &= 2 \cdot 10^{-1} \text{ cm}, \\
A &= A' = 25^\circ, & \rho_2 &= 7.5 \cdot 10^2 \text{ cm}, \\
D &= 5 \cdot 10^{-3}, & z_0 &= 1 \cdot 10^5 \text{ cm}.
\end{aligned}
\tag{32.37}$$

$$\begin{aligned}
s &= 3, & \rho_1 &= \rho_* = 4.3 \text{ cm}, \\
\tau_0 &= \tau_{0B} = 1, & \rho_2 &= 2.8 \cdot 10^4 \text{ cm}, \\
A &= A' = 25^\circ, & & \\
D &= 4.3 \cdot 10^{-2}, & z_0 &= 1 \cdot 10^5 \text{ cm}.
\end{aligned}
\tag{32.38} \quad \underline{/105}$$

The parameters of the Eq. (32.28) model were selected such that they satisfy observational data, and, at the same time, provide for possibly obtaining a broader range of variance, one including not only macroscopic particles, but fine dust as well. This selection leads one to expect first, good concordance between the theoretical and the observed phase curve, and, second, a quite clearly expressed difference between the Eq. (32.37) model phase curve, and the curves for models without variance.

The selection of values for the parameters τ_0 , z_0 , and the volumetric density, D , provides the concordance with the data from observations. This is done by taking a value for the latter which, in accordance with the data listed in Table 7, should result in an amplitude close to that observed.

The latitude in the variance interval (almost seven orders of magnitude) for a comparatively large amplitude, is provided for by an extremely moderate value, $s = 2$. At the same time, ρ_2 was selected such that the Eq. (32.23) condition is satisfied. This means that for all particles in the variance interval, including ρ_2 , the nonlinear section of the phase curve is within the limits of the observed interval of phase angles.

Another model, Eq. (32.38), was taken for purposes of comparison. Here, on the other hand, a maximum $s = 3$, was taken, something that resulted in a substantial increase in ρ_1 , ρ_* , and ρ_2 , otherwise the amplitude would be very small. Because of the large ρ_2 , the Eq. (32.23) condition is not satisfied. As has already been mentioned above, this results in a reduction in the actual amplitude as compared with that calculated using Eq. (32.10). /106

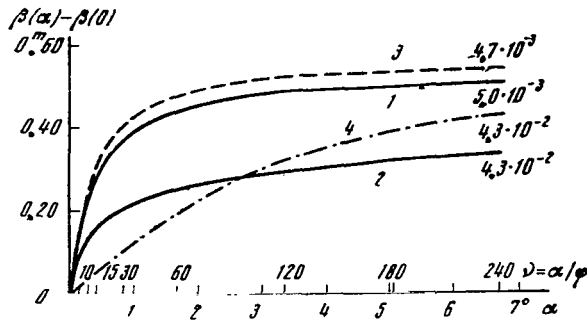


Figure 28. Effect of variance of particle radius, ρ , on the shape of the phase curve.

1, 2 - curves for the Eqs. (32.37) and (32.38) models with variance of ρ , respectively; 3, 4 - their analogs, obtained for models without variance of ρ , for the same values of the parameters A , τ_0 , and z_0 . D values are shown near the curves.

Calculations have resulted in the phase curves shown in Figure 28 (curves 1 and 2). For purposes of demonstrating how the variance of ρ affects the shape of the phase curve, the figure also shows two phase curves for a model without variance of ρ , one of which, curve 3, is the analog of curve 1; the other, curve 4, is the analog of curve 2. The values of the parameters A , τ_0 , and z_0 are equal for the pairs of curves, 1-2, and 2-4, respectively, and so are the values of the most important parameter, D (precisely or approximately), so that the difference in the shape of the compared curves must be equated solely to the effect of variance of ρ .

As will be seen from the figure, when $s = 3$ these differences are much greater than when $s = 2$. This can be explained by the fact that with increase in s there is an increase in the contribution made by the small particles to the total luminous flux from the ring, and, consequently, in the influence of the small particles on the resultant phase curve. Generally speaking, every ρ value has its "partial" phase curve, with the initial (linear) and transitional (non-linear) sections shorter and steeper the smaller ρ as compared with z_0 . The resultant phase curve for the model as a whole is the mean weighted curve, as it were, of all the partial curves. That is why, in particular, curve 4 (models of single, extremely large, particles) is an extremely flat curve, whereas curve 2 (models of particles with a variety of sizes) rises quite sharply from $\alpha = 0$, and approaches saturation much more rapidly.

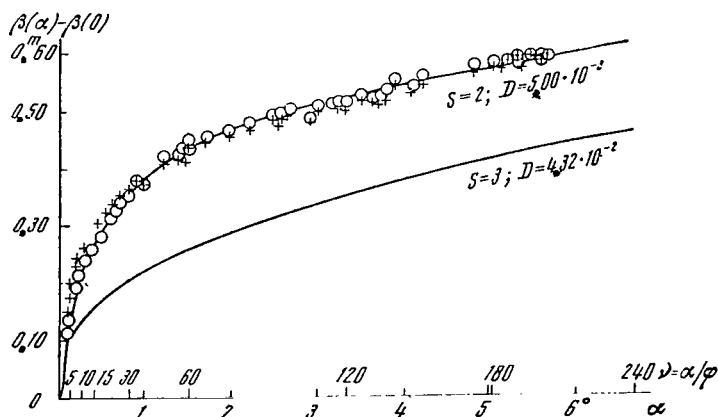


Figure 29. Comparison between observations and theoretical phase curves for Eqs. (32.37) and (32.28) models, with variance in sizes of particles considered.

Solid curves are the theoretical phase curves. The circles and crosses are the blue and visual stellar magnitudes of ring brightness according to Franklin and Cook (1965), respectively. The luminous fluxes from the A and B rings have not been separated; $\beta_B(0) - \beta_C$ has been taken equal to $-0^m.115$.

Figure 29 compares the theoretical phase curves with the observations. We used Franklin and Cook's observational data (1965). We see that the concordance of the $s = 2$ model with the observations is quite satisfactory, particularly for blue stellar magnitudes. The visual stellar magnitudes develop a small, systematic, discrepancy with theory when $\alpha < 0^\circ 30'$. The authors believe that this discrepancy is a real one and that it is the result of diffraction in the microscopic, transparent, frozen droplets forming the surface of the particles (the latter are assumed to be macroscopic). It probably is too soon to take these conclusions as final. As a matter of fact, in the photoelectric photometry provided by Franklin and Cook the luminous fluxes from the A and B rings were not distinguishable from each other (#12). The authors assert (on the basis of their simultaneous photographic photometry) that the observed phase curves for the A and B rings are absolutely identical. This assertion cannot be verified, unfortunately, because the authors have not published their photographic phase curves for the A and B rings. It is possible that there is a little difference in the A and B ring curves, but this cannot be detected within the limits of error for photographic photometry.

But there are serious observational facts pointing to an A ring light scattering with its own features: (1) the polarization of the light reflected by the A ring is significantly different from that for the B ring (#11); (2) when A' is extremely small the brightness of the A ring can exceed the brightness of 108 the B ring (Barnard, 1909), whereas when the openings are of medium, or large size, the reverse is true; (3) as calculation shows (Bobrov, 1956b, p. 907), the difference in the A and B ring brightnesses cannot be explained by the simple difference in τ_0 . Evidently, the scattering properties of the rings are not entirely identical. Consequently, the nonconcordance with theory mentioned when $\alpha < 0^\circ 30'$ may be due solely to the A ring. The only way to resolve this is to make direct photoelectric photometry of the surface brightness of the A and B rings individually.

As will be seen from Figure 29, the behavior of the observed brightness values near $\alpha = 0$ possibly indicate that the value (-0.115) taken from $\beta_B(0) - \beta_c$ is somewhat (absolutely) inflated. There is reason to think, therefore, that in fact the s value is not 2.0, as in Figure 29, but is between 2 and 3. Figure 30 shows our attempt to illustrate this graphically. We should point out that the mean values of s for meteorites observed in the vicinity of the earth, as well as for the material responsible for the Fraunhofer component of the solar corona have this same order of magnitude.

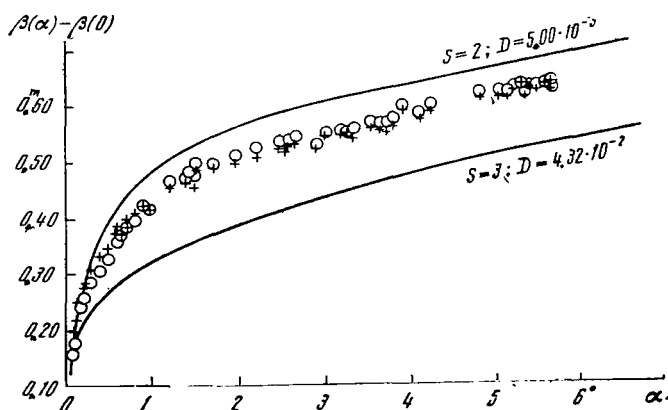


Figure 30. The same as Figure 29, but the assumption is that $\beta_B(0) - \beta_c = -0^m.060$.

In Figure 30, $\beta_B(0) - \beta_c$ is taken as equal to $(-0^m.060)$, a magnitude which is more reasonable than $(-0^m.115)$.

#33. Other Solutions

Franklin and Cook recently published (1965) formulas for calculating the phase function of the mutual shading effect. They considered two cases: (1) the cone-cylinder approximation, which considers particles large enough so the effect of diffraction along the length of the shadow can be ignored; and (2) the cone-cone approximation for microscopic particles, when the volume of the shielding is not a cylinder, or a cone. The details can be found in the original paper.

Case 1 is the complete equivalent of the case which we had considered at the time, and which is described in this chapter. Analysis of case 2 led Franklin and Cook to the conclusion that the rings possibly consist of particles with $\rho \sim 300$ microns, and they should have exceptionally small physical thickness, $z_0 \sim 3 - 10$ cm. Discussing these values, the authors are silent with respect to the more serious argument against case 2, that of the very short life of a formation such as this. We discussed this question in #17, and found that the life of rings consisting of particles of $\rho \sim 300$ microns is about $5 \cdot 10^7$ years, or 10^{-2} the life of the solar system. Consequently, the assumption must be that the ring material has been renewed some 100 times during the life of the solar system, or that the rings are very young, and that we now see them only because of an occasional, fortuitous coincidence. Both /109 possibilities have a very low order of probability. The authors themselves tend more to the view that the actual structure of the rings corresponds more to case 1 than to case 2. To be added is the fact that thanks to the international observations made of Saturn in 1966, it became possible to reduce the first estimates of the order of the thickness of the rings to $z_0 \sim 3$ to 4 km.

#34. Discussion of the Results. Values of the Principal Physical Parameters of the Rings.

By the end of Chapter IV (#19), we were able to obtain some idea of the structure of the B ring, and of the properties of its typical particle, based on analysis of observational data. It was found that the B ring is a many-particle thickness system, and that the particles themselves are macroscopic, very scarred bodies with a spherical albedo of a $\alpha \sim 0.5$ to 0.6 . In this system, when $\tau_0 \sim 1$, the phase behavior of the brilliance in the region of small α will be determined for the most part by the effect of the mutual shading of the

particles by each other, so the next step should be to apply the theory of mutual shading to the B ring in order to check and refine previously derived conclusions with respect to the structure of the ring, and to obtain a quantitative estimate of its principal physical parameters. In this section, once the theory of mutual shading is explained, and its predictions are compared with observations, we can discuss the results obtained and compile a summary of the values of the ring parameters representing those that appear to be most probable at this stage of the research.

Let us point out, first of all, that the theory of mutual shading is what makes it possible to use observations to establish whether the rings are a one-particle thickness system, or a many-particle thickness system.

Let us postulate the existence of the first possibility. In that case, the observed shape of the phase curve for the rings will, in the main, be due to the Gehrels-Hapke opposition effect (#17). The effect of mutual shading will be slight when A is not too small, because the cone of the shadow of the eclipsing particle will lie almost entirely outside the layer in which the particles are located. But with reduction in A to a few degrees, the situation changes. When $A \sim 3^\circ$, the length of the section of the shadow of the particle within the limits of the layer reaches a value of several tens ρ . The probability of mutual shading increases significantly, and the phase effect will be stronger for large and medium A .

The situation is different in the case of the many-particle thickness layer. For the majority of the particles the shadow falls entirely within the layer, regardless of A , so the probability of mutual shading always is great (providing D is not too small). The transition from large A to small is reflected only in the increase in the magnitude $\tau_0/\sin A$; that is, in the optical thickness along the incident ray. When $\tau_0 \sim 1$, this has little effect on the magnitude of the phase effect. /110

Accordingly, in the case of the ring with a one-particle thickness, the phase curve will show a substantial increase in the phase factor at any point in the observed interval, α , for small A , and, consequently, a significant increase in the total amplitude of the change in brightness. The phase curve will be relatively insensitive to change in A in the case of the ring with a many-particle thickness.

The program of international cooperation in observing Saturn's rings in 1966, included among its many facets the obtaining of phase curves for the rings for small A. Although the analysis of the observations is not complete as of this time, the preliminary data indicate that the phase curve for the B ring obtained in 1966, evidently is identical with the curve obtained for large and medium A; that is, this ring is a many-particle thickness system.

Let us point out as well that the comparison of the phase curves calculated in terms of the theory of mutual shading, with the observed phase curves for the B ring, confirms the assumption of extensive scarring of the surface of ring particles. This can be seen from the fact that in order to obtain concordance between theory and observations, it is necessary to add to the nonlinear phase curve for the mutual shading effect a linear component with a phase factor of the order of $0^m.024$ per degree of phase (or somewhat higher, if one recalls the phase factor for the center of Saturn's disk). Obviously, this component is none other than the individual particle phase curve. The magnitude of the phase factor found is quite large, and extremely close to that for the moon, the extensive surface scarring of which is certainly not in doubt.

So, the theory of mutual shading first of all confirms the correctness of the preliminary conclusions arrived at in #19 concerning the B ring structure, and the properties of its particles. Beyond that, the theory makes it possible to arrive at certain new conclusions with respect to the structure of the ring, as well as to make a quantitative estimate of its principal physical parameters. In fact, we established the following in #31 and #32.

1. The shape of the phase curve for the ring indicates the presence of a marked variance in the sizes of the particles forming the ring. The exponent s in the Eq. (32.1) variance law is close to 2.5, a value that is, in general, typical of meteor material in the solar system.
2. The volumetric density, D , of the ring material is of the order of 10^{-2} .
3. Ring thickness, z_0 , must be known in order to estimate ring particle sizes. In our models, Eqs. (32.37) and (32.38), we used $z_0 = 1$ km. The edge-on observations of the rings made in 1966, confirm this value by order of magnitude. When $z_0 = 1$, and $s = 2.5$, we find that 90 percent of the reflecting surface be-

longs to particles in the interval $2 \text{ cm} \leq \rho \leq 2 \cdot 10^2 \text{ cm}$, where ρ is particle /111
radius.

4. Knowing D , and the geometric dimensions of the rings, and approximating $D_A = D_B$, and that $D_C = 0$, we can estimate the total mass of the rings \mathfrak{M}_r . If $z = 3 \text{ km}$, and the particle density is of the order of 1 gram/cm^3 (ice), $\mathfrak{M}_r = 1 \cdot 10^{24}$; that is, about $1/70^{\text{th}}$ the mass of the moon.

In conclusion, we should like to emphasize the fact that even in its present form the theory of mutual shading still does not take into consideration all the main features of Saturn's ring structure. Specifically, it fails to consider that D is a function of z , and that with increase in z the relative number of small particles should increase. The estimates of physical parameters of the rings presented here therefore should be considered simply as preliminary.

Notations in the Formulas
Used in the Theory of the Effect of Mutual Shading

(Chapter VII, #29-34)

- a - albedo of particle
- A, A' - angles of elevation of the sun and earth above the plane of Saturn's rings
- b_1 - component of ring brightness attributable to first order scattering
- Δb - component of ring brightness attributable to multiple scattering
- $b = b_1 + \Delta b$ - total ring brightness
- $b_B(\alpha)$ - brightness of the B ring for phase angle equal to α
- $b_B(0)$ - same, when $\alpha = 0$ (at time of precise opposition of Saturn)
- C - cylinder of shielding (see Figures 23 and 25)
- $D = 4/3 (\pi \rho^3 N)/R$ - volumetric density (part of ring volume occupied by particles)
- $F(\alpha)$ - natural phase function of ring particle
- K - constant in the particle size distribution law in Eq. (32.1)
- M - point on element of surface $d\epsilon$ of eclipsed particle (Figures 23 and 25)
- N - number of particles in ring volume
- P - volume contained between expanding and compressing cones of the volume of probability, V (Figure 25)
- p - probability of particle falling into volume V
- ρ_p - natural phase coefficient for the particle (the change in its stellar magnitude for change in phase angle of 1°)
- R - ring volume
- s - exponent in the particle size distribution law
- U - cone of shading (Figures 23 and 25)
- V - "volume of probability." The element $d\epsilon$ will be shielded from the earth (completely) or from the sun (completely or partially) when a particle falls into this volume. $V = C + U - W$ when the penumbra is ignored; $V = C + U + P - W$ when the penumbra is taken into consideration

W - part of V, total of C and U; $w = (\varphi/\pi\rho^3)W$

$x = \varphi z / (\rho \sin A)$ - auxiliary variable replacing the variable z

/113

$x_0 = \varphi z_0 / (\rho \sin A)$

z - depth of element de of eclipsed particle (Figures 23 and 25) measured from the plane of the rings, π , closest to the sun

z_0 - ring thickness

α - phase angle at Saturn (the angle sun-Saturn-earth)

$\beta = -2.5 \log b + C$ - the stellar magnitude of brightness. If it is measured in stellar magnitudes for a square second of arc, and the brightness b is in apostilbs, $C = 13.92$

δ - density

$v = \alpha/\varphi$ - auxiliary variable replacing the variable α

ρ - **particle** radius

ρ_1, ρ_2 - minimum and maximum particle radius values

$\bar{\rho}$ - mean particle radius

ρ_* - minimum radius of particles the eclipsing effect of which is not yet taken into consideration

$\varphi = 1'.676$ - the angular radius of the sun for an observer at the mean distance of Saturn

Subscripts S, Sh, M, and D designate the surface, shallow, middle and deep layers of the rings (for explanations see the corresponding sections of the text). The subscript c is the designation for the center of Saturn's disk.

REFERENCES

1. Allen, C.W., Astrofizicheskiye velichiny [Astrophysical Magnitudes], IL, 1960. /114
2. Arkad'yev, V.K., "Fresnel Diffraction," ZhRFKhO, Physics Department, Vol.44, No.4, 1912, p.145.
3. Barabashov, N.P., Semeykin, B.Ye., "Monochromatic Photometry of Saturn and Its Rings," Astron. zh., Vol.3, 1933, p.381.
4. Barabashov, N.P., Chekirda, A.T., "O raspredelenii yarkosti na diske Saturna i o yarkosti yego kolets," Trudy Khar'k. astron. obs. [On the Distribution of Brightness on the Disk of Saturn and on the Brightness of Its Rings, Proceedings of the Khar'kov Astronomical Observatory], Vol.2 (10), p.9.
5. Barnard, E.E., "Observations of the Eclipse of Iapetus in the Shadows of the Globe, Crape Ring, and Bright Ring of Saturn, 1889 Nov.1," Monthly Not., Vol.50, 1890, p.107.
6. Barnard, E.E., "Observations of Saturn's Ring at the Time of Its Disappearance in 1907," Monthly Not., Vol.68, 1908, p.346 (a).
7. Barnard, E.E., "Additional Observations of the Disappearances and Reappearances of the Rings of Saturn in 1907/08," Monthly Not., Vol.68, 1908, p.360 (b).
8. Barnard, E.E., "Recent Observations of the Rings of Saturn," Monthly Not., Vol.69, 1909, p.621.
9. Barnard, E.E., "Photographic Measures of Saturn and Its Rings," Astrophys. J., Vol.40, 1914, p.259.
10. Bell, L., "The Physical Interpretation of Albedo. II. Saturn's Rings," Astrophys. J., Vol.50, No.1, 1919.
11. Belopol'skiy, A.A., "Issledovaniye smeshcheniy liniy v spektre Saturna i yego kol'tsa," Izv. SPb. Akad. nauk. [An Investigation of Displaced Lines in the Spectrum of Saturn and Its Ring, News of the Saint Petersburg Academy of Sciences], Vol.3, No.4, 1895, p.379.
12. Belopol'skiy, A.A., "A Spectrographic Examination of Saturn's Rings," Astron. Nachr., Vol.139, No.3313, 1896.
13. Berry, A., Kratkaya istoriya astronomii [A Short History of Astronomy], GITTL, 1946.
14. Bobrov, M.S., "On the Physical Interpretation of the Phase Curve of Saturn's Rings," Astron. zh., Vol.17, No.6, 1940, p.1.
15. Bobrov, M.S., "Toward the Question of the Thickness of Saturn's Rings,"

- Astron. zh., Vol.33, 1956, p.161 (a).
16. Bobrov, M.S., "On the Structure of Saturn's Rings. III. An Evaluation of the Dimensions of Particles and the Mass of the Rings," Astron. zh., Vol.33, 1956, p.904 (b).
 17. Bobrov, M.S., Derivation of the Theoretical Phase Function of Brightness of Saturn's Rings and a Comparison of It with Observations," Astron. zh., Vol.37, 1960, p.306.
 18. Bobrov, M.S., "Theoretical Phase Curves of the Shadow Effect on Saturn's Rings. I. Derivation of Formulas," Astron. zh., Vol.37, 1960, p.306.
 19. Bobrov, M.S., "A Summation of the Theory of the Shadow Effect on Saturn's Rings on the Occurrence of Particles of Non-Identical Dimensions," Astron. zh., Vol.38, 1961, p.669.
 20. Bobrov, M.S., "On an Observation of Occultations of Stars by Saturn's Rings," Astron. zh., Vol.39, 1962, p.669.
 21. Bobrov, M.S., "Sovremennoye sostoyaniye voprosa o strukture i poryadke tolshchiny kolets Saturna," Tr. Astrofiz. in-ta AN KazSSR [The Modern Status of the Question on the Structure and Order of Thickness of Saturn's Rings, Proceedings of the Astrophysical Institute of the Academy of Sciences of the Kazakh SSR], Vol.9, No.83, 1967.
 22. Brower, D., Clemence, J.M., "Orbits and Masses of Planets and Satellites," IN: Planety i sputniki [Planets and Satellites], edited by Kuiper and Middlehurst, IL, 1963, ch.3.
 23. Walter, H., "Scattered Light Intensity of Large Spherical Particles," Optik, Vol.14, 1957, p.130.
 24. Walter, H., "Scattered Light Intensity of Large Spherical Particles. II," Optik, Vol.16, 1959, p.401. /115
 25. Wood, R.W., "Monochromatic Photography of Jupiter and Saturn," Astrophys. J., Vol.43, 1916, p.310.
 26. Harris, D.L., "Integral Photometry and Colorimetry of Planets and Satellites," IN: Planety i sputniki [Planets and Satellites], edited by Kuiper and Middlehurst, IL, 1963, ch.8.
 27. Gehrels, T., "The Light-Curve and Phase Function of 20 Massalia," Astrophys. J., Vol.123, 1956, p.331.
 28. Gehrels, T., "Photometric Studies of Asteroids. VI. Photographic Magnitudes," Astrophys. J., Vol.125, 1957, p.550.
 29. Gehrels, T., Coffeen, T., Owings, D., "Wavelength Dependence of Polarization. III. The Lunar Surface," Astron. J., Vol.69, 1964, p.826.

30. Hertzprung, E., "Comparison Between the Surface Brightness of the Rings and Central Body of Saturn," Astron. Nachr., Vol.208, 1919, p.81.
31. Giese, R.N., Bary, E., Bullrich, K., Vinnemann, C.D., "Tables of the Diffusion Functions and the Scattering Cross Section of Homogeneous Spherules Based on the Mie Theory, Refractive Index 1.50," Abhandl. Dtsch. Akad. Wiss. Berlin. Kl. Math., Phys. und Techn., No.6, 1961, p.1.
32. Goldsbrough, G.R., "The Influence of Satellites Upon the Form of Saturn's Ring," Philop. Trans. A, Vol.222, 1921, p.101.
33. Goldsbrough, G.R., "Cause of Encke's Division in Saturn's Rings," Proc. Roy. Soc. London A, Vol.101, 1922, p.280.
34. Goldsbrough, G.R., "The Stability of Saturn's Rings," Philos. Trans. A, Vol.244, 1951, p.1.
35. Goldsmith, W., Udar [Collision], Construction Literature Press, 1965.
36. Greaves, W.M.H., "On the Behavior of a Small Body Within the Cassini Division of Saturn's Ring," Monthly Not., Vol.83, 1922, p.71 (b).
37. Gurevich, L.E., Lebedinskiy, A.I., "Ob obrazovanii planet. I. Gravitatsionnaya kondensatsiya," Izv. AN SSSR, seriya fiz. [On the Formation of the Planets. I. Gravitational Condensation," News of the Academy of Sciences of the USSR, physics series], Vol.14, 1950, p.765.
38. Danjon, A., "Photometry and Colorimetry of the Planets Mercury and Venus," Bull. astron., Vol.14, 1949, p.315.
39. Deslandres, H., "A Search for Spectrals on the Rings of Saturn," C. r. Acad. sci., Vol.120, 1895, p.1155.
40. Dollfus, A., "Investigations of the Polarization of Planets," IN: Planety i sputniki [Planets and Satellites], edited by Kuiper and Middlehurst, IL, 1963, ch.9 (a).
41. Dollfus, A., "Visual and Photographic Observations of Planets at Pic du Midi," IN: Planety i sputniki [Planets and Satellites], edited by Kuiper and Middlehurst, IL, 1963, ch.15 (b).
42. Dollfus, A., "A New Satellite of Saturn," C. r. Acad. sci., Vol.264, 1967, p.822.
43. Dollfus, A., "The Discovery of Janus, Saturn's Tenth Satellite," Sky and Telescope, Vol.34, No.3, 1967.
44. Dollfus, A., Focas, J.H., "Photometry of Saturn's Rings As Seen Through the 1966 Slit," preprint of the Meudon Observatory, 1968, Astron. and Astrophysics, Vol.2, No.3, 1969.

45. Jeffreys, H., "The Relation of Cohesion to Roche's Limit," Monthly Not., Vol.107, 1947, p.260 (a).
46. Jeffreys, H., "The Effects of Collisions on Saturn's Rings," Monthly Not., Vol.107, 1947, p.263.
47. Drake, F.D., "Microwave Spectrum of Saturn," Nature, Vol.195, 1962, p.893.
48. Duboshin, G.N., "Ob ustoychivosti kolets Saturna," Trudy GAISH [On the Stability of Saturn's Rings, Proceedings of GAISH], Vol.14, 1940, p.172.
49. Davies, R.D., Beard, M., Cooper, B.F.C., "Observation of Saturn at 11.3 Centimeters," Phys. Rev. Letters, Vol.13, 1964, p.325. /116
50. Davies, R.D., Williams, D., "Observations of the Continuum Emission From Venus, Mars, Jupiter, and Saturn at 21.2 cm Wavelength," Planet. and Space Science, Vol.14, 1966, p.15.
51. Zheleznyakov, V.V., "On the Configuration of the Magnetic Field of Saturn," Astron. zh., Vol.41, 1964, p.955.
52. Seeliger, H.H., "Frequency of Occultations by Saturn," Astron. Nachr., Vol.100, 1881, p.177.
53. Seeliger, H.H., "Toward a Theory of the Illumination of the Large Planets, and Particularly of Saturn," Abhandl. Bayer. Akad. Wiss., 2 Kl., Vol.16, 1887, p.467.
54. Seeliger, H.H., "On the Illumination of Dusty Masses," Abhandl. Bayer. Akad. Wiss., 2 Kl., Vol.18, 1893, p.1.
55. Zlotnik, Ye.Ya., "On the Influence of the Rings on the Exosphere and Magnetic Field of Saturn," Astron. zh., Vol.44, 1967, p.581.
56. Yabushita, S., "Stability Analysis of Saturn's Rings With Differential Rotation," Monthly Not., Vol.133, 1966, p.247.
57. Carmichel, H., "Photometric Measures of Saturn and of Its Ring," Ann. astrophys., Vol.21, 1958, p.231.
58. Kiladze, R.I., "Nablyudeniye kolets Saturna v period prokhozhdeniya Zemli cherez ploskost' kolets v 1966 godu," Doklad na Simpoziume po fizike Luny i planet [Observation of Saturn's Rings in the Period of Earth's Passage Through the Plane of the Rings in 1966, Report at a Symposium on the Physics of the Moon and the Planets], Kiev, October, 1968.
59. Keeler, J.E., "Spectroscopic Proof of the Meteoric Constitution of Saturn's Rings," Astrophys. J., Vol.1, 1895, p.416.
60. Kirkwood, D., "The Zone of Asteroids and the Ring of Saturn," Proc. Amer. Philos. Soc., Vol.21, 1884, p.263.
61. Kowalewsky, S.V., "Additions and Comments to Laplace's Examination of

- the Shape of Saturn's Ring," Astron. Nachr., Vol.111, 1885, p.38.
62. Kozyrev, N.A., "Vodyanoy par v kol'tse Saturna i yego teplichnyy effekt na poverkhnosti planety," Izv. GAO AN SSSR v Pulkove [Water Vapor in Saturn's Ring and Its Greenhouse Effect on the Planet's Surface, News of the GAO of the Academy of Sciences of the USSR in Pulkova], No.184, 1968, p.99.
 63. Kuiper, G.P., Atmosfera Zemli i planet [Atmospheres of the Earth and Planets], IL, 1951, pp.378-379.
 64. Kuiper, G.P., Trans. Internat. Astron. Union, Vol.9, 1957, p.254 (a).
 65. Kuiper, G.P., "Infrared Observations of Planets and Satellites," Astron. J., Vol.62, 1957, p.245 (b).
 66. Cook, J.J., Cross, L.G., Bair, M.E., Arnold, C.B., "Radio Detection of the Planet Saturn," Nature, Vol.188, 1960, p.393.
 67. Cook, A.F., Franklin, F.A., "Optical Properties of Saturn's Rings. I. Transmission," Smiths. Contribs. Astrophys., Vol.2, 1958, p.377.
 68. Cook, A.F., Franklin, F.A., "Rediscussion of Maxwell's Adams Prize Essay on the Stability of Saturn's Rings. I," Astron. J., Vol.69, 1966, p.179.
 69. Cook, A.F., Franklin, F.A., "Rediscussion of Maxwell's Adams Prize Essay on the Stability of Saturn's Rings. II," Astron. J., Vol.71, 1966, p.10.
 70. Kutuza, B.G., Losovskiy, B.Ya., Salomonovich, A.Ye., "Radioizlucheniye Saturna na $\lambda = 8$ mm," Dokl. AN SSSR [Radio Emission of Saturn at $\lambda = 8$ mm, Reports of the AN SSSR], Vol.161, 1965, p.1301.
 71. Laplace, P.S., Mécanique céleste, Vol.3, sect. 46, 1802.
 72. Lebedinets, V.N., "Absolyutnaya fotograficheskaya fotometriya Yupitera i Saturna so svetofil'trami," Trudy Khar'k. astron. obs. [Absolute Photographic Photometry of Jupiter and Saturn With Filters, Proceedings of the Khar'kov Astronomical Observatory], Vol.12, 1957, p.167.
 73. Lyot, B., "Research on the Polarization of Light of the Planet and of Certain Terrestrial Substances," Ann. Obs. Meudon, Vol.8, 1929, pp. 56-62, 147-150.
 74. Lyot, B., "Aspect of the Planet at Pic du Midi Through a 60 cm Lens," Astronomie, Vol.67, 1953, p.3.
 75. Low, F.J., "Infrared Brightness Temperature of Saturn," Astron. J., Vol.69, 1964, p.143.
 76. Low, F.J., "Observations of Venus, Jupiter, and Saturn at $\lambda 20 \mu$," Astron. J., Vol.71, 1966, p.391.

77. Lowell, P. "Saturn's Rings, Astron. Nachr., Vol.184, 1910, p.177.
78. Maggini, M., "The Recent Disappearance of Saturn's Ring," Ricerca scient., ser.2, Vol.1, No.5-6, year 8, 1937.
79. Maxwell, J.C., "On the Stability of the Motion of Saturn's Rings," Cambridge, 1859 (reprinted in Scientific Papers of J.C. Maxwell, Vol.1, Cambridge Univ. Press, 1890).
80. Maksumov, D.D., Astronomicheskaya optika [Astronomical Optics], GTTI, 1946.
81. Meinel, A., "Quality of the Astronomical Image and Selection of a Site an Observatory," IN: Teleskopy [Telescopes], edited by Kuiper and Middlehurst, IL, 1963, p.196.
82. Menzel, D.H., Coblentz, W.W., Lampland, C.O., "Planetary Temperatures Derived From Water-Cell Transmission," Astrophys. J., Vol.63, 1926, p.177.
83. Mertz, L., "Astronomical Infrared Spectrometer," Astron. J., Vol.70, 1965, p.548.
84. Mertz, L., Coleman, I., "Infrared Spectrum of Saturn's Ring," Astron. J., Vol.71, 1966, p.747.
85. Minnaert, M., Svet i tsvet v prirode [Light and Color in Nature], Fizmatgiz, 1958.
86. Moroz, V.I., "On the Infrared Spectra of Jupiter and Saturn (0.9-2.5 μ)," Astron. zh., Vol.38, 1961, p.1080.
87. Müller, G., "Determinations of the Brightness of the Large Planets and Several Asteroids," Potsdam Publ., Vol.8, 1893, p.193.
88. Murray, B.C., Wildey, R.L., "Stellar and Planetary Observations at 10 Microns," Astrophys. J., Vol.137, 1963, p.692.
89. Pavlov, A.V., "On the Resolving Power of the Eye," Byull. VAGO, No.29 (36), 1961, p.39.
90. Pettit, E., Nicholson, S.B., Popul. Astron., Vol.32, No.601, 1924, p.614.
91. Rabe, W., "Investigations of the Diameters of the Large Planets," Astron. Nachr., Vol.234, 1928, p.153.
92. Radziyevskiy, V.V., "Radiation Deceleration in the Solar System and the Growth of Saturn's Rings," Astron. zh., Vol.29, 1952, p.306.
93. Wright, W.H., "Photographs of Saturn Made by Light of Different Colours," Publs. Astron. Soc. Pacific, Vol.39, 1927, p.231.
94. Russell, H.N., "On the Illumination of the Dark Side of Saturn's Rings,"

Astrophys. J., Vol.27, 1908, p.230.

95. Russell, H.N., "The Stellar Magnitudes of the Sun, Moon, and Planets," Astrophys. J., Vol.43, 1916, p.103.
96. Rose, W.K., Bologna, G.M., Sloanaker, R.M., "Linear Polarization of the 3200 Mc/sec Radiation From Saturn," Phys. Rev. Letters, Vol.10, 1963, p.123.
97. Roche, E.A., "The Figure of a Fluid Mass Subjected to the Attraction of a Distant Point," Acad. de Montpellier (Sciences), Vol.1, 1850).
98. Rougier, G., "Photoelectric Photometry of the Moon," Ann. Obs. Strasbourg, Vol.2, No.3, 1933, p.205.
99. Slipher, E.C., "Phenomena in Connection With the Earth Transit of the Plane of Saturn's Rings in 1920-21," Popul. Astron., Vol.30, 1922, p.8.
100. Sobolev, V.V., Perenos luchistoy energii v atmosferakh zvezd i planet [Transfer of Radiant Energy in the Atmospheres of Stars and Planets], GITI, 1956.
101. Stebbins, J., Kron, G.E., "Six-Colour Photometry of Stars," Astrophys. J., Vol.123, 1956, p.440.
102. Stebbins, J., Jacobsen, T.S., "Further Photometric Measures of Jupiter Satellites and Uranus, With Tests of the Solar Constant," Lick Obs. Bull., Vol.13, 1928, p.180.
103. Struve, H., "Observations of Saturn's Satellites at the 30-inch Pulkova Refractor," Publ. Obs. Poulkova, ser.2, Vol.11, 1898, p.232.
104. Sytinskaya, N.N., "Investigation of the Threshold of Contrast Sensitivity of Vision at Low Values of Brightness," Uch. zap. LGU, seriya matem. nauk, No.18, 1949, p.158.
105. Texereau, J., "Observing Saturn's Edgewise Rings, October, 1968," Sky and Telescope, Vol.33, No.4, 1966, p.226. /118
106. Timiryazev, A.K., Kineticheskaya teoriya materii [The Kinetic Theory of Matter], 3rd edition, Moscow, Uchpedgiz, 1956, ch.4.
107. Tikhov, G.A., "Dvukhtsvetnyye fotografii Marsa i Saturna, poluchennyye pri pomoshchi pulkovskogo 30-dyuymovogo refraktora sposobom svetofil'trov," Izv. Russk. astron. ob-sa [Dichromatic Photographs of Mars and Saturn, Obtained Using the Pulkova 30-inch Refractor by Means of Filters, News of the Russian Astronomical Observatory], Vol.17, No.5, 1911.
108. Welch, W.J., Thornton, D.D., Lohman, R., "Observations of Jupiter, Saturn, and Mercury at 1.53 μ m," Astrophys. J., Vol.146, 1966, p.799.
109. Feibelman, W.A., "Concerning the 'D' Ring of Saturn," Nature, Vol.214, 1967, p.793.

110. Fesenkov, V.G., "Photometric Observations of the Planet Saturn," Astron. Nachr., Vol.226, 1926, p.127; Astron. Nachr., Vol.229, 1927, p.227; Astron. Nachr., Vol.231, 1928, p.9.
111. Franklin, F.A., Cook, A.F., "Optical Properties of Saturn's Rings. II. Two-colour Phase Curves of the Two Bright Rings," Astron. J., Vol.70, 1965, p.704.
112. Hagihara, Y., "Stability of the Solar System," IN: Planety i sputniki [Planets and Satellites], edited by Kuiper and Middlehurst, IL, 1963, ch.4.
113. Hapke, B., "A Theoretical Photometric Function for the Lunar Surface," J. Geophys. Res., Vol.68, 1963, p.4571.
114. Hapke, V., van Horn, H., "Photometric Studies of Complex Surfaces, With Applications to the Moon," J. Geophys. Res., Vol.68, 1963, p.4545.
115. Heath, M.B.B., "Saturn in 1957," J. Brit. Astron. Assoc., Vol.68, 1958, p.57.
116. Hepburn, P.H., (1) "Dimensions of Saturn and His Rings as Measured on Prof. Barnard's Photograph on 1911 Nov.19"; (2) "Observations of the Transparency of Ring A, and Other Details Appearing on the Photograph," Monthly Not., Vol.24, 1914, p.721.
117. Hughes, M.P., "Planetary Observations at a Wavelength of 6 cm," Planet. and Space Sci., Vol.14, 1966, p.1017.
118. Chandrasekhar, S., Perenos luchistoy energii [Transfer of Radiant Energy], IL, 1953.
119. Chandrasekhar, S., Elbert, D., Franklin, A., "The X and Y Functions for Isotropic Scattering. I," Astrophys. J., Vol.115, 1952, p.244.
120. Shayn, G.A., "On the Intensity Distribution in the Spectrum of Saturn and His Ring," Tsirk. Pulk. obs., Vol.13, 1935, p.9.
121. Sharonov, V.V., "An Experiment on the Absolute Determination of the Brightness Coefficient of Saturn's Surface," Byull. Yerevanskoy astron. obs., 1935.
122. Sharonov, V.V., "Absolute Photographic Photometry of Saturn's Disk," Tsirk. GAO AN SSSR, No.26-27, 1939, p.37.
123. Sharonov, V.V., Priroda planet [Nature of the Planets], Fizmatgiz, 1958.
124. Shoenberg, E., "On the Illumination of the Planets," Publ. Obs. Dorpat, Vol.24, 1917.
125. Shoenberg, E., "Photometric Examinations of Jupiter and the System of Saturn," Ann. Acad. Sci. Fennicae, ser.A, Vol.16, No.5, 1921.

126. Schoenberg, E., Theoretische Photometrie. Handbuch der Astrophysik [Theoretical Photometry. Handbook of Astrophysics], Vol. 2, Part 1, Berlin, 1929, p. 1.
127. Schoenberg, E., "New Investigations of Saturn's Ring," Vierteljahresschr. Astron. Ges., Vol. 68, 1933, p. 387.
128. Shifrin, K.S., Rasseyaniye sveta v mutnoy srede [Light Scattering in a Scattering Medium], GTTI, 1951.
129. Shnyrev, G.D., Grechushnikov, B.N., Moroz, V.I., "An Investigation of the Infrared Spectrum of Saturn by the Fourier Transform Method," Astron. tsirk., No. 302, 1964, p. 1.
130. Aitken, R.G., "Observations of Saturn's Rings in 1907." Lick Obs. Bull., Vol. 4, 1907, p. 181.

NATIONAL AERONAUTICS AND SPACE ADMINISTRATION
WASHINGTON, D.C. 20546

OFFICIAL BUSINESS
PENALTY FOR PRIVATE USE \$300

FIRST CLASS MAIL

POSTAGE AND FEES PAID
NATIONAL AERONAUTICS AND
SPACE ADMINISTRATION



034 001 C1 H 30 720526 S00903DS
DEPT OF THE AIR FORCE
AF WEAPONS LAB (AFSC)
TECH LIBRARY/WLOL/
ATTN: E LOU BOWMAN, CHIEF
KIRTLAND AFB NM 87117

NASA-451

POSTMASTER: If Undeliverable (Section 112
Postal Manual) Do Not Ret

"The aeronautical and space activities of the United States shall be conducted so as to contribute . . . to the expansion of human knowledge of phenomena in the atmosphere and space. The Administration shall provide for the widest practicable and appropriate dissemination of information concerning its activities and the results thereof."

— NATIONAL AERONAUTICS AND SPACE ACT OF 1958

NASA SCIENTIFIC AND TECHNICAL PUBLICATIONS

TECHNICAL REPORTS: Scientific and technical information considered important, complete, and a lasting contribution to existing knowledge.

TECHNICAL NOTES: Information less broad in scope but nevertheless of importance as a contribution to existing knowledge.

TECHNICAL MEMORANDUMS: Information receiving limited distribution because of preliminary data, security classification, or other reasons.

CONTRACTOR REPORTS: Scientific and technical information generated under a NASA contract or grant and considered an important contribution to existing knowledge.

TECHNICAL TRANSLATIONS: Information published in a foreign language considered to merit NASA distribution in English.

SPECIAL PUBLICATIONS: Information derived from or of value to NASA activities. Publications include conference proceedings, monographs, data compilations, handbooks, sourcebooks, and special bibliographies.

TECHNOLOGY UTILIZATION PUBLICATIONS: Information on technology used by NASA that may be of particular interest in commercial and other non-aerospace applications. Publications include Tech Briefs, Technology Utilization Reports and Technology Surveys.

Details on the availability of these publications may be obtained from:

SCIENTIFIC AND TECHNICAL INFORMATION OFFICE

NATIONAL AERONAUTICS AND SPACE ADMINISTRATION

Washington, D.C. 20546